OPTIMIZING THE PERFORMANCE OF VISIBLE LIGHT COMMUNICATION SYSTEM WITH ANGULAR DIVERSITY

A THESIS SUBMITTED TO
GRADUATE SCHOOL OF NATURAL AND APPLIED SCIENCES
OF
KOCAELİ UNIVERSITY

BY

AAMIR ULLAH KHAN

IN PARTIAL FULFILLMENT OF THE REQUIREMENTS
FOR
THE DEGREE OF MASTER OF SCIENCE
IN
ELECTRONICS AND COMMUNICATIONS ENGINEERING

KOCAELİ 2020

OPTIMIZING THE PERFORMANCE OF VISIBLE LIGHT COMMUNICATION SYSTEM WITH ANGULAR DIVERSITY

A THESIS SUBMITTED TO
GRADUATE SCHOOL OF NATURAL AND APPLIED SCIENCES
OF
KOCAELİ UNIVERSITY

BY

AAMIR ULLAH KHAN

IN PARTIAL FULFILLMENT OF THE REQUIREMENTS
FOR
THE DEGREE OF MASTER OF SCIENCE
IN
ELECTRONICS AND COMMUNICATIONS ENGINEERING

Assoc.Prof.Dr. Sultan ALDIRMAZ ÇOLAK		
Supervisor,	**Kocaeli University**	**.....**
Assoc.Prof.Dr. Kerem KÜÇÜK		
Jury member,	**Kocaeli University**	**.....**
Asst.Prof.Dr. Yasin ÇELİK		
Jury member,	**Aksaray University**	**.....**

Thesis Defense Date: 20.07.2020

ACKNOWLEDGMENT

At first, I would like to express my gratitude and reverence to ALLAH Almighty, who gave me the strength, ability, knowledge, and guidance to continue my research studies as well as the perseverance to complete my Master of Science in Electronics and Communications Engineering. Without the grace and blessings of Allah Almighty, I believe, it would not have been possible.

I would like to express my sincere gratitude to my supervisor, Assoc. Prof. Dr. Sultan Aldırmaz Çolak for her continuous support, guidance, and motivation throughout my research studies. Her professional approach and practical knowledge helped me to complete my research in the best possible way.

I take pride in acknowledging the insightful guidance of Asst. Prof. Dr. Yasin Çelik for his invaluable time, comments, suggestions, and contributions to my research work. I am also very thankful to the Scientific and Technological Research Council of Turkey (TÜBİTAK) for their support in my research. I am also very thankful to all the academic personnel of the Electronics and Communications Engineering Department at Kocaeli University, Turkey.

Last but not least, I am very grateful to my parents for their unconditional love, support, and prayers. I am very thankful to my brother and sister for their love and support.

July, 2020 Aamir Ullah Khan

CONTENTS

LIST OF FIGURES

LIST OF TABLES

LIST OF SYMBOLS AND ABBREVIATIONS

α	: Incidence angle
α_{mn}	: Irradiance angle at LED n w.r.t PD m
A_{PD}	: Active area of PD
β_{mn}	: Incidence angle at PD m w.r.t LED n
C_d	: Capacitance of PD
C_g	: Gate capacitance of FET
C_{max}	: Maximum capacity
η_{lu}	: Luminous efficiency
η_{pow}	: Power efficiency
η_{qe}	: Quantum efficiency
E_{recv}	: Received electrical energy
E_s	: Mean emitted electrical energy
Γ	: FET channel noise factor
g_m	: Trans-inductance of FET
$H(0)$	: DC channel gain
$\mathbf{H}$. $\|.\|_F$	: Frobenius norm
I_{avg}	: Mean emitted optical power
I_p	: Photo-current
k_b	: Boltzmann's constant
k	: FOV coefficient
L_{max}	: Maximum visibility
M	: Number of LEDs
m	: Lambertian emission order
N_0	: Spectral density of noise
N	: Number of PDs
N_{ca}	: Number of carriers passing through PN junction
N_{ext-ph}	: Number of externally emitted photons
$\Omega_{1/2}$	: LED's semi-angle calculated at half power
Ω_{sp}	: Spatial angle
$\overline{\sigma^2_{Nj}}$	: Mean square noise current for the j^{th} receiver
Φ_{e-flux}	: Electric flux
P_{elec}	: Electrical input power
Φ_{flux}	: Luminous flux
P_{in-max}	: Maximum value of the transmitter's optical power
P_{op}	: Optical power
$P_{recv-LoS}$	: Power received through LoS
$P_{recv-NLoS}$	: Power received through NLoS
P_{thresh}	: Threshold value of maximum permissible power to ensure eye safety
P_{trans}	: Transmitted optical power
q	: Charge on an electron

$R_0(\alpha)$: Lambertian radiation intensity
R : Responsivity of photodetector
$R_{feedback}$: Feedback resistor
R_H : Rank of the channel matrix
R_{spec} : Spectral efficiency
σ^2_{shot} : Shot noise
σ^2_{th} : Thermal noise
$\sigma^2_{th–FET}$: Thermal noise from FET channel resistance
$\sigma^2_{th–FET}$: Thermal noise from FET channel resistance
$\sigma^2_{th–R_{feedback}}$: Thermal noise from feedback resistor
$\sigma^2_{tot–noise}$: Total noise present in a VLC system
SNR_{elec} : Average electrical power per transmit antenna
T_k : Absolute temperature
T_s : Symbol duration
$V(\lambda)$: Eye sensitivity level
ξ : Irradiance angle

Abbreviations

ACO-OFDM : Asymmetrically Clipped Optical Orthogonal Frequency Division Multiplexing
ADC : Analog-to-Digital Converter
ADO-OFDM : Asymmetrically Clipped DC biased Optical Orthogonal Frequency Division Multiplexing
AI : Artificial Intelligence
ADR : Angular Diversity Receiver
AOR : Angle Oriented Receiver
APD : Avalanche Photodiode
AWGN : Additive White Gaussian Noise
BER : Bit Error Rate
CAGR : Compound Annual Growth Rate
CSI : Channel State Information
DAC : Digital-to-Analog Converter
DCO-OFDM : DC biased Optical Orthogonal Frequency Division Multiplexing
DD : Direct Detection
DLoS : Directed Line of Sight
DMT : Discrete Multitone
EA : Elevation Angle
EC : European Commission
EM : Electromagnetic Spectrum
FET : Field Effect Transistor
FOV : Field of View
I2V : Infrastructure to Vehicle
ICT : Information and Communication Technologies
IEEE : Institute of Electrical and Electronics Engineers
IM : Intensity Modulation

IoT : Internet of Things
IR : Infra-red
ISI : Inter Symbol Interference
ITS : Intelligent Transport System
JEITA : Japan Electronics and Information Technology Industries Association
LD : Laser Diode
LED : Light Emitting Diode
LoS : Line of Sight
Li-Fi : Light Fidelity
M2M : Machine-to-Machine
MIMO : Multiple Input Multiple Output
MISO : Multiple Input Single Output
ML : Maximum Likelihood
MMSE : Minimum Mean Square Error
MRC : Maximum Ratio Combining
N-ADR : Non-Angular Diversity Receiver
NDLoS : Non-directed Line of Sight
NRZ-OOK : Non-Return Zero On-Off Keying
OFDM : Orthogonal Frequency Division Multiplexing
O-LEDs : Organic Light Emitting Diodes
O-MIMO : Optical Multiple Input Multiple Output
OOK : On-Off Keying
OWC : Optical Wireless Communication
P2P : Point-to-Point
PD : Photodetector
PEP : Pairwise Error Probability
PIN Diode : Positive Intrinsic Negative Diode
PLC : Power Line Communication
POF : Plastic Optical Fibre
PSD : Power Spectral Density
RAN : Radio Access Networks
RC : Repetition Coding
SMP : Spatial Multiplexing
SSL : Solid State Lighting
V2V : Vehicle to Vehicle
V-BLAST : Vertical-Bell Laboratories Layered Space-Time
VC : Vehicular Communications
VLC : Visible Light Communication
VLCA : Visible Light Communication Association
VLCC : Visible Light Communications Consortium
VL-ID : Visible Light ID System
VPPM : Variable Pulse Position Modulation
WDM : Wavelength Division Multiplexing
WLEDs : White Light Emitting Diodes
WPLEDs : White Phosphors Light Emitting Diodes
WWRF : Wireless World Research Forum
ZF : Zero Forcing

GÖRÜNÜR IŞIK HABERLEŞMESİNDE AÇISAL ÇEŞİTLEME İLE SİSTEM PERFORMANSININ EN İYİLENMESİ

ÖZET

Telsiz bağlantılar günümüzde hayatımızın önemli bir parçası haline geldi. Telsiz cihazların sayısı yüksek veri hızlarına olan talep ve sürekli bağlantıda olma talebi her geçen gün artmaktadır. Nesnelerin İnterneti (Internet of Things, IoT) ve Yapay Zeka (Artificial Intelligence, AI) ile ilgili hizmetlerin ortaya çıkmasıyla birlikte, yüksek veri hızı ve mutlak bağlantı ihtiyacı gelecekte daha da artacaktır. Ancak böyle bir artış, tüm yeni kullanıcıları birlikte yer alabileceği etkin bir yöntem gerektirir. Radyo frekans spektrumu şuan çok sıkışık durumdadır. Araştırmacılar, sözkonusu bu yeni kullanıcıları iletişim sistemine dahil edebilmek için, lisanssız bandları ve kaynakları henüz işletilmeyen görünür ışık spektrumunu kullanmaya karar verdiler, böylece Görünür Işık İletişim (Visible Light Communication, VLC) sistemlerinin temelini oluşturdular. VLC sistemi, elektromanyetik spektrumunun bir parçası olan görünür ışık ile iletişimin gerçekleştirildiği bir sistemdir ve çoklu Işık Yayan Diyotlardan (Light Emitting Diodes, LEDs) ve Fotodetektörlerden (Photodetectors, PDs) oluşur. Bunların içinde iletişim elektromanyetik spektrumun görünür kısmı aracığıyla gerçkleşir. VLC, özellikle iç mekan ortamlarında çok sayıda uygulamaya sahiptir. VLC için mevcut optik bant genişliği birkaç THz'dir, ancak elektrik bant genişliği sadece birkaç MHz ile sınırlıdır. Yüksek veri hızı gereksinimini karşılamak için Çok Girişli Çok Çıkışlı (Multiple-Input Multiple-Output, MIMO) teknikleri benimsenmiştir.

İç mekan MIMO-VLC sistemleri için kritik zorluklardan biri kanal korelasyonudur. İç ortam nedeniyle, özellikle görüş hattı sahıp (Line of Sight, LoS) senaryolar düşünüldüğünde sönümleme bileşenleri yoktur. Sonuç olarak, iç mekan MIMO-VLC kanalları yüksek derecede korelasyona girerek sadece düşük çeşitlilik kazancı sağlar. Benzer şekilde, bir MIMO-VLC sistemindeki çoklu veri akışlarının başarılı bir şekilde çözülmesi de yüksek kanal korelasyonu tarafından önlenir ve bu da düşük performansa neden olur. Bu nedenle, ilişkili kanal matris girişlerinin bu zorluğunun üstesinden gelmek için bir mekanizma mevcut olmalıdır. Kanal ilintisini en aza indirmek için, Açısal Çeşitlilik Alıcı (Angular Diversity Receiver, ADR) yapısı kullanılabilir. Bir ADR'de, kanal matrisinin elemanları PD'lerin normal vektörlerine bağlıdır. ADR tabanlı bir MIMO-VLC sistemi, PD'lerin normal vektörlerinin farklı yönlere yönlendirileceği bir şekilde tasarlanır. İlgili normal vektörler PD'lerin Yükseklik Açılarına (Elevation Angle, EA) bağlıdır, bu nedenle EA'ların değiştirilmesi ile ilgili normal vektörler değiştirilebilir. EA tüm PD'ler için aynı kabul edilir, dolaysıyla sabit bir EA için, MIMO-VLC sisteminde sabittir.

Bu tezde, Piramit Alıcı (Pyramid Receiver, PR) adı verilen özel bir ADR türü ele alınmıştır. Değişken EA'ya sahip bir iç mekan MIMO-VLC sistemi öneriyoruz. Değişken EA MIMO-VLC sisteminde, PD'lerin EA'ları birbirinden bağımsız olarak değişir. Böyle bir MIMO-VLC sisteminde, her PD'nin kendi özgün optimum EA değeri vardır, bu da kanal ilintisinin düşük olmasına neden olur. Yapılan benzetimlerde, sabit

ve değişken yükselme açılarına sahip 4x4, 4x5 ve 5x5 MIMO-VLC sistemleri ele alınmış, performansları kapasite ve Bit Hata Oranı (Bit Error Rate, BER) ölçütleri cinsinden karşılaştırılmıştır. Ayrıca, birçok iç mekan MIMO-VLC sistemleri için optimum veri hızı performansı sağlayacak şekilde uygun alıcı konumları belirlenmiştir. İç mekan MIMO-VLC sistemlerinin BER performansını belirlemek için Tekrarlı Kodlama (Repetition Coding, RC) ve Uzamsal Çoğullama (Spatial Multiplexing, SMP) gibi iletim şemaları da ele alınmış ve performansları karşılaştırılır. ADR tabanlı MIMO-VLC sisteminin performansı, Açısal Olmayan Çeşitlilik Alıcı (Non-angular Diversity Receiver, N-ADR) tabanlı MIMO VLC sistemi ile de karşılaştırılmıştır.

Sonuçlar, önerilen yöntemin tüm iç mekan MIMO-VLC sistemleri için daha yüksek veri hızı elde ettiğini göstermektedir. Önerilen yöntemin BER sonuçları da diğer sistemlerin BER sonuçlarından daha iyidir. Ayrıca, Görüş Alanı (Field-of-View, FoV), LED verici dizi uzunluğu ve alıcının yatay yönlendirme açısı gibi faktörlerin ele alınan sabit ve değişken EA MIMO-VLC sistemlerinin performansın üzerindeki etkisi de bu tezde incelenmiş ve tartışılmıştır.

Anahtar Kelimeler: Çok-Girdili Çok-Çıktılı (MIMO), Görünür Işık İletişimi (VLC), Optik Kablosuz İletişim (OWC), Yükselme Açısı (EA) .

OPTIMIZING THE PERFORMANCE OF VISIBLE LIGHT COMMUNICATION SYSTEM WITH ANGULAR DIVERSITY

ABSTRACT

Wireless connectivity is becoming an essential part of our life nowadays. The number of wirelessly connected devices and the demand for high data rates and continuous connectivity is increasing day by day. With the emergence of the Internet of Things (IoT) and Artificial Intelligence (AI) associated services, the need for high speed and absolute connectivity would only grow in the future. Such an increase, however, requires an efficient mechanism to accommodate all the new users. The Radio Frequency (RF) spectrum is already very congested. In order to accommodate these new users, researchers decided to harness unlicensed and mostly unexploited resources in the visible light spectrum for communication, thus, becoming the foundation for Visible Light Communication (VLC) systems. A VLC system is composed of multiple Light Emitting Diodes (LEDs) and Photodetectors (PDs) in which communication takes place via visible part of the Electromagnetic (EM) spectrum. VLC has numerous applications specifically in indoor environments. The available optical bandwidth for VLC is several THz, however, the electrical bandwidth is limited to only several MHz. In order to accommodate the high data rate requirement, Multi-Input Multi-Output (MIMO) techniques are adopted.

One of the critical challenges for the indoor MIMO-VLC systems is the channel correlation. In an indoor MIMO-VLC system, Line of Sight (LoS) links exist between an LED-based transmitter and a PD based receiver. Due to the indoor environment, there are no fading components present, especially when LoS scenarios are considered. As a result, indoor MIMO-VLC channels become highly correlated resulting in only small diversity gain. Similarly, successful decoding of multiple data streams in a MIMO-VLC system is also prevented by a high channel correlation, resulting in poor performance. Therefore, a mechanism must be in place to overcome this challenge of correlated channel matrix entries. In order to minimize the channel correlation, an Angular Diversity Receiver (ADR) can be employed. In an ADR, the channel matrix entries depend on the respective of normal vectors of the PDs. An ADR based MIMO-VLC system is designed in such a way that the normal vectors of PDs are directed in different directions. The respective normal vectors depend on Elevation Angles (EAs) of the PDs, thus, by varying the EAs, the respective normal vectors can be changed. The EA is assumed the same for all the PDs resulting in a fixed EA MIMO-VLC system.

In this thesis, we consider the work of a special type of ADR called Pyramid Receiver (PR) and propose a new variable EA based indoor MIMO-VLC system. In the variable EA MIMO-VLC system, the EA of the PDs is varied independently of one another. In such a MIMO-VLC system, each PD has its own unique optimum EA value which results in a further reduction in channel correlation. In the simulations, 4x4, 4x5 and 5x5 MIMO-VLC systems with fixed and variable EAs were handled and their performances were compared in terms of capacity and Bit Error Rate (BER). Furthermore, suitable

receiver positions resulting in optimum throughput performance have been highlighted for multiple considered indoor MIMO-VLC systems. In order to determine the BER performance of the indoor MIMO-VLC systems, transmission schemes like Repetition Coding (RC) and Spatial Multiplexing (SMP) are considered and compared. The performance of the ADR based MIMO-VLC system is also compared with the Non-Angular Diversity Receiver (N-ADR) based MIMO-VLC system.

The results show that the proposed method achieves higher throughput for all the considered indoor MIMO-VLC systems. The BER results of the proposed method also show improvement for some respective receiver positions. Furthermore, the impact of factors including Field-of-View (FOV) angle, LED transmitter array length, and the horizontal orientation angle of the receiver on the performance of the considered fixed and variable EA MIMO-VLC systems have also been investigated and discussed in this dissertation.

Keywords: Multiple-Input Multiple-Output (MIMO), Visible Light Communication (VLC), Optical Wireless Communication (OWC), Elevation Angle (EA).

INTRODUCTION

Wireless connectivity has become an absolute necessity nowadays. It is no more regarded as a luxury but as an utter need of time. Due to technical developments, the cost of handheld devices has become relatively lower over the years, due to which their availability is no more an issue. According to the Wireless World Research Forum (WWRF), it is projected that by 2020, 7 billion people will be served by 7 trillion devices. Similarly, it is also expected that the number of wireless connected devices will reach 1000 times of the human population in the coming years [1].

Moreover, the scope of communication is also expected to shift from human to human and human to machine mode to the Machine to Machine (M2M) mode in the coming years. In a similar manner, the Internet of Things (IoT), where every device is connected to a virtual network, will bring a massive surge of connected devices providing humans with new prospects of corporate businesses and consumer services. As the number of devices connected online increases, it also results in a significant increase in the amount of traffic generated by these devices.

Recent studies have projected that by 2022, 77 exabytes of traffic will have to be transported via mobile networks every month and forecast a Compound Annual Growth Rate (CAGR) of 46 percent for the period 2017-2022 [2]. This high volume of data traffic certainly leads to a greater need for spectrum to support wireless services provided by these devices. The best propagation conditions to meet the need of wireless devices can be found in the Radio Frequency (RF) spectrum. But the RF spectrum is already very congested, therefore, to accommodate these new devices and meet the ever-growing demand for connectivity, researchers have started looking for new alternative solutions. In this process, Visible Light Communication (VLC) caught the eye of the researchers.

VLC is gaining much attention from academia and industry over recent years. The research in VLC is being conducted in different directions. Most of the research is focused on the improvement of the performance metrics including data rate, capacity, and reliability of the VLC systems. Different technologies such as Orthogonal Frequency

Division Multiplexing (OFDM) and Optical Multiple-Input Multiple-Output (O-MIMO) have been introduced to enhance the data rate of VLC systems. Similarly, heterogeneous networks composed of VLC and RF or Infrared (IR) networks along with Power Line Communication (PLC) have also been recently investigated by many researchers. An indoor wireless VLC system is one of the exciting fields of VLC. An indoor wireless VLC can be used for simultaneous data transmission and localization. In such a system, illumination is the primary function followed by communication. So any indoor wireless VLC system must obey the standards and principles of illumination and must be jointly optimized with illumination.

An indoor VLC system is generally composed of several Light Emitting Diodes (LEDs) and Photodetectors (PDs). The spectral efficiency of an indoor VLC system can be increased by adopting MIMO techniques. MIMO can increase the data rate without any additional bandwidth expansion. However, due to an indoor environment, the channel matrix of the indoor MIMO-VLC system may become highly correlated. As a result, a rank deficient channel matrix is obtained affecting the throughput and Bit Error Rate (BER) performance of the system. To improve the performance of an indoor MIMO-VLC system, it is therefore of utmost importance to have uncorrelated entries in the channel matrix.

Different methods have been explored by researchers to obtain uncorrelated channel matrix for an indoor MIMO-VLC system. An aperture based receiver for an indoor MIMO-VLC system is investigated in [3]. It is shown that a well-designed receiver can receive signals from different directions with low multi-stream interference. This results in a well-conditioned channel matrix. A MIMO system may employ a special type of receiver called “Angular Diversity Receiver (ADR)”. In ADRs, the entries in the channel matrix depend on the respective normal vectors PDs. The PDs are arranged in such a manner that the normal vectors of the PDs point in different directions from one another. As a result, a highly uncorrelated channel matrix is obtained [4]. A special type of ADR called “Pyramid Receiver (PR)” is demonstrated in [5]. In PR, the PDs are arranged in such a way that the receiver resembles a pyramid. The Elevation Angles (EAs) of PDs were varied so that normal vectors would point in different directions. Thus, highly uncorrelated channel matrix was obtained for PR. However, in [5], the

EAs for the PDs were assumed the same, resulting in a fixed EA MIMO-VLC system.

However, certain aspects regarding ADR were not addressed in the literature. This thesis is designed to explain and discuss those aspects in detail and provide convincing conclusions regarding the performance of an indoor MIMO-VLC system for ADRs. One of the aspects that this thesis is going to address is the independent variation of EA for all the PDs and its effects on the VLC system's capacity and BER performance for indoor MIMO-VLC systems. In a similar manner, different factors and their impact on the performance of multiple considered MIMO-VLC systems are also explored in this thesis. These factors include the Field-of-View (FOV) angle, LED transmitter array length, and horizontal orientation of the receiver. The proposed methodologies and obtained results will provide very important insight regarding the performance of indoor MIMO-VLC systems. This will help us to understand the role of different factors in the performance of indoor MIMO-VLC systems.

The thesis is organized as follows: In Chapter-1, the background and development of VLC technology along with the motivation behind this thesis is provided. In Chapter-2, the basic characteristics of optical transceiver along with noise characteristics are provided. Different types of link topologies and propagation models adopted in VLC systems are also elaborated. Chapter-3 provides a detailed description of the system model. Different types of receivers and transmission mechanisms adopted in this thesis are also explained in this chapter. In Chapter-4, the performance of different considered MIMO-VLC systems is elaborated and compared. This chapter provides insight into different factors and their effect on the performance of the MIMO-VLC systems. Chapter-5 concludes this thesis and provides future directions.

1. BACKGROUND AND MOTIVATION

Several campaigns have been launched over the past few years to reduce the emission of carbon dioxide (CO_2). The CO_2 emission has caused a rise in the earth's temperature. A prominent example of such initiatives is the Paris Agreement in 2015. In this agreement, 196 nations came together and set a goal of limiting the global mean increase of temperature below 2° Celsius. As a result, carbon emission can be reduced by 60% by 2050 [6]. In the same way, the European Commission (EC) has also planned to reduce CO_2 emission by 40% by 2030. As the number of internet-connected devices increases, so does the volume of data traffic increasing the carbon footprint of mobile networks. Global Greenhouse Gas (GGHG) emission data shows that electricity production is the leading contributor to GGHG i.e. 29% of which 8% originates from computers, network equipment, data centers, and other Information and Communication Technologies (ICT) devices excluding smartphones. Similarly, it has been shown that mobile devices production, Radio Access Networks' (RANs) operation, and the operation of data center and data transport accounts for 30%, 29% and 19% of the total carbon footprint of mobile communications, respectively [7].

Artificial lighting constitutes one of the major sources of electricity consumption, estimated to be 19% of total electricity usage. This poses the challenge of making the light sources more energy-efficient. The benefits of using LEDs based lighting are twofold i.e. being more energy efficient and reduction in carbon footprint. In [6], it has been shown that fluorescent light and LED technologies can reduce the life-cycle of GGHG emissions by 60-85% as compared to incandescent lights. Over the past few years, Solid State Lighting (SSL) sources such as white LEDs (WLEDs) have started to replace traditional sources of lighting e.g. fluorescent light sources. It has been predicted that the LED lighting market scale will reach US$ 98.5 billion by 2023 from US$ 69.7 billion in 2017. Similarly, LED lighting market penetration will reach 63% in 2022 from 22% in 2017. With the technical advancements and mass production of LEDs in markets, prices have become more reasonable over the years. An LED lamp can be

bought at a cost of US$ 3-5. Similar price trends are also observed in Europe and North America [8, 9]. According to [6], by 2050, 90% penetration of LED lighting, along with the expected future advances in LED efficiency, would result in the reduction of the total amount of energy consumed for lighting. The LEDs based lighting technology will revolutionize the lighting techniques and replace the traditional means of illumination globally in the near future.

1.1. Visible Light Communication (VLC)

Optical Wireless Communication (OWC) is a form of optical communication that utilizes visible, IR, or Ultraviolet (UV) light for communication. In VLC, the visible part of the spectrum in the range around 390 nm to 750 nm as shown in Figure 1.1 adopted from [10], is exploited for communication between an LED-based transmitter and a PD-based receiver. Air acts as a medium between source and destination. Such a network is also called Light Fidelity (Li-Fi). In VLC, we have around 400 THz of optical bandwidth, however, the electrical bandwidth is limited to several MHz due to the limitations of the electrical technology [11]. Some of the key attributes of VLC are:

1. Low design complexity transceivers,
2. Energy efficient,

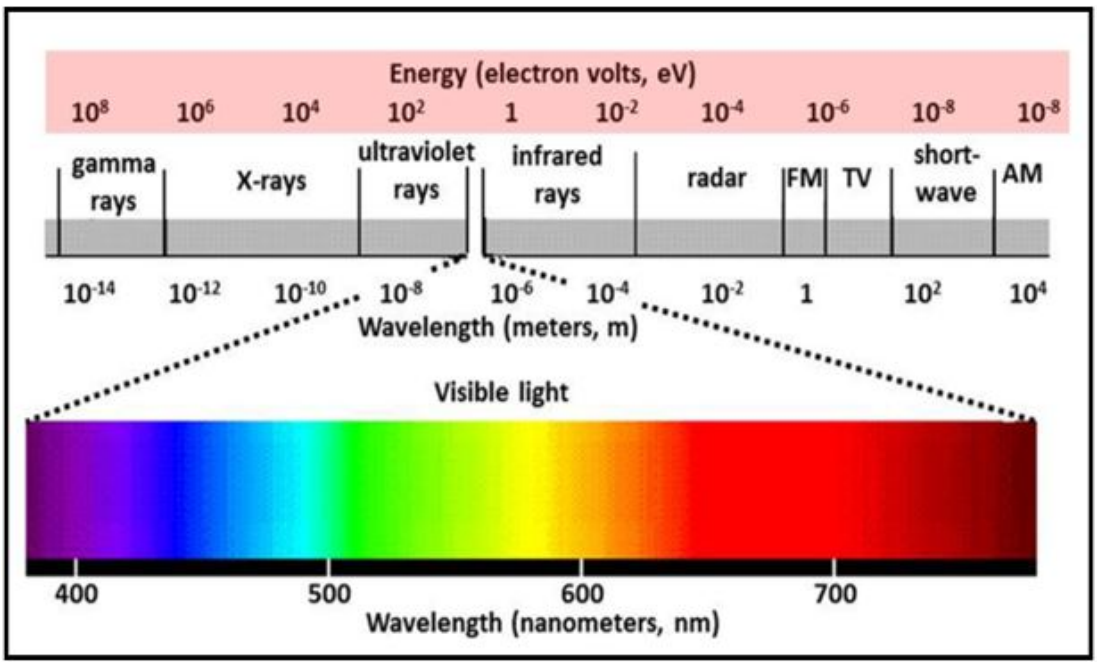

Figure 1.1. Electromagnetic spectrum with classification of communication bands

3. More economical,
4. Greater life expectancy (as LEDs are employed),
5. No electromagnetic interference to RF or electric-based equipment.

The purpose of simultaneous illumination and wireless communication can be realized by building light transceivers in LED light fixtures. In recent years, research has been conducted on multiple wireless and wired systems for backbone technologies of VLC. Some of the backbone technologies for VLC network architecture include [12–15]:

1. Broadband PLC (IEEE 1901, ITU-T G.9960/61),
2. 60 GHz Millimeter (mm) wave,
3. Low-cost Plastic Optical Fibre (POF)-based backbone technology.

As a result of these backbone technologies, the range of the VLC network can be extended throughout the building instead of just a single room.

1.1.1. Development history of VLC standards

The first VLC system based on LED technology was demonstrated by the researchers in the year 1999 [16]. After the first system was successfully demonstrated, VLC became a topic of interest from all the researchers around the globe. Researchers started to investigate possible applications, range of transmissions, data rates, and mobility levels of VLC. The researchers from Japan were the leaders in manufacturing blue LEDs and they established the first Visible Light Communications Consortium (VLCC) in 2003. This consortium brought together researchers from industry and academia to conduct further research in this green technology. By 2007, VLCC proposed a further two standards i.e. VLC system standard and Visible Light ID System (VL-ID) standard [17]. The Japan Electronics and Information Technology Industries Association (JEITA) later accepted these standards as CP-1221 and CP-1222, respectively. The VL-ID system can be used for the applications of location-based services and digital signage. In 2013, CP-1223 was introduced as a VLC beacon system. These systems have a very low data rate i.e. up-to 4.8 kbps [18].

To further enhance the research activities and expand the commercialization of VLC, the Institute of Electrical and Electronics Engineers (IEEE) standardized VLC and

published as IEEE 802.15.7. This standard is defined for both the physical and Media Access Control (MAC) layer for short-range OWCs. The modulation techniques of On-Off Shift Keying (OOK), Variable Pulse Position Modulation (VPPM), and Color Shift Keying (CSK) are proposed in this standard. The maximum data rate that can be achieved for indoor communication can be up to 96 Mb/s according to the standard [19]. However, data rates can be significantly improved by the applications of MIMO systems and different modulation schemes. In May 2014, the Visible Light Communication Association (VLCA) replaced VLCC to further expand the research, plan the development process, and standardized the advanced VLC systems [17, 20].

1.1.2. VLC applications

With the advent of the IoT, the seamless network connectivity for billions of users comprising people and machines is one of the biggest challenges of time. The requirement of different IoT based applications is very diverse from one another. Some applications require very high data rates whereas some require ultra-reliable and secure communication. VLC technology can accommodate the requirements of those applications as VLC can offer high data rates and secure communication. Not to mention the ease of availability (as LEDs have already been employed for illumination purposes), thus making VLC an ultimate choice for future wireless applications.

One of the many applications of VLC is in the Intelligent Transport System (ITS). Most of the accidents occur due to slow response or inability to make the right decision at the right time of the driver. Approximately 1.2 million people die and 50 million people are injured as a result of road accidents every year [21, 22]. To ensure the safety of drivers and others, Vehicle to Vehicle (V2V) and Infrastructure to Vehicle (I2V) are proposed under the ITS domain. As ITS require robust and secure communication between vehicles and infrastructures, VLC is an ideal candidate to replace or complement the existing congested RF-based ITS systems [23, 24]. Further, a heterogeneous network consisting of VLC and RF-based communication schemes could present a more reliable system for Vehicular Communications (VC).

VLC can also be used in smart cities in which the government, people, infrastructure, and economy are seamlessly connected. VLC can provide us with reliable and high

data rate links to connect all the enablers. Already employed lighting technology in the shape of street lights, billboards, and park lights can be used for high speed and energy-efficient network connectivity for applications like utility services. It will help us free the congested RF spectrum for other applications. Similarly, street lights and other lighting infrastructures can be used as hot-spots for high data rate connectivity of users [25].

Another application of VLC can be in advertisement billboards. Those large advertisement billboards could be made of hundreds of high-intensity LEDs and can serve as a hotspot to provide outdoor high-speed network connectivity for users. The nanometer wavelength of VLC cannot penetrate objects, rendering it safe to be used in environments like hospitals where we want to minimize the health risks associated with RF radiations. VLC can be used for monitoring patients, M2M communications, and all other networking applications.

1.2. Motivation

After the first successful representation of the VLC system in 1999, researchers have directed their efforts in improving the performance of the VLC systems. Different techniques including equalization, pre-equalization, post-equalization, OFDM, and O-MIMO have been explored by researchers in the literature. MIMO techniques have been used extensively in indoor environments as it offers system performance improvement without any surplus bandwidth extension. In an indoor MIMO-VLC system, Line of Sight (LoS) component is usually present between an LED-based transmitter and a PD-based receiver. No fading components are present in an indoor environment results in making the channel entries highly correlated. As a result, a rank deficient channel matrix is obtained. The performance of an indoor MIMO-VLC system highly depends on the rank of the channel matrix.

Different approaches have been adopted by the researchers to avoid rank deficient channel matrices for indoor MIMO-VLC systems. One of the approaches is to use a specifically designed receiver i.e. ADR to avoid rank deficient channel matrices. In such a receiver, uncorrelated channel matrix is obtained by placing PDs in such a way

that normal vectors of PDs point in different directions [4]. A similar approach was adopted in [5], where a special receiver based on the principles of ADRs called PR was explored by the authors. In PR, every PD was assigned with a fixed EA. As a result of the positions of the PDs, the respective normal vectors would be different from one another. Such an arrangement results in an uncorrelated channel matrix.

In this dissertation, a modified PR model is proposed. In the modified model, the PDs are allowed to have different independent EAs as compared to fixed EAs. We investigate the effects of the independent EAs on the rank of the channel matrices and the resulting performance of the different indoor MIMO-VLC schemes. In a similar way, the performance of different considered MIMO-VLC systems is determined for different FOV angles. Similarly, the role of LED transmitter array length and the horizontal orientation of the receiver in the performance of MIMO-VLC systems is also investigated. This gives us an insight into the role of the different factors on the performance of the MIMO-VLC systems. A comparison is provided in terms of throughput and BER for fixed and variable EA systems for different considered MIMO-VLC systems.

1.3. Literature Review

The Bells Photophone, developed in 1880, became the foundation of the first OWC system and resulted in the discovery of the fiber optic communication system. The first fiber optic communication system was developed in 1975 and it could achieve the data rate of 45 Mbps [26]. VLC is a form of OWC in which no guided media such as a fiber optic cable is used. It is a wireless communication that uses air as a medium suitable for distances up to 2-3 meters. The VLC systems mostly employ WLED-based transmitters whose modulation bandwidth is very limited. As a result, the performance of the VLC systems is not very efficient. Therefore, many researchers have conducted their research on improving the VLC system performance and presented different methodologies for improving the performance.

In [27], a simple equalization method is explored, improving the performance of the VLC system. It has been shown that the data rate is nearly doubled when an equalizer

is used as compared to an unequalized channel. A maximum data rate of 32 Mbps is achieved with Non-Return Zero-On-Off Keying (NRZ-OOK) for a BER of 10^{-6}. Similarly, the performance of the VLC system can be improved by the application of the pre-equalization technique. In [28], researchers have achieved a data rate of 80 Mbps by applying this technique to expand the modulation bandwidth.

In [29], the authors reported a data rate of 513 Mbps Point-to-Point (P2P) VLC link with the application of Discrete Multitone (DMT) modulation. The same group continued their efforts to improve the performance of a VLC system and achieved a data rate of 803 Mbps for Red-Green-Blue-LEDs (RGB-LEDs). Wavelength Division Multiplexing (WDM) along with DTM was considered by the authors [30]. Similarly in [31], high data rates of 1 Gbps and 2.1 Gbps at usual illumination level were reported for single-channel and WDM based transmission respectively. Similarly, the FOV angle is also a very important factor in determining the performance and coverage of a MIMO-VLC system. With the application of a wide FOV angle, a data rate of up to 100 Gbps has been recorded in [32]. For indoor communications, the challenge of complete coverage can be tackled by employing wide FOV communication systems.

In a similar way, to improve the optical efficiency of the MIMO-VLC system, different methods have been proposed in the literature [33–35]. In [33], OFDM has been shown a suitable scheme for VLC for achieving high data rates because of combating Inter-Symbol Interference (ISI) and utilizing spectrum more efficiently. As traditional OFDM results in polar (complex) and both positive and negative valued signals, however, in VLC the signal must be real and positive all the time as negative signals cannot be modulated using Intensity Modulation Direct Detection (IM/DD) technique. Due to this limitation, in [34] three different types of Optical-OFDM (O-OFDM) techniques named Asymmetrically Clipped Optical OFDM (ACO-OFDM), DC biased Optical OFDM (DCO-OFDM) and Asymmetrically Clipped DC biased Optical OFDM (ADO-OFDM) specifically designed for IM/DD systems are compared and analyzed. To improve the performance of the MIMO-VLC system, channel correlation must be reduced. Power imbalance and pre-coding techniques have been explored by the researchers to reduce channel correlation. In [36], the effect of the power imbalance between transmitters and link blockage on channel correlation has been explored.

Similarly, the channel correlation can also be minimized by employing aperture-based receivers. In [3], the authors have shown that by the application of aperture based receivers, the channel correlation can be reduced resulting in a well condition channel matrix. Similarly, the MIMO channel correlation can also be reduced by changing the physical orientation of the receiver, or the angles of the PDs in the receiver. The authors, in [4, 5], have shown that by the application ADRs, the resulting channel matrix entries can be made highly uncorrelated. An uncorrelated MIMO-VLC system results in better performance.

1.4. Scope of the Thesis

The main objective of this thesis is to investigate the effect of EA along with different factors including the FOV angle, LED transmitter array length and horizontal orientation of receiver, on the performance of multiple considered indoor MIMO-VLC ADR based systems. Capacity and BER are the chief performance metrics considered in this thesis. In this respect, we consider three different VLC systems i.e. four transmitters and four receivers (4×4), four transmitters and five receivers (4×5), and five transmitters and five receivers (5×5) MIMO schemes and evaluate system performance for each system. The 4×4 MIMO-VLC system serves as a benchmark for performance comparison and provides an insight on how the performance of different considered MIMO-VLC systems changes when a PD or LED is added to the MIMO-VLC system. Some of the key features of the thesis are mentioned:

1. Capacity across the entire indoor available area has been evaluated and the optimum receiver position resulting in maximum capacity (C_{max}) has been calculated,
2. A new approach of independent variation of EA has been introduced. In this method, the PDs are allowed to have different EAs from one another,
3. Performance comparison between fixed and variable EA systems has been recorded in terms of capacity and BER,
4. The effect of FOV angle, LED transmitter array length and horizontal orientation of receiver on the performance has also been demonstrated and evaluated.

2. VLC SYSTEM AND CHANNEL CHARACTERISTICS

This chapter is intended to introduce the basic building blocks of a VLC system along with the channel characteristics, different types of noise, and interference present in a VLC system. According to [6], with around 90% saturation in the worldwide market by 2050 would make the LED lighting the most common source of illumination. In OWC, many SSL sources can serve the purpose of transmitters and receivers. Incoherent WLEDs and coherent Laser Diodes (LDs) are the most commonly employed sources in the VLC system whereas Positive Intrinsic Negative (PIN) diode and Avalanche Photodiode (APD) are among the most commonly employed receivers. The generation of white light with LEDs along with some basic properties of LEDs is elaborated in this chapter. Different types of link topologies that can be faced in a VLC environment is also a part of this chapter. The various types of noise and interference encountered in a VLC system along with its impact on the performance of the system is also mentioned in this chapter.

2.1. Transmitter Sources in VLC

The conventional sources of light such as incandescent and fluorescent light bulbs can be used as transmitter sources in VLC. However, SSL devices e.g. LEDs, Organic-LEDs (O-LEDs), and LDs are preferred to be used in VLC because they can be flickered at a much greater rate as compared to other conventional light sources. This makes SSL sources ideal for the scenarios at which a high data rate is desired. Some of the key attributes of the light sources adopted for communication are mentioned below:

1. High bandwidth and appropriate wavelength,
2. Fast response time,
3. Energy-efficient, cost-effective and a long lifetime,
4. Linear power-current characteristics,
5. Direct modulation ability by varying the driving current.

The LEDs and LDs are fabricated in such a fashion that the light emitted from them covers the IR and visible part of the EM spectrum [37]. LEDs and LDs have the properties of small size, stability, lower forward voltage, and drive current, ability to transmit light at a single particular wavelength, and secure data transmission. Moreover, the power supplied by both devices is of equal magnitude (10-50 mW) [38]. For applications in which very high throughput and optical power are required, LDs are preferred over LEDs. Data rates of the order Gbps can be achieved by the application of high power LDs. However, high power LDs have some associated risks for human eye safety and care must be taken while employing LDs in an indoor environment. Moreover, LDs are not considered very suitable for the purpose of illumination, thus rendering LDs not desirable in an indoor environment. The choice of whether using an LED or LD as a transmitter depends upon the application at hand and its salient features including beam profile, optical power, and current properties and switching speed. A comparison between some of the basic LED and LD characteristics is provided in Table 2.1.

2.1.1. White light generation with LEDs

Every color in the visible spectrum can be produced with LEDs, however, white light, in the 480-750 nm range of the visible spectrum, is the most commonly used for the purpose of illumination. At the same time, WLEDs are the most commonly employed sources i.e., transmitters in VLC systems as white light provides higher energy efficiency (up to 85%) and a higher switching rate as compared to other sources, which is a well-desired trait in VLC systems. White light discharge from an LED can be obtained by the combination of phosphorous with blue/UV LEDs or by the application of a mixture of multi-color LEDs. There are generally two methods that can be adapted to manufacture WLEDs. Different types of WLEDs are available among which some are mentioned below:

1. UV-based WLEDs: In this method, a UV LED is precoated with red/blue/green phosphors to emit white light [39, 40].

Table 2.1. Basic characteristics of LEDs and LDs

Characteristics	**LED**	**LD**
Optical output power	Low Power	High Power
Optical spectral width	From 25 to 100 nm	From 0.01 to 5 nm
Electrical-Optical conversion efficiency	From 10% to 20%	From 30% to 70%
Modulation bandwidth	From tens of KHz to hundreds of MHz	From tens of KHz to tens of GHz
Human eye safety	Considered safe for the human eye	Must be made safe for the human eye
Reliability	High	Moderate
Cost	Low	Moderate to high
Directionality	Beam is broader and dispersal	Highly directional with low beam divergence
Noise	No noise present	Relative light intensity noise present

2. White Phosphors LEDs: In this method, the phosphor is incorporated in the body of a blue LED. As a result, some of the blue light-emitting from LED is converted into yellow light. White light is emitted from the LED when the remaining blue light diffuses with yellow light [39–41].
3. RGB-LEDs: In this method, light from a mixture of LEDs is mixed to emit white light from the LED. Here red, green and blue lights are mixed together to emit white light from the LED. RGB-LEDs consist of multiple emitters and combining optics enclosed in a single package [42].

It can be seen that white phosphors LEDs (WPLEDs) are a simpler choice but RGB-LEDs can result in performance enhancement with the potential of WDM. It can provide higher data rates utilizing the individual bandwidths of RGB-LED components. However, as individual LEDs are switched on at arbitrary intervals, it makes the process of providing white color balance a more challenging task [37].

2.1.2. Basic properties of an LED

In this section, some of the basic properties of an LED will be discussed.

2.1.2.1. Luminous intensity and efficiency

Luminous intensity is often used to describe the brightness of an LED whereas luminous efficiency describes an LED's radiation pattern in the visible spectrum. Luminous intensity is mathematically calculated by taking a derivative of luminous flux (Φ_{flux}) with respect to spatial angle (Ω_{sp}) i.e., d / d Ω_{sp} (Φ_{flux}). Luminous flux is defined as the total emitted flux weighted or scaled appropriately to reflect the varying sensitivity of the human eye to different wavelengths of light and can calculated from energy flux Φ_{e-flux} as:

$$\Phi_{flux} = L_{max} \int V(\lambda)\ \Phi_{e-flux}(\lambda)\ d\lambda, \tag{2.1}$$

where $V(\lambda)$ and L_{max} are relative eye sensitivity and maximum visibility, respectively. The value of L_{max} is calculated to be 683 lm/W at a wavelength (λ) of 555 nm. The transmitted total optical power can be calculated by integrating Φ_{e-flux} in all the possible directions and is given as [37]:

$$P_{tot-op} = L_{max} \int_{Amin}^{Amax} \int_{0}^{2\pi} \Phi_{e-flux}(\lambda)\ d\theta\ d\lambda, \tag{2.2}$$

where the values of A_{min} and A_{max} can be determined from the photodiode sensitivity curve. Hence, the Equation (2.1) can also be represented as:

$$\Phi_{flux} = L_{max} \int V(\lambda)\ P_{tot-op}(\lambda)\ d\lambda. \tag{2.3}$$

Luminous efficiency is defined as the ratio of luminous flux to the applied input electrical power and is given by [37]:

$$\eta_{lu} = \frac{\Phi_{flux}}{P_{elec}} = \frac{L_{max} \int V(\lambda)\ \Phi_{e-flux}(\lambda)\ d\lambda}{IV}\ \text{lm/W}. \tag{2.4}$$

The radiation intensity at the receiving plane for an LED lighting with Lambertian radiation pattern is given by:

$$Int(\xi) = Int(0)\ \cos^{m}(\alpha), \tag{2.5}$$

where ξ and Int(0) are irradiance angle and luminous intensity center, respectively. Lambertian emission order is represented by m in Equation (2.5). A standard for full illumination with a mean level of 350 lux for home and office environments is set by international lighting standard organization [26].

2.1.2.2. Power efficiency

Power efficiency is simply the ratio of optical output power P_{op} to the electrical input power P_{elec} given by [37]:

$$\eta_{pow} = \frac{P_{op}}{P_{elec}} = \frac{N_{ext-ph} \times hf}{N_{ca} \times q \times V}, \tag{2.6}$$

where N_{ext-ph} represents number of photons emitted externally, $h = 6.626 \times 10^{-34}$ Js is the Planck's constant, f denotes frequency, N_{ca} represents number of carriers passing through the PN junction, $q = 1.69 \times 10^{-19}$ C is the charge on an electron, and V is the voltage.

2.2. Wireless Optical Receiver

In the VLC system, the PD is used to convert the light energy incident upon it and generate electrical current at its output. The generated electric current is proportional to the square of the received optical power and is given by:

$$I_p = \eta_{qe} \frac{qP_{recv-op}}{hf} (1 - e^{\gamma l}), \tag{2.7}$$

where γ is the absorption coefficient which depends on the PD's medium, $P_{recv-op}$ is the received optical power, and l is the length of PD's active region. The η_{qe} represents quantum efficiency which is defined as the number of electron-hole pair generated by a PD to the incident photons in a certain amount of time and can be represented as [43]:

$$\eta_{qe} = \frac{\text{Number of electrons out}}{\text{Input number of photons}}. \tag{2.8}$$

The photo-current I_p can also be represented as $I_p = RP_r$ where R is called responsivity of PD and is calculated as:

$$R = \frac{\lambda q \eta_{qe}}{hc} = \frac{\lambda}{1.24} \eta_{qe}, \tag{2.9}$$

where λ is the wavelength of the incident light on the PD. Several factors affect the performance of a PD or a VLC system as a whole. These factors are:

1. Large detection surface area of PDs,
2. High sensitivity and responsivity,
3. Low noise resulting in better Signal-to-Noise Ratio (SNR) performance,
4. Small size and fast response time,
5. High values of reliability and a lower cost.

Two types of PDs are most commonly used in VLC systems, meeting all the requirements mentioned above. They are:

- PIN PD,
- APD.

The APD provides an inherent current gain as a result of repeated electron ionization process which results in higher sensitivity of APD as compared to PIN PD. PIN PD has shown better results at high optical wavelengths whereas APD is preferred for shorter wavelengths.

2.2.1. Elements of an optical receiver

The receiver in most OWC determines the performance of the system rather than the transmitter. The receiver in a VLC system is composed of multiple components including a concentrator, an optical filter, a photodiode, and an amplifier as shown in Figure 2.1 adopted from [26]. VLC systems are prone to noise. Both the natural and artificial sources of light act as noise sources in a VLC environment. It is therefore of significant importance to employ both electrical and optical filters to remove the unwanted DC noise components in the recovered data. The scattered sunlight can be very easily removed by the application of an electrical filter [44]. The optical filters are employed to remove the noise components resulting from artificial lighting sources. The current generated by PDs is proportional to the amount of light incident on the PDs. This current is converted into the voltage by the application of a trans-impedance amplifier [37].

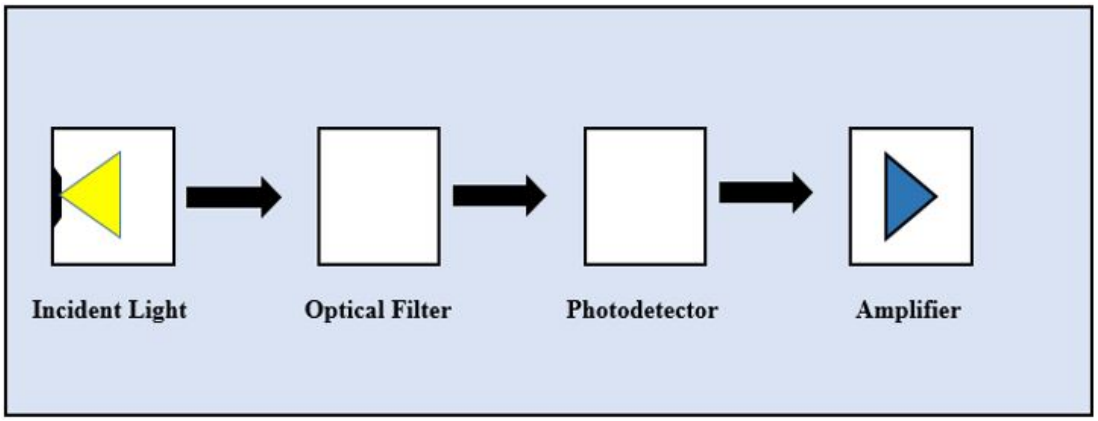

Figure 2.1. Components of an optical receiver

2.3. VLC Link Topologies and Characteristics

The optical path loss and multipath interference are the two most important factors that are associated with the performance of a link in a VLC system. It is very important to understand the characteristics of the link between a transmitter and a receiver in a VLC system so that an efficient VLC system can be designed and implemented. Numerous considerations must be take into account while designing a high-speed VLC link as OWC is a very challenging medium. In an indoor scenario, the light may reflect off many surfaces including ceiling, furniture, and walls but will not penetrate through opaque objects. In an outdoor environment, light is dispersed and absorbed as a result of atmospheric conditions. Links in a typical indoor VLC system can be classified into four types [37]:

1. Directed LoS (DLoS) link topology,
2. Non-directed LoS (NDLoS) link topology,
3. Diffused link topology,
4. Tracked link topology.

This classification is mainly based on the presence of a LoS link and degree of directionality between a transmitter and a receiver.

2.3.1. Directed LoS link topology

DLoS links are mostly employed for P2P communication in a VLC based indoor system. DLoS link does not suffer from multipath induced signal distortion. Similarly, ambient

sources of light have very little impact on the performance of the DLoS link when used in conjunction with a narrow FOV receiver [45]. Furthermore, DLoS links can provide very high data rates for links covering a distance from a few meters to kilometers [46]. However, there are some disadvantages associated with the DLoS links as well. As the coverage provided by a single link is very small, it gives rise to the problem of coverage for mobile users. In DLoS links, the transmitter and receiver must remain in close alignment and thus it restricts free mobility of users.

2.3.2. Non-directed LoS link topology

This type is of link topology is considered most suitable for indoor applications, more specifically for point-to-multipoint broadcast applications. A wide beam transmitter along with a wide FOV receiver is commonly employed. In addition to the LoS link, multiple signal reflections resulting from the surfaces within a room are also present as shown in Figure 2.2 adopted from [37]. This results in achieving a greater coverage area. As observed in DLoS link topology, the NDLoS link does not require alignment

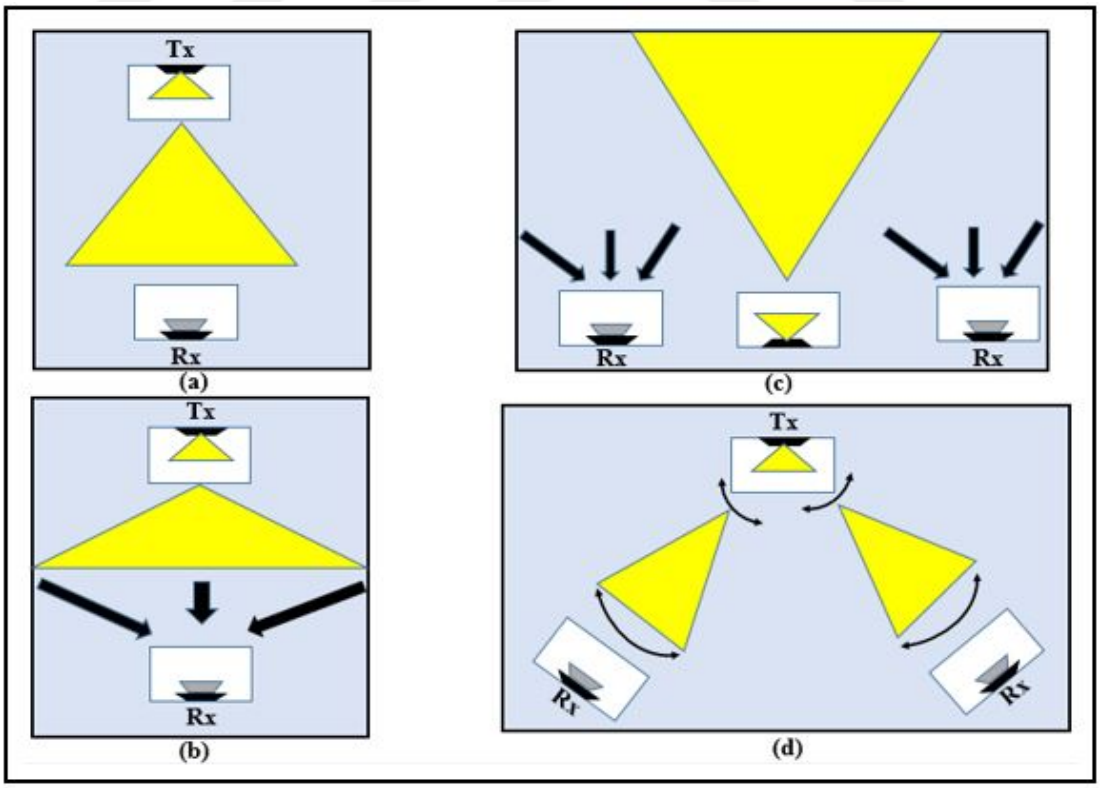

Figure 2.2. VLC link topologies a) DLoS Link b) NDLoS Link c) Diffuse Link d) Tracked Link

between transmitter-receiver pair, thus excellent mobility can be achieved with this type of topology. High-proportions of the transmitted signal are detected at the PD as a result of reflections from the surfaces of the objects within the room, thus overcoming the problem of blocking. However, the NDLoS links result in a high optical path loss. Similarly, as the PD receives the transmitted signal after reflections from the surfaces of objects within the room, it may result in inducing multi-path dispersion. However, for indoor applications, as the size of PD is comparatively bigger as compared to the wavelength of the light, ISI is produced [47, 48]. ISI results in limiting the data rate in a room to only several hundreds of Mbps.

2.3.3. Diffuse link topology

In this topology, a wide FOV transmitter emits visible light directly at the ceiling of the room, whereas a wide FOV receiver receives the reflected light from the ceiling [49, 50]. This link is also called a non-directed non-LoS link as there is no LoS component present in this type of topology. As no LoS path is required to be maintained between a transmitter and receiver, diffuse links are immune to shadowing and blockage and supports a greater mobility. However, diffuse links result in a high optical path loss i.e., about 50-70 dB for a meagre horizontal separation of 5 m between transmitter and receiver [51]. As the PD receives the reflections from the ceiling and objects within a room, the diffuse links can also suffer from multipath induced dispersion and ISI. As a result, the performance of diffuse link is further degraded and higher optical power values are required to maintain acceptable BER performance.

2.3.4. Tracked link topology

In this type of link topology, diffuse, and tracked directed links are used in conjunction to achieve high-speed communication links. The connectivity is achieved via the diffuse link whereas a tracked directed link is employed to achieve high data rates. High bandwidth is available as a result of employing a narrow beam transmitter and a narrow FOV receiver, reducing the number of multipath signals. Similarly, by pointing a directive receiver towards the transmitter as shown in Figure 2.2, the interference from the sun can also be reduced resulting in improved system performance.

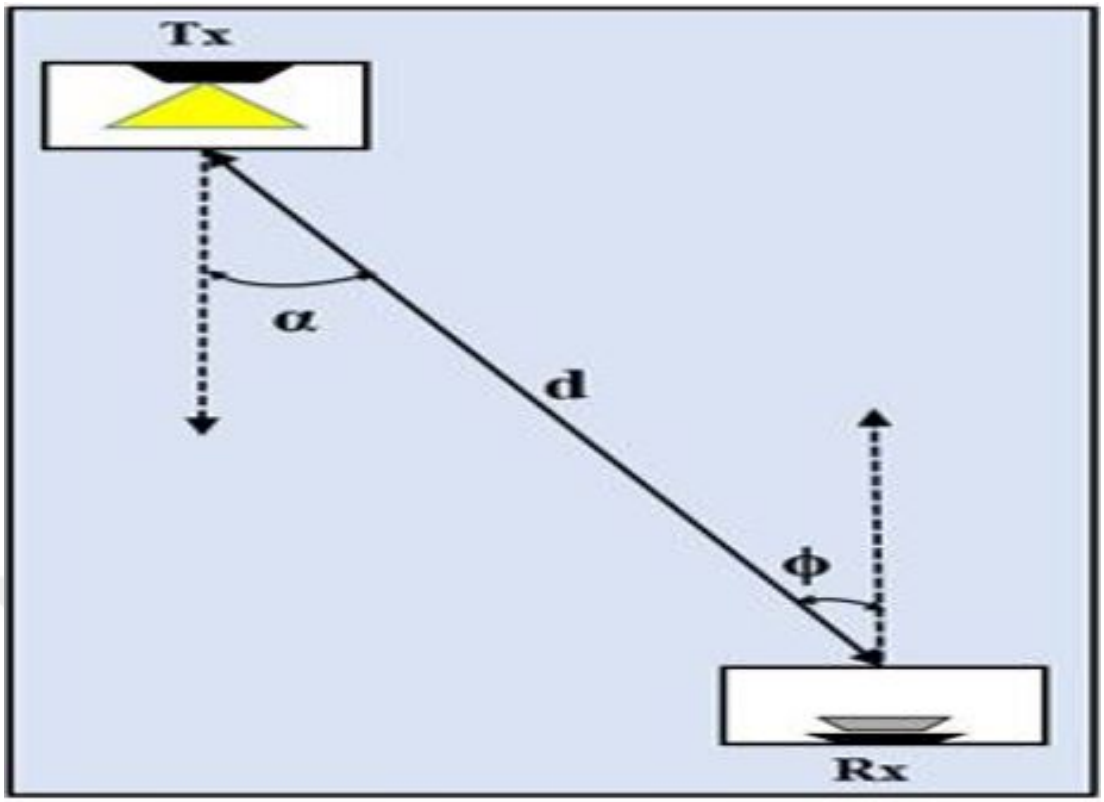

Figure 2.3. LoS propagation model between an LED and a PD

2.4. LoS Propagation Model

An indoor VLC system uses an LED/LD as a transmitter whereas PD is used as a receiver. The radiation intensity for the propagation model depicted in Figure 2.3 can be represented as:

$$Q(\alpha) = P_{trans} R_0(\alpha), \tag{2.10}$$

where P_{trans} and $R_0(\alpha)$ represent the transmitted power and Lambertian radiation intensity pattern, respectively. The Lambertian intensity pattern can be represented as:

$$R_0(\alpha) = \frac{(m_i + 1)}{2\pi} \cos^{m_i}(\alpha) \tag{2.11}$$

where m_i represents the Lambertian emission order expressing the directivity of the source beam and is given by:

$$m_i = -\frac{\ln(2)}{\ln(\cos \Omega_{1/2})}, \tag{2.12}$$

where $\Omega_{1/2}$ is the semi-angle of the LED calculated at half power. It can be clearly seen that $R_0(\alpha)$ is the combination of two angles:

1. The LED's half power semi-angle ($\Omega_{1/2}$),
2. The angle of incidence (α).

In a VLC system, the role of the PD is to collect all the incident light for all the angles ϕ that falls under the FOV angle. Therefore, the effective PD area is given as:

$$A_{\text{effective}}(\phi) = \begin{cases} A_{PD}\cos(\phi) & 0 \leq \phi \leq 90^\circ \\ 0 & \phi > 90^\circ, \end{cases} \tag{2.13}$$

where A_{PD} is the PD's area and $\phi \leq 90^\circ$ is the FOV. A larger PD area is more suitable for an indoor VLC system. However, a larger PD area also results in the following problems:

1. A reduction in receiver bandwidth because of the increased junction capacitance,
2. A significant increase in noise levels received at the receiver,
3. Increase in manufacturing and implementation costs.

The DC gain $H_{LoS}(0)$ for a LoS link for a receiver at a distance of d from the transmitter and with an incidence angle (α) can be calculated and given by:

$$H_{LoS}(0) = \begin{cases} \frac{A_{PD}\,(m_i+1)}{2\pi d^2}\cos^{m_i}(\alpha)\,T_s(\phi)\cos\phi, & 0 \leq \phi \leq 90^\circ \\ 0 & \text{elsewhere,} \end{cases} \tag{2.14}$$

where A_{PD} is the PD area, and $T_s(\phi)$ is the signal transmission of the optical filter. For the LoS link, the power received at the receiver is represented as:

$$P_{recv-LoS} = H_{LoS}(0)\,P_{trans}. \tag{2.15}$$

2.5. Non-LoS Propagation Model

For NDLoS and diffuse link topologies, the estimate of the received power at the receiver is more complex as compared to the LoS propagation model. The optical path loss in the NLoS propagation model depends on many variable factors. Some of the factors that play a vital role in optical path loss are listed below:

1. The dimensions of the room,

2. The reflectivity of the ceiling, room, and walls,
3. The presence of the objects in the room,
4. The respective position and orientation of the LED/LD and PD.

The received power has two components as shown in Figure 2.4, and is represented as:

$$P_{recv-NLoS} = \begin{matrix} \left(H_{LoS}(0) + H_{NLoS}(0)\right) P_{trans} = \ldots \\ \ldots \left(H_{LoS}(0) + \sum_{Reflect} H_{Reflect}(0)\right) P_{trans}, \end{matrix} \quad (2.16)$$

where $H_{Reflect}(0)$ represents the DC channel gain on reflection points.

The optical power associated with two or more reflections is very small in magnitude. Similarly, the arrival time of the signal undergoing two or more reflections is greater as compared to the signal undergoing only one reflection. Therefore, for the high-speed NLoS links, generally signals with only one reflection are considered. Thus the received power depends on the LoS link component and the first reflected NLoS component. The $H_{Reflect}(0)$ DC channel gain can be mathematically expressed as [26]:

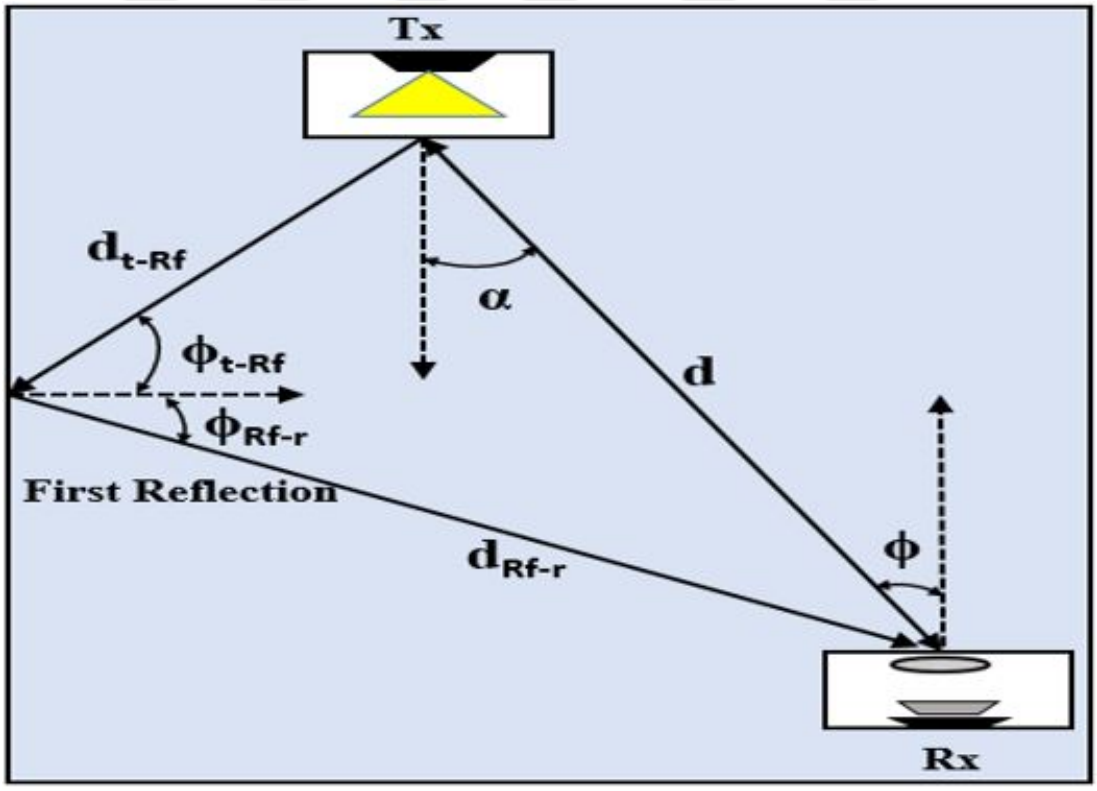

Figure 2.4. NLoS propagation model

$$H_{Reflect}(0) = \begin{cases} \frac{(m_i+1)\,\rho_{Rf}\,A_{PD}\triangle A}{2\pi d_{t-Rf}^2 d_{Rf-r}^2}\,\cos^{m_i}(\alpha)\,\cos(\phi_{t-Rf})\,... \\ ...\,\cos(\phi_{Rf-r})\,T_s(\phi)\,\cos(\phi), \quad 0 \leq \phi \leq 90^\circ \\ 0 \qquad\qquad\qquad\qquad\qquad\qquad \phi > 90^\circ. \end{cases} \tag{2.17}$$

In Equation (2.17), d_{t-Rf} represents the distance from the transmitter to the reflective point whereas d_{Rf-r} is the distance from the reflective point to the receiver. Similarly, ϕ_{t-Rf} is the angle of incidence to the reflecting point whereas ϕ_{Rf-r} is the irradiance angle to the receiver. The ρ_{Rf} represents the reflectivity factor whereas $\triangle$A is the small portion of the area considered as a reflecting point.

2.6. Noise in a VLC System

The performance of a VLC link highly depends on the types and level of noise present either in the optical link or in the receiver. Various types of noises including shot noise, photodetector dark current shot noise and excess noise, background radiation and relative intensity noise, and thermal noise can occur in a VLC system. However, in this thesis, we will only discuss shot and thermal noises as they are the most dominant sources of noise in a VLC system.

2.6.1. Shot noise

In VLC systems, the shot noise is the dominant noise as compared to the thermal noise. The shot noise arises in environments where ambient light is also present along with the transmitted signal. For a constant optical-power transmitter, the mean number of photons generated by the transmitter remains the same. However, the number of photons generated per second varies and follows a Poison distribution which results in the shot or quantum noise. The shot noise is normally present in all PDs because of the difference in the rate of arrival of photons from data transmitters and background radiation [37]. The shot noise is represented mathematically as [26]:

$$\sigma_{shot}^2 = 2\,qRP_n, \tag{2.18}$$

where q represents electron charge, R represents PD's responsivity and P_n denotes the average power of the ambient source of light.

2.6.2. Thermal noise

The thermal noise is present in all the receivers consisting of active and resistive elements. Electrons in a conducting material are in a constant state of motion and moves freely. They continuously collide with the atom or molecules of the substance. As a result of this random motion, thermal noise is produced. The thermal noise is labeled as white noise, as the Power Spectral Density (PSD) of thermal noise is frequency independent. However, the thermal noise depends on the temperature. The mathematical expression of thermal noise can be divided into two parts [26]. The first part describes the mathematical expression for feedback resistor ($R_{feedback}$) as given by:

$$\sigma^2_{th-R_{feedback}} = \frac{4k_B T_k}{R_{feedback}} I_2 R_b, \tag{2.19}$$

where T_k represents absolute temperature, $k_B = 1.3807 \times 10^{-23}$ J/K is the Boltzmann's constant and I_2 is the noise bandwidth factor. The second part shows the thermal noise expression from Field Effect Transistor (FET) channel resistance and is given by [26]:

$$\sigma^2_{th-FET} = \frac{16\pi^2 k_B T_k}{g_m} \Gamma (C_d + C_g)^2 I_3 R_B^3, \tag{2.20}$$

where Γ represents FET channel noise factor, g_m and C_g represents FET's trans-inductance and gate capacitance respectively. C_d is the capacitance of PD and whereas I_3 is the noise bandwidth factor with a value of 0.0868. The total thermal noise can be calculated by adding Equation (2.19) and Equation (2.20) i.e.,

$$\sigma^2_{th} = \sigma^2_{th-R_{feedback}} + \sigma^2_{th-FET}. \tag{2.21}$$

Similarly, the total noise in a VLC system can be calculated as a sum of shot noise and thermal noise and can be expressed as:

$$\sigma^2_{tot-noise} = \sigma^2_{shot} + \sigma^2_{th}. \tag{2.22}$$

2.7. Baseband Model and System Characteristics of an OWC System

An indoor OWC system does not suffer from multipath propagation, however, they are prone to ISI that can lead to affect the system's performance. The equivalent baseband model of an IM/DD modulated OWC system is shown in Figure 2.5 and can be mathematically represented as:

$$y(t) = Rs(t) \otimes h(t) + w(t). \tag{2.23}$$

In Equation (2.23), the $\otimes$ symbol represents convolution between the instantaneous optical power of signal $s(t)$ and baseband channel impulse response $h(t)$. Similarly, $w(t)$ is the signal independent link noise and R is the responsivity of the PD.

It is important to note that an OWC system is different from the traditional RF system. In an OWC system, the instantaneous optical power is directly proportional to the current generated at the PD, whereas, the instantaneous power represents the amplitude of the signal in the RF domain. As a result, there are certain constraints on the instantaneous optical power in an OWC system.

One of the constraints is that $s(t)$ should remain positive at all times i.e.,

$$P_{in-max} \geq s(t) \geq 0, \tag{2.24}$$

where P_{in-max} represents the maximum value of the transmitter's optical power. Similarly, the average power value of the $s(t)$ should not exceed the power threshold value P_{thresh} that ensures eye safety. This can be mathematically expressed as:

$$P_{thresh} = \lim_{T\to\infty} \frac{1}{2T} \int_{-T}^{T} s(t)\,dt \tag{2.25}$$

where P_{thresh} is the determined value of the maximum permissible power ensuring eye safety. In a similar manner, the SNR in traditional RF channels depends on the average

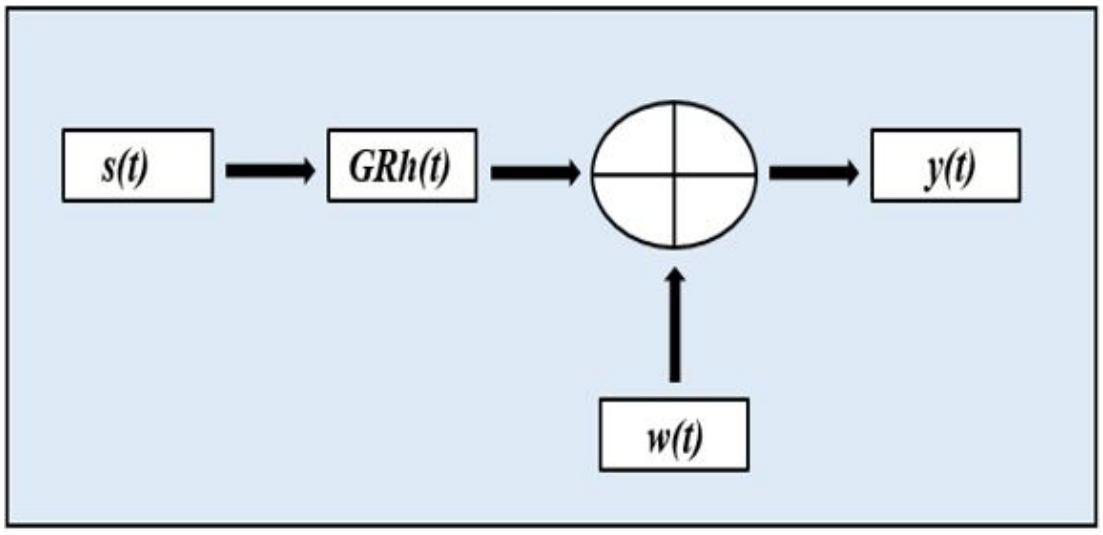

Figure 2.5. A baseband model of an OWC system

power received at the receiver i.e., $P_{RF-recv}$. However, in OWC, SNR is proportional to the square of the average received optical signal power i.e., $P_{op-recv}$. This can be expressed as:

$$SNR = \frac{R^2 H^2(0) P_{op-recv}^2}{R_b N_0}, \tag{2.26}$$

where N_0 and $H(0)$ represent the noise spectral density and DC channel gain whereas R_b represents the bit rate. The channel DC gain is given by:

$$H(0) = \int_{-\infty}^{\infty} h(t)\, dt. \tag{2.27}$$

3. SYSTEM MODEL FOR INDOOR MIMO-VLC SYSTEMS

This chapter provides the basic idea of the system model adopted in this dissertation. In this chapter, we discuss the basic properties of Non-ADRs (N-ADRs) and ADRs. This chapter also provides insight into the coordinate system adopted for different MIMO-VLC systems along with the adopted simulation parameters. Mathematical relationships for determining the capacity and BER performance of multiple MIMO-VLC systems are also a part of this chapter.

3.1. MIMO-VLC System

In indoor environments, multiple LEDs are normally used to achieve uniform illumination. These LEDs can be used to transmit data to a single or multiple receivers, thus, resulting in a Multiple-Input Single-Output (MISO) or a MIMO system. The usage of a MISO or a MIMO system results in decreasing the probability of a complete link blockage. It also helps in achieving the desired rate of mobility in an indoor environment. In a MIMO system, separate independent data streams can be sent from the LEDs resulting in high data speed and multiplexing gain as compared to the MISO system. The application of MIMO techniques along with its impact on the system performance has been investigated by many researchers for the RF domain. In the RF domain, the interference and scattering make the channel uncorrelated and independent, allowing MIMO systems to attain better performance. The MIMO techniques applied for the RF domain are of the same significance for optical communications and can be adopted to improve the performance of the VLC systems.

A typical M $\times$ N MIMO-VLC system model is shown in the Figure 3.1 [1]. In the system model, 4 LEDs are used to achieve simultaneous illumination and communication. The receiver is also composed of 4 PDs to receive the incident photons. The vertical and horizontal distance between the LEDs is represented by d_{tx}. In a similar manner, the distance between the PDs is represented by d_{rx}, which is much

[1] In Figure 3.1, the circles with cross sign within represent LEDs whereas simple circles represent PDs.

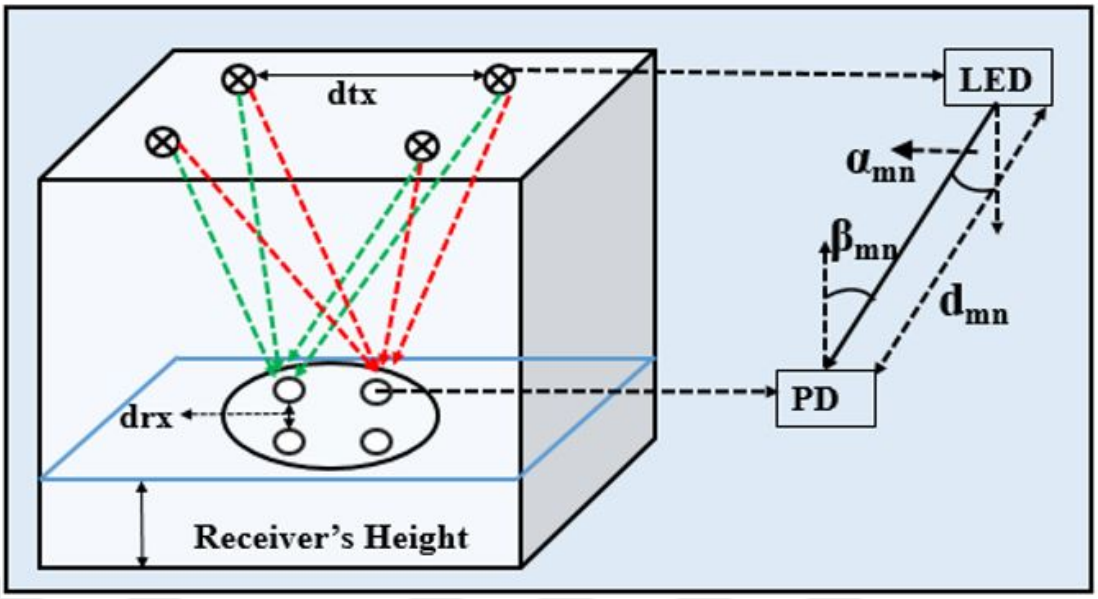

Figure 3.1. Indoor MIMO-VLC model

smaller as compared to d_{tx}. As the geometric orientation of the PDs in the receiver is different from one another, every PD receive a signal with different strength depending on its position and distance from the LEDs. The signal received at the receiver can be represented as:

$$\mathbf{y} = \mathbf{Hs} + \mathbf{w}, \tag{3.1}$$

where **s** represents the transmitted signal, **w** is the encountered Additive White Gaussian Noise (AWGN) noise signal whereas **y** is the received signal. The channel matrix **H** is of the order (N × M) and can be represented as:

$$\mathbf{H} = \begin{bmatrix} h_{11} & \dots & h_{1M} \\ . & . & . \\ . & . & . \\ . & . & . \\ h_{N1} & \dots & h_{NM} \end{bmatrix}. \tag{3.2}$$

The Equation (3.1) can be expanded and represented as:

$$\begin{bmatrix} y_1 \\ y_2 \\ . \\ . \\ y_N \end{bmatrix} = \begin{bmatrix} h_{11} & h_{12} & .. & .. & h_{1N} \\ h_{21} & h_{22} & .. & .. & h_{2N} \\ . & . & . & . & . \\ . & . & . & . & . \\ h_{M1} & h_{M2} & .. & .. & h_{MN} \end{bmatrix} \begin{bmatrix} x_1 \\ x_2 \\ . \\ . \\ x_M \end{bmatrix} + \begin{bmatrix} w_1 \\ w_2 \\ . \\ . \\ w_N \end{bmatrix}, \tag{3.3}$$

where the Channel State Information (CSI) i.e., h_{mn} between a n^{th} LED and m^{th} PD can be represented as:

$$h_{mn} = \begin{cases} \frac{A_{PD}\,(m_i+1)}{2\pi d_{mn}^2}\,\cos^{m_i}(\alpha_{mn})\,\cos(\beta_{mn}), & 0 \leq \beta_{mn} \leq \phi \\ 0 & \phi > \beta_{mn}, \end{cases} \tag{3.4}$$

where ϕ is the FOV angle, A_{PD} is the area of the PD, m_i is the Lambertian emission order and d_{mn} is the distance between the m receiver and n transmitter.

The j^{th} received signal can be expressed as:

$$r^{th} = RP_{trans} \sum_{l=1}^{1} h_{mn} \,.\, M_l + \sqrt{\overline{\sigma_{Nj}^2}}, \tag{3.5}$$

where R is the responsivity of the PD, P_{trans} is the average transmitted optical power and $\overline{\sigma_{Nj}^2}$ represents the mean-square noise current.

In literature, various equalizers for MIMO-VLC systems have been investigated by researchers. These algorithms include:

1. Zero forcing (ZF) equalizer,
2. Minimum mean square error (MMSE) equalizer,
3. Maximum likelihood (ML) equalizer,
4. Vertical bell labs layered space-time (V-BLAST) equalizer.

The ZF equalizer inverts the frequency response of the channel. The inverted frequency response is applied to the received signal vector to remove the channel effects. The ZF forces the ISI to be 0 in a noise-free case. However, the ZF algorithm also tends to amplify the noise greatly for the cases in which the channel matrix (**H**) has a small magnitude. To remove the channel effects, we need a matrix such that when combined with **H** will produce the identity matrix i.e., **PH=I**. For ZF, **P** can be mathematically expressed as [5]:

$$P = \left\{\mathbf{H}^H\mathbf{H}\right\}^{-1}\mathbf{H}^H, \tag{3.6}$$

where $\mathbf{H}^H$ represents Hermitian transpose of **H**. Similarly, an MMSE equalizer adopts the approach to minimize the Mean Square Error (MSE) which is an important aspect to determine the estimator quality. MMSE does not eliminate ISI components completely

like the ZF equalizer. However, MMSE minimizes the noise power and ISI components in the output. In order to do that, the MMSE approach tries to find a matrix **P** which minimizes the criterion,

$$\mathrm{E} = \left\{ \left[\mathbf{Py} - \mathbf{s}\right] \left[\mathbf{Py} - \mathbf{s}\right]^{\mathrm{H}} \right\}, \tag{3.7}$$

where **s** and **y** are transmitted and received signal vectors whereas **P** can be expressed as [37]:

$$\mathrm{P} = \left\{ \mathbf{H}^{\mathrm{H}}\mathbf{H} + \mathbf{wI} \right\}^{-1} \mathbf{H}^{\mathrm{H}}, \tag{3.8}$$

where **w** is the noise vector. When compared with Equation (3.6), the only difference is the **wI** term. For the cases in which no noise is present i.e., **w** = 0, the MMSE equalizer reduces to ZF equalizer. The computational complexity of these equalizers varies with ZF equalizer being the least computational complex and ML equalizer being the most complex. In [52], authors have observed that only a negligible gain can be achieved by adopting a more complex decoding algorithm for MIMO-VLC systems.

3.2. System Model

In this dissertation, we consider an indoor M × N MIMO-VLC system composed of M number of white LEDs and N number of PDs where M = {4, 5} and N = {4, 5}. The values of M and N are selected in such a way that M ≤ N. This gives us the possibility

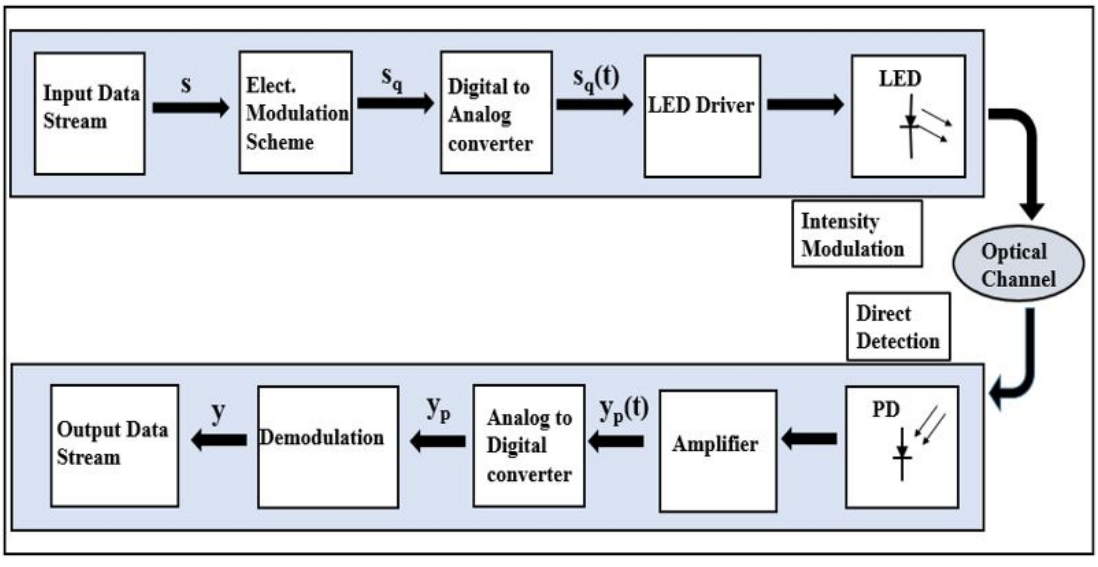

Figure 3.2. Block diagram of a VLC system

of having three different indoor MIMO-VLC systems i.e., 4×4, 4×5 and 5×5. IM/DD is employed as optical modulation and demodulation scheme respectively. Shot and thermal noises are modelled as AWGN and added at the receiver in the electrical domain. In our system model, we have only considered LoS signal components. The different stages of a VLC system are shown in Figure 3.2.

At first, the signal to transmit is modulated using unipolar K-PAM for its output being real and positive. The q_{th} modulated signal is represented as $\mathbf{s_q}\ \varepsilon\ [0, ..., (K-1)]$ where K is modulation size of the constellation alphabet. This modulated signal is grouped into a vector of length M which is denoted by $\mathbf{s} = [s_0, s_1, s_2, ..., s_{M-1}]^T$. The $\mathbf{s_q}$ signal is sent to Digital to Analog Converter (DAC) to form $\mathbf{s_q(t)}$ and is sent to the optical transmitter. In the optical transmitter, optical modulation i.e., IM is performed and data is sent to the optical receiver via the optical channel. The receiver is generally composed of the components given in Figure 2.1. The current generated at PD as a result of incident photons is sent to an amplifier. The amplified signal is sent to the Analog to Digital Converter (ADC) to generate $\mathbf{y_p}$ to form a receive vector of length N as $\mathbf{y} = [y_0, y_1, y_2, ..., y_{N-1}]^T$. The transmitted data is recovered by performing electrical demodulation on the received digital signal "$\mathbf{y}$".

The overall system can be represented similarly as given in Equation (3.1). In Equation (3.1), the $\mathbf{s}$ represents the message signal and is a column vector of the order $(M \times 1)$ where M is the number of LEDs. The $\mathbf{y}$ is the received signal whereas $\mathbf{w}$ is the noise signal encountered. Both $\mathbf{y}$ and $\mathbf{w}$ are column vectors of the order $(N \times 1)$ where N is the number of PDs. The noise vector i.e., $\mathbf{w} = [w_0, w_1, w_2, ..., w_{N-1}]^T$, indicates Independent Identically Distributed (i.i.d) samples of AWGN with $w_p \sim \mathcal{N}\ (0, N_0/2)$ where N_0 is the PSD of one sided noise power [37]. The sum of shot noise variance σ^2_{shot} and thermal noise variance $\sigma^2_{thermal}$ is equal to the total noise variance $\sigma^2_{tot-noise} = N_0/2$. The channel matrix $\mathbf{H}$ is of the order $(N \times M)$ as given in Equation (3.2). The entries of the channel matrix $\mathbf{H}$ for a specific LED i.e., n and PD i.e., m for both N-ADRs and ADRs can be given as:

$$h_{mn} = \frac{A_{PD}\ (m_i + 1)}{2\pi d^2_{mn}}\ \cos^{m_i}(\alpha_{mn})\ \cos^{k}(\beta_{mn})\ , \tag{3.9}$$

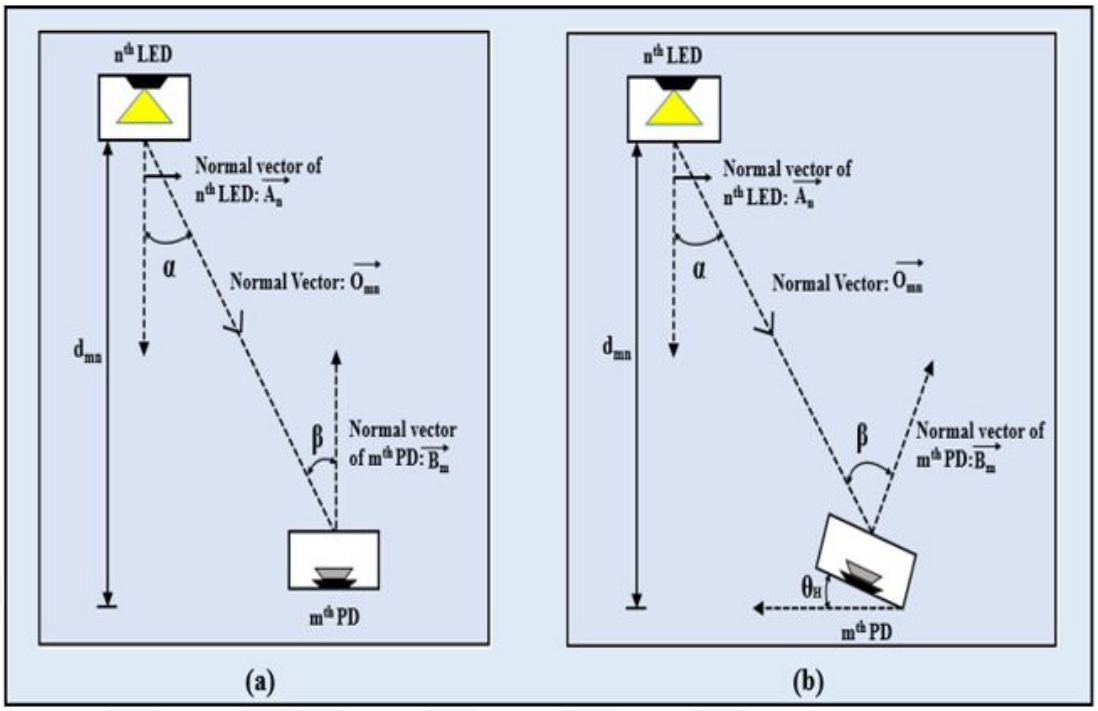

Figure 3.3. The geometry of transmitter-receiver pair: a) N-ADR b) ADR

where α_{mn} and β_{mn} must be within range of [–90°, 90°], otherwise $h_{mn} = 0$. In Equation (3.9), A_{PD} represents the active area of PD, α_{mn} is the irradiance angle at LED n with respect to PD m, β_{mn} is the incident angle at PD m with respect to LED n, d_{mn} is the distance between LED n and PD m, k represents the FOV coefficient, whereas m_i is the Lambertian emission order given by the Equation (2.12).

For a single particular link between an LED and a PD, we have three vectors of interest as shown in Figure 3.3. These vectors are:

1. $\overrightarrow{A_n}$ is the normal vector in the direction of irradiance from LED n,
2. $\overrightarrow{O_{mn}}$ is the vector from the LED n to the PD m,
3. $\overrightarrow{B_m}$ is the normal vector in the direction of incident light from the of the PD m.

By using these vectors α_{mn} and β_{mn} can be calculated as [5]:

$$\cos(\alpha_{mn}) = \frac{\overrightarrow{A_n} \cdot \overrightarrow{O_{mn}}}{\|\overrightarrow{A_n}\| \|\overrightarrow{O_{mn}}\|}, \tag{3.10}$$

$$\cos(\beta_{mn}) = \frac{\overrightarrow{O_{mn}} \cdot \overrightarrow{B_m}}{\|\overrightarrow{O_{mn}}\| \|\overrightarrow{B_m}\|}. \tag{3.11}$$

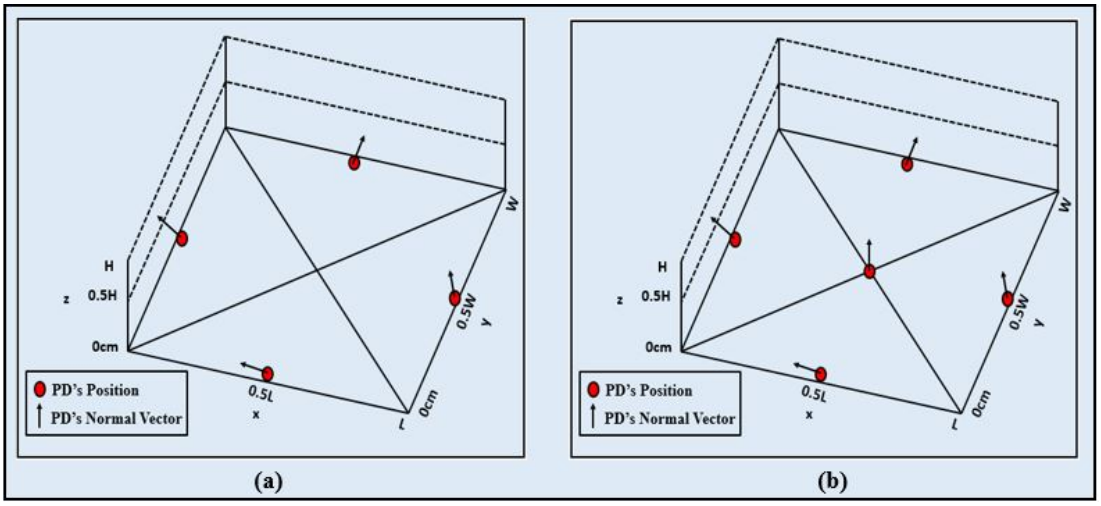

Figure 3.4. Normal vectors representation of PR for (a) 4×4 MIMO-VLC system (b) 4×5 & 5×5 MIMO-VLC system

In our system model, we have assumed that perfect CSI is present at the receiver i.e., CSI-R. Similarly, we have allocated the same power to each LED ensuring equal power allocation. The estimated received signal can be calculated by the application of the ML-MIMO detection technique at the receiver. The decoder selects a signal as received signal by comparing the received signal **y** with all the possible potential received signal vectors. A signal vector resulting in minimum Euclidean distance is selected as the actual received signal $\widehat{s}$. The process of ML decoding can be expressed mathematically as [36]:

$$\widehat{s} = \arg\max_{s} \rho_y\,(y \mid s, \mathbf{H}) = \arg\min_{s} \|y - \mathbf{H}s\|_F^2 . \tag{3.12}$$

In Equation (3.12), $\rho_y\,(y \mid s, \mathbf{H})$ represents the conditional probability density function whereas **H.** $\|.\|_F$ represents the Frobenius norm. The channel capacity of MIMO-VLC system assuming equal power allocation is given by [5]:

$$Cap = \sum_{i}^{R_H} \log_2 \left[1 + \frac{SNR_{elec}}{M} \lambda_i\right] \tag{3.13}$$

In Equation (3.13), λ_i represents i^{th} eigenvalue of ($\mathbf{H}^*\mathbf{H}$) whereas R_H represents the rank of MIMO channel matrix. The average electrical power per transmit antenna is given by $SNR_{elec} \triangleq P_{elec}/N_0$, whereas P_{elec} is the constraint on the transmit power.

3.3. Angular Diversity Receivers (ADRs)

In ADRs, the PDs are arranged in such a manner that the resulting normal vectors of the PDs would point in different directions. In this way, although very closely packed, different entries in the channel matrix are generated for the Angle Oriented Receiver (AOR) [4]. In this dissertation, we are considering a special ADR called PR. The PR got its name due to the fact that PDs on it are pointing in different directions just like the faces of a triangle except for its base. There are different ways in which this objective can be reached. One way is to arrange the PDs in the form of a pyramid with N-gon base for 4×4 MIMO-VLC system and (N-1)-gon for 4×5 and 5×5 MIMO-VLC systems as the N^{th} PD is located at the center of the receiver as shown in Figure 3.4. As the normal vectors from PDs depend on the EA of the PDs, there are generally two methods in which PDs can be arranged.

1. Fixed EA system: In this method, we assume that the EA of all the PDs, resulting in an optimum performance at different considered positions of the receiver, is the same for all the PDs. As a result, we have a single optimum EA for a considered position of the receiver [5]. As the position of the receiver varies, so does the optimum EA value depending on the distance between LEDs and PDs and the respective FOV angle.
2. Variable EA system: In this method, we assume that the EA of all the PDs resulting in optimum performance can be different from one another for the considered position of the receiver. As a result, we have a different optimum EAs for different PDs for a considered position of the receiver [11]. The EA values for PDs depends on the respective position of the receiver, along with the FOV angle.

3.3.1. The coordinate system for ADRs

The position and orientation of LEDs and PDs are specified by their respective normal vectors in [x, y, z, θ, ϕ] format. The originating position of a vector is represented by (x, y, z) in the Cartesian coordinate, θ represents the EA from the positive z-axis whereas ϕ represents the azimuth angle from the positive x-axis as shown in Figure 3.5. θ and ϕ should be in range [0, 180°) and [0, 360°) respectively.

The m^{th} PD placed at $\left(x_{PD}^{m}, y_{PD}^{m}, z_{PD}^{m}\right)$ has its normal vector $\vec{B}_m$ specified by $\left[x_{PD}^{m}, y_{PD}^{m}, z_{PD}^{m}, \theta_{PD}^{m}, \phi_{PD}^{m}\right]$ for $1 \leq m \leq N$ as shown in Figure 3.5. As for the 4×5 and 5×5 MIMO-VLC systems, the N^{th} PD is considered to be at the center of the receiver. Its normal vector is represented as $\left[x_{PD}^{N}, y_{PD}^{N}, z_{PD}^{N}, \theta_{PD}^{N}, \phi_{PD}^{N}\right] = \left(x_{PD}^{N}, y_{PD}^{N}, z_{PD}^{N}, 0, 0\right)$. For the remaining PDs i.e., $1 \leq m \leq (N-1)$, the normal vectors are represented in a similar fashion as that of 4×4 MIMO-VLC system.

In a similar manner for 4×4 and 4×5 MIMO systems, the LED placed at $\left(x_{LED}^{n}, y_{LED}^{n}, z_{LED}^{n}\right)$ has its normal vector $\vec{A}_n$ specified by $\left[x_{LED}^{n}, y_{LED}^{n}, z_{LED}^{n}, \theta_{LED}^{n}, \phi_{LED}^{n}\right]$ for $1 \leq n \leq M$ using the same coordinate system as depicted in Figure 3.5. For 5×5 MIMO-VLC system, the M^{th} LED is located at the center of the room. Its normal vector is represented as $\left[x_{LED}^{M}, y_{LED}^{M}, z_{LED}^{M}, \theta_{LED}^{M}, \phi_{LED}^{M}\right] = \left(x_{LED}^{M}, y_{LED}^{M}, z_{LED}^{M}, 0, 0\right)$. For the remaining LEDs i.e., $1 \leq n \leq (M-1)$, the normal vectors are represented in a similar fashion as that of 4×4 and 4×5 MIMO-VLC systems.

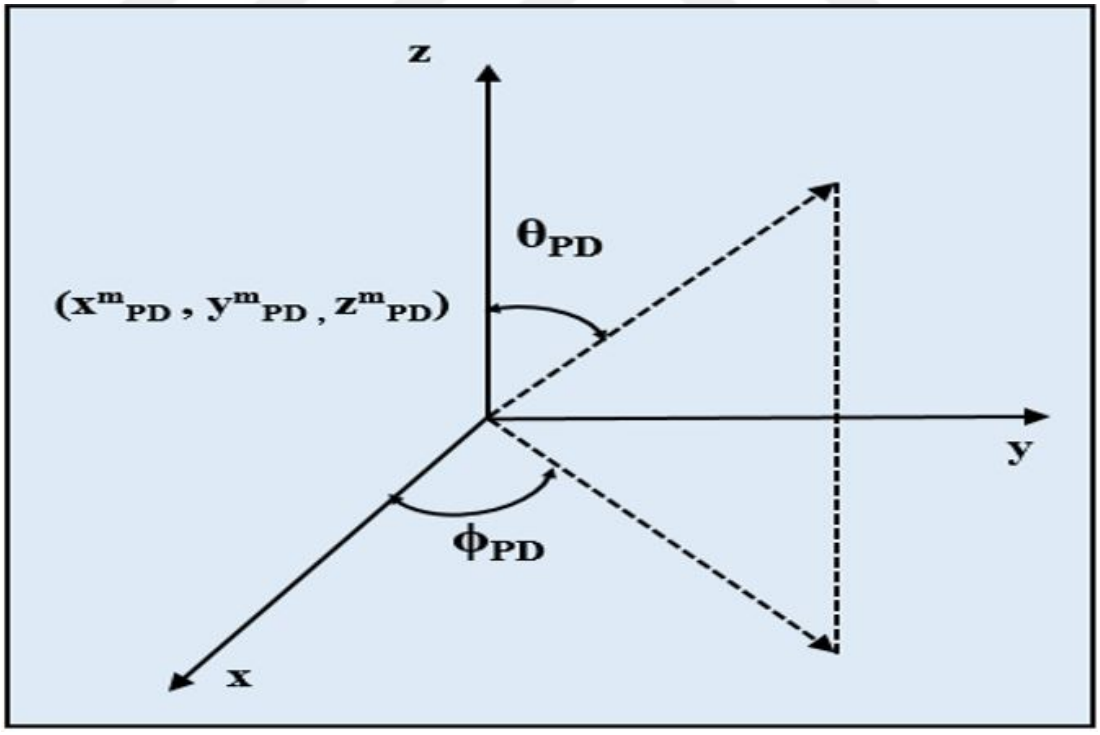

Figure 3.5. The coordinate system for PDs placement

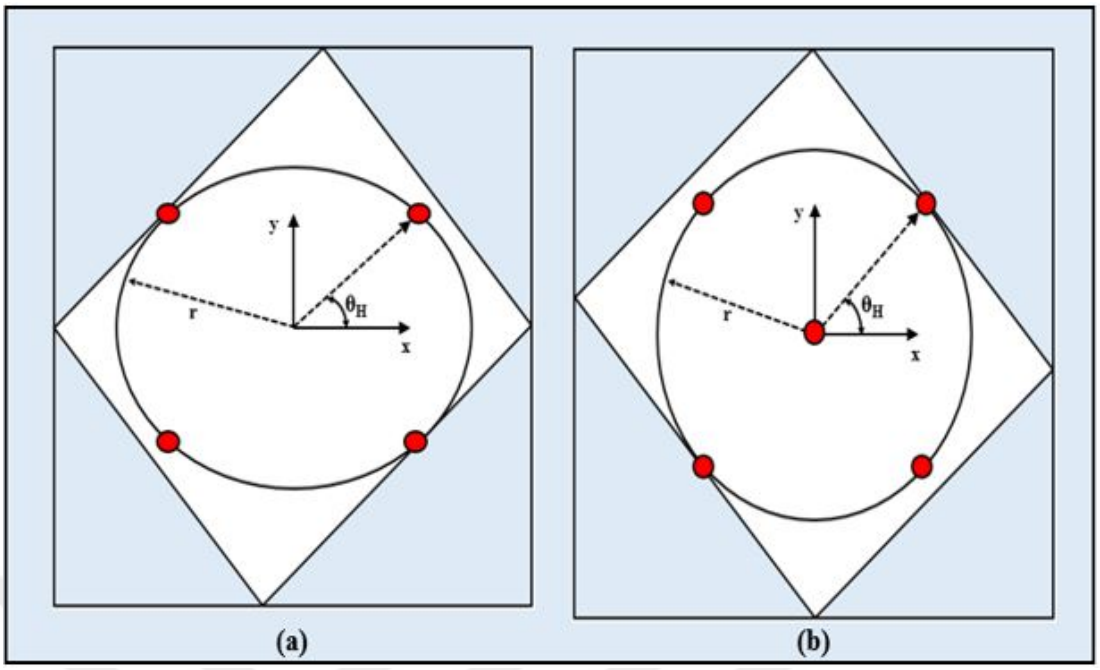

Figure 3.6. PD placement in PR for (a) Y= N (b) Y= (N-1), where Y denotes number of PDs

3.3.2. PDs placement in PR

The PDs are arranged uniformly in a circle of radius r for $1 \leq m \leq Y$ where $Y = \{N, N-1, N-1\}$ for 4×4, 4×5 and 5×5 MIMO-VLC systems, respectively. The coordinates for PDs are given by:

$$\left(x_{PD}^{m},\, y_{PD}^{m},\, z_{PD}^{m}\right) = \left(x_{PD} + \frac{r\cos 2(m-1)\pi}{Y},\, y_{PD} + \frac{r\sin 2(m-1)\pi}{Y},\, h_{PD}\right), \tag{3.14}$$

where $\left(x_{PD}, y_{PD}\right)$ represents the (x, y) coordinates of the center of PR and h_{PD} is the height of the receiver from the ground's surface [5]. As EAs of PDs can be same or different from one another, therefore, the orientation of PD m is defined as:

1. The EA θ_{PR} can be same or different from one another,
2. In order to have all the azimuth angles symmetrically assigned, the azimuth angle should be arranged such that $\phi_{PD}^{m} = \frac{2(m-1)\pi}{Y}$.

For all the considered scenarios of MIMO-VLC systems, the PR's horizontal orientation can be varied by ϕ_H resulting in azimuth angle to be equal to $\phi_{PD}^{m} + \phi_H$. The horizontal orientation can be introduced intentionally to improve the performance of MIMO-VLC system or it can arise from random orientation of the PR. Although the PDs in a PR are placed very close to each other, the orientation of PDs in each case is very different from

one another as shown in Figure 3.4, resulting in different entries in channel matrix. As mobility, orientation and small size are very important factors of modern day handheld devices, the PR is small, compact and suitable for handheld devices.

3.4. Non-Angular Diversity Receivers (N-ADRs)

In N-ADRs, the normal vectors of the PDs point straight up towards the LEDs. The receiver is assumed to be placed along with the surface of the ground or the table. The distance between the PDs i.e., d_{rx} is very small and the distance of all the PDs from the LEDs can be assumed almost equal. As the normal vectors of all the PDs point in the same direction along with almost the same distance from LEDs, the channel matrix entries become highly correlated. The PDs normal vector representation is shown in Figure 3.3, where the normal vectors of LEDs and PDs point in opposite directions.

3.4.1. The coordinate system for N-ADRs

The position and orientation of LEDs and PDs are specified by their respective normal vectors in [x, y, z, θ, ϕ] format. However, θ and ϕ are always 0 as the normal vectors of the PDs are always in the same direction i.e., upwards. For all the considered MIMO-VLC systems, the PD placed at $\left(x^m_{PD}, y^m_{PD}, z^m_{PD}\right)$ has its normal vector $\vec{B}_m$ specified by $\left[x^m_{PD},\ y^m_{PD},\ z^m_{PD},\ 0,\ 0\right]$ for $1 \leq m \leq N$. Similarly, the LED placed at $\left(x^n_{LED},\ y^n_{LED},\ z^n_{LED}\right)$ has its normal vector $\vec{A}_n$ specified by $\left[x^n_{LED},\ y^n_{LED},\ z^n_{LED},\ 0,\ 0\right]$ for $1 \leq n \leq M$.

The PDs in the N-ADR is arranged as shown in Figure 3.7. The horizontal orientation angle of the N-ADR is considered to be 0°.

3.5. Optical MIMO Transmission Schemes

In this section, we will introduce Repetition Coding (RC) and Spatial Multiplexing (SMP) O-MIMO transmission schemes along with their respective Spectral Efficiency (R_{spec}). This will provide us with a foundation to compare the BER performance of multiple MIMO-VLC systems. This will also provide us with opportunity to compare the BER performance of fixed and variable EA MIMO-VLC systems.

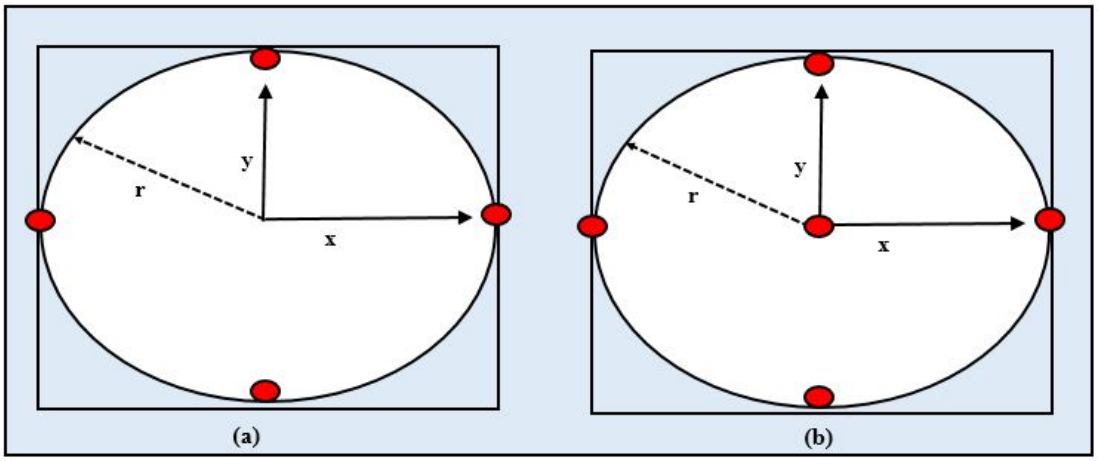

Figure 3.7. PD placement in N-ADR for (a) Y= N (b) Y= (N-1) where Y denotes number of PDs

3.5.1. Repetition coding

The simplest transmission technique that can be adopted for MIMO-VLC systems is RC. In RC, the same symbol information is sent from all the LEDs such that $s_0 = s_1 = s_2 = \ldots = s_M$, thus, resulting in a transmit-diversity gain. The application of RC results in better performance as the intensities coming from different LEDs constructively add up at the receiver, enhancing the received optical power. In our system model, we have considered a unipolar K-PAM for which RC achieves a R_{spec} of $\log_2(K)$ bit/s/Hz. The intensity levels for K-PAM is given by [36]:

$$I_i^{K-PAM} = \frac{2I}{K-1} \text{ i for i } = 0, 1, \ldots, (K-1), \tag{3.15}$$

where I represents the mean emitted optical power. Similarly, the mean emitted electrical energy i.e., E_s of the optical signals can be represented as [36]:

$$E_s = (r_{op-e} I)^2 T_s. \tag{3.16}$$

In Equation (3.16), $r_{op\text{-}e}$ represents the optical-to-electrical coefficient, whose value is chosen as 1 $A\sqrt{\Omega}$/ W without the loss of generality. T_s is the symbol duration. To keep the mean optical power emitted from all LEDs constant, the values of intensities given in Equation (3.15) is divided by the total number of LEDs.

As the intensities from different LEDs add up at the receiver, the received optical power for PD "m" can be calculated as [36]:

$$I_{recv-m} = \sum_{n=1}^{M} \frac{1}{M} h_{mn}. \tag{3.17}$$

At the receiver, Maximum Ratio Combining (MRC) is employed for combining the N received signals. The electrical SNR after MRC is given by [36]:

$$\frac{E_{recv}}{N_0} = \frac{T_s}{N_0} \sum_{m=1}^{N} \left(\sum_{n=1}^{M} \frac{I}{M} h_{mn} \right)^2 = \frac{E_s}{N_0 M^2} \sum_{m=1}^{N} \left(\sum_{n=1}^{M} h_{mn} \right)^2. \tag{3.18}$$

The equations for the lower bound of BER and BER of an RC employed MIMO-VLC system are given in Equations (6) and (7) of [36], respectively.

3.5.2. Spatial multiplexing

Another important transmission mechanism that is commonly employed in a MIMO-VLC system is SMP. RC results in enhanced reliability. However, that reliability comes at a cost of R_{spec} as the same information is sent from all the LEDs. To have a more spectral efficient MIMO-VLC system, SMP is adopted as a transmission technique. In SMP, independent data streams from all the LEDs are simultaneously used for the data transmission. Therefore, SMP results in a better R_{spec} of M $\log_2$ (K) bit/s/Hz as compared to RC's R_{spec} of $\log_2$ (K) bit/s/Hz.

In our system model, we have kept the modulation scheme and mean transmission power the same for RC and SMP. The available optical power is divided equally among all the LEDs such that all LEDs have the same optical power. For the calculation of BER for SMP employed MIMO-VLC system, a Pairwise Error Probability (PEP) is considered. PEP is defined as the probability when the decoder mistakes the actually transmitted signal vector $s_{m^{(1)}}$ as $s_{m^{(2)}}$ and is given by [36]:

$$PEP_{SMP} = PEP\left(s_{m^{(1)}} \rightarrow s_{m^{(2)}}\right) = Q\left(\sqrt{\frac{r_{op-e}^2 T_s}{4N_0} \left\| \mathbf{H}\left(\mathbf{s}_{m^{(1)}} - \mathbf{s}_{m^{(2)}}\right) \right\|_F^2} \right). \tag{3.19}$$

The BER for a SMP employed MIMO-VLC system is given in Equation (10) of [36].

4. CAPACITY AND BER PERFORMANCE OF INDOOR MIMO-VLC SYSTEMS

In this chapter, a comprehensive performance comparison is presented for fixed and variable EA indoor MIMO-VLC systems. The performance of the ADR based MIMO-VLC is also compared with N-ADR (classical receiver) based MIMO-VLC system. The impact on the performance of the considered MIMO-VLC systems by different factors including the FOV angle, LED transmitter array length, and horizontal orientation angle of the receiver has also been discussed in this chapter. A comparison in terms of BER performance for RC and SMP transmission schemes have also been discussed and elaborated in this chapter.

4.1. Simulation Setup and Parameters

In order to determine the performance of the considered MIMO-VLC systems, we have considered a room with 4 m x 4 m x 2.7 m dimensions. The LEDs are placed in a square form in the ceiling of the room such that the center of the square and the room coincide with each other. LED's downward normal angle is considered the same for all LEDs i.e., $\theta_{PR} = [0^{\circ},\ 180^{\circ})$. The LEDs are separated from one another by a distance called LED transmitter array distance i.e., d_{tx}. Similarly, we have considered 7 receiver positions across the room in accordance with the reference study [5]. The PDs in the receiver are arranged in a circular fashion with a radius of 0.5 cm, which makes the separation between the PDs equal to 1 cm as shown in Figure 4.1 and Figure 4.2.

[1] In reference study [5], we are presented with a fixed EA MIMO-VLC system in which the EA is considered the same for a specific receiver position. However, we are interested to find the effect of a variable EA on the performance of MIMO-VLC systems. To find the optimum values of EAs, we vary the EA of PDs in the range 0° to 90° and note down the values resulting in an optimized capacity performance.

[1] In Figures 4.1 and 4.2, the red circles represent the receiver composed of 4 PDs (not the individual PD), the yellow circle with a cross sign within represent LED position whereas the green circle with a cross sign within represent the case where the LED and the receiver is located at the same location.

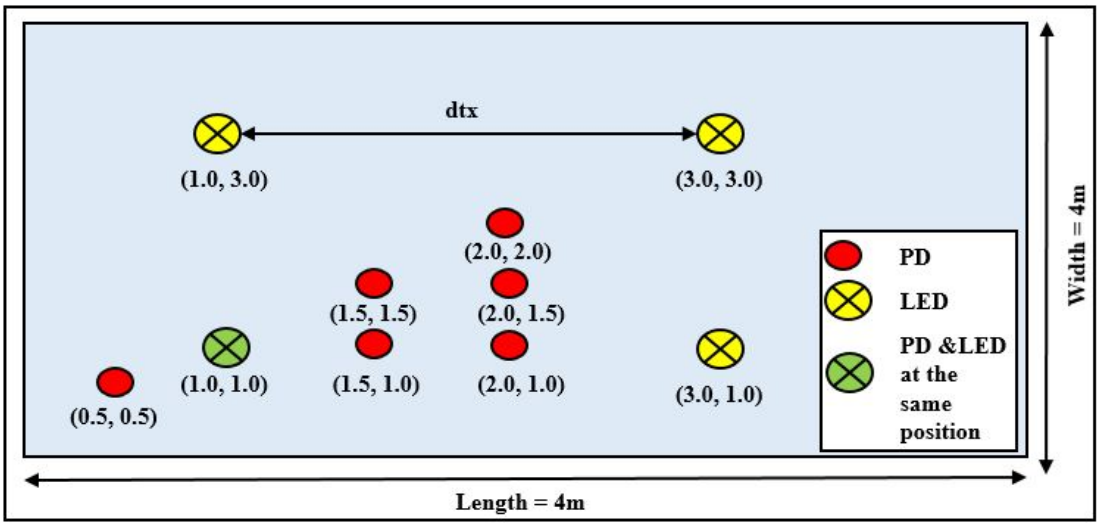

Figure 4.1. LED's placement and considered receiver positions for 4×4 MIMO-VLC system

A combination of different optimum EAs is achieved for all the considered receiver positions. To conduct a fair comparison between the capacity performance of a fixed and variable EA MIMO-VLC system, we have kept the modulation size constant i.e., 4-PAM. Similarly, we are also interested in finding suitable receiver positions, other than the considered receiver positions, across the entire room. To achieve the capacity coverage of a MIMO-VLC system, we have considered a step size of 0.4 m along the length and width of the room. As the receiver consists of 4 PDs with a separation of 1 cm between PDs, we can only consider the possible receiver positions in length and width up-to 3.6 m. The positions $(4.0,\ X,\ 0.8)$ and $(X,\ 4.0,\ 0.8)$, where X represents

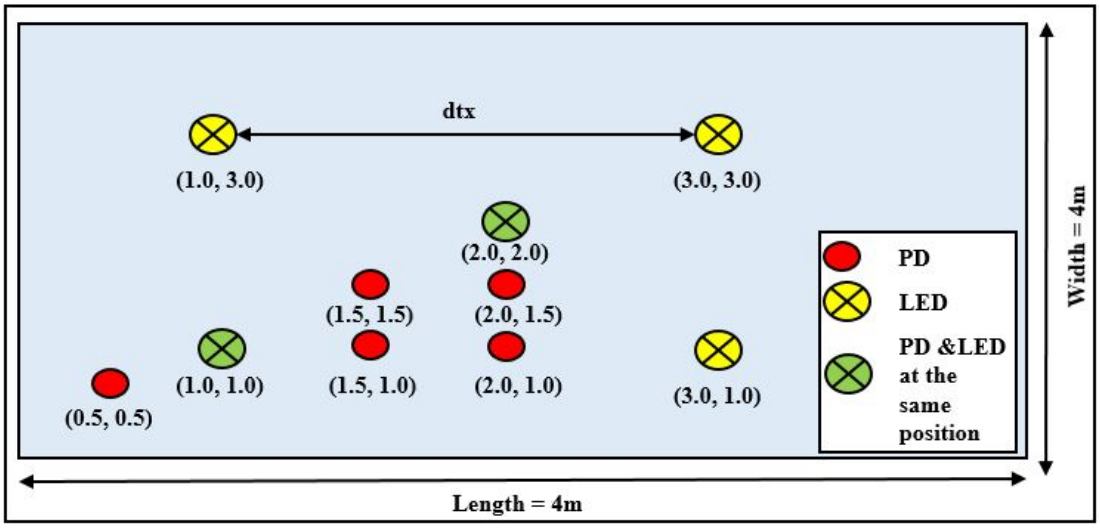

Figure 4.2. LED's placement and considered receiver positions for 4×5 & 5×5 MIMO-VLC systems

the respective width and length values, cannot be considered because they represent the boundary of the room. Moreover, the receiver is assumed to be at a height of 0.8 m from the surface of the ground throughout this dissertation.

In a similar manner, to determine the BER performance of the 4×4 and 5×5 MIMO-VLC systems, we have considered RC and SMP as transmission schemes. To present a fair comparison between the BER performance of RC and SMP employed MIMO-VLC systems, we have considered the R_{spec} of 4 bit/s/Hz and 8 bit/s/Hz for 4×4 MIMO-VLC system whereas for 5×5 MIMO-VLC system we have considered R_{spec} of 5 bit/s/Hz and 10 bit/s/Hz. As a result, we have adopted different modulation sizes for both the transmission schemes in accordance with the reference study [36]. As we are interested to explore the effect of different parameters such as FOV angle, LED transmitter array length, and horizontal orientation angle of the receiver on the performance of MIMO-VLC systems, we have considered the below-mentioned factors in our simulations:

1. The effect on the performance of fixed and variable EA MIMO-VLC systems by different FOV angles is explored. For this purpose, we have considered FOV angles of 60° and 90°,
2. The LED transmitter array length plays a very important role in generating uncorrelated channel matrix entries. Therefore, it is varied from 0.5 m to 3.5 m and its impact on the performance of the MIMO-VLC system is determined,
3. The horizontal orientation angle of the receiver is varied between 0° and 180° for fixed and variable EA MIMO-VLC systems and the respective changes in the

Table 4.1. Parameters for MIMO-VLC System

Parameter	**Value**
Number of LEDs (M)	{4,5}
Number of PDs (N)	{4,5}
Mean emitted optical power (I)	1 W
Semi Angle at half power $\Omega_{1/2}$	60°
Active Area of PD (A_{PD})	15 mm^2
FOV Coefficient (k)	1.4738
Height of LEDs (h_{LED})	2.7 m
Height of PDs (h_{PD})	0.8 m
SNR_{elec}	160 dB

capacity performance are examined.

The rest of the simulation parameters adopted in this dissertation are listed in Table 4.1.

4.2. Capacity Performance of a 4x4 MIMO-VLC System

In this section, we will compare the capacity performance of fixed and variable EA indoor MIMO-VLC systems. The performance of ADRs is also compared with N-ADRs. Similarly, the variation in the capacity performance of the MIMO-VLC system with respect to the FOV angle, LED transmitter array length and horizontal orientation angle of the receiver has also been explored in this section.

4.2.1. Capacity variation with respect to EA and fixed EA MIMO-VLC system

The capacity performance of ADR based indoor MIMO-VLC system depends on the EA of the PDs. In order to explore the variation in capacity performance with respect to EA, we vary the EA in the range from 0° to 90° for each PD separately. The respective capacity graph is plotted for all the considered receiver positions for a FOV angle of 90° and LED transmitter array length of 2 m. The capacity performance of position 6 (2.0, 2.0, 0.8) is better as compared to other considered receiver positions as shown in Figure 4.3. As position 6 (2.0, 2.0, 0.8) is located at the center of the room, it achieves a C_{max} value of 38.16 bit/s/Hz whereas position 0 (0.5, 0.5, 0.8), being located at the corner of the room, results in a throughput value of only 25.04 bit/s/Hz. For all the considered

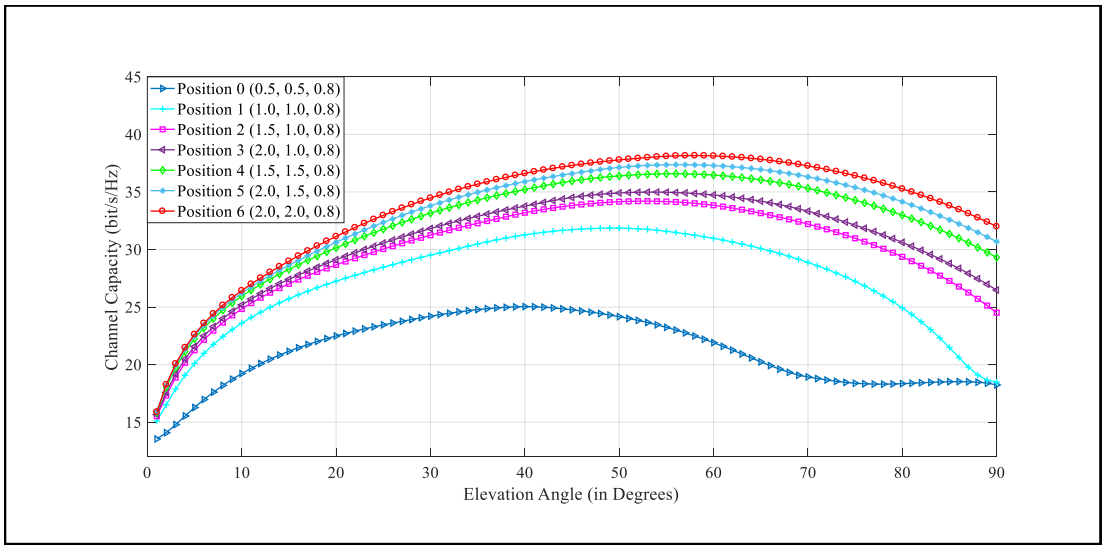

Figure 4.3. Capacity variation with EA for considered receiver positions

Table 4.2. Optimum fixed EAs that result in C_{max} for considered receiver positions for FOV angle of 90°

Considered Positions of the Receiver (x,y,z)	**C_{max} of the fixed EA system (bit/s/Hz)**	**Optimum EAs (in Deg) of the fixed EA system $[\theta_{m1}\ \theta_{m2}\ \theta_{m3}\ \theta_{m4}]$**
Position 0 (0.5, 0.5, 0.8)	25.04	[40 40 40 40]
Position 1 (1.0, 1.0, 0.8)	31.86	[49 49 49 49]
Position 2 (1.5, 1.0, 0.8)	34.20	[53 53 53 53]
Position 3 (2.0, 1.0, 0.8)	34.99	[54 54 54 54]
Position 4 (1.5, 1.5, 0.8)	36.58	[56 56 56 56]
Position 5 (2.0, 1.5, 0.8)	37.37	[56 56 56 56]
Position 6 (2.0, 2.0, 0.8)	38.16	[58 58 58 58]

receiver positions, the capacity initially rises with the EA angle as shown in Figure 4.3. The capacity curve depends on the respective EA value. The EA value determines the entries in the channel matrix, which in turn, determines the rank of the channel matrix. For every respective receiver position, there is an optimum EA value resulting in C_{max}. This optimum EA is considered the same for all the PDs i.e., $\theta_i = \theta_m$. Such a system results in a fixed EA MIMO-VLC system. After the optimum EA value, the capacity value drops until the FOV limit is reached. The optimum EAs along with C_{max} values for considered receiver positions are given in Table 4.2.

4.2.2. 4x4 Variable EA MIMO-VLC system

To find the optimum variable EA for each PD resulting in an overall optimum capacity performance, we vary the EA of each PD from 0° to 90°. The optimum EA values for individual PDs are recorded which results in C_{max}. The C_{max} for the fixed and variable EA MIMO-VLC systems along with optimum variable EA values for a FOV angle of 90° is given in Table 4.3.

As can be seen from the values of C_{max} in Table 4.3, that variable EA MIMO-VLC system performs better as compared to a fixed EA MIMO-VLC system, specifically at

Table 4.3. Optimum variable EAs that result in C_{max} for considered receiver positions for FOV angle of 90°

Considered Positions of the Receiver (x,y,z)	**C_{max} of the fixed EA system (bit/s/Hz)**	**C_{max} of the variable EA system (bit/s/Hz)**	**Optimum EAs (in Deg) of the variable EA system $[\theta_{m1}\ \theta_{m2}\ \theta_{m3}\ \theta_{m4}]$**
Position 0 (0.5, 0.5, 0.8)	25.04	26.44	[74 68 1 68]
Position 1 (1.0, 1.0, 0.8)	31.86	32.50	[64 68 16 68]
Position 2 (1.5, 1.0, 0.8)	34.20	34.46	[56 69 25 64]
Position 3 (2.0, 1.0, 0.8)	34.99	35.08	[60 61 50 51]
Position 4 (1.5, 1.5, 0.8)	36.58	36.66	[55 66 34 65]
Position 5 (2.0, 1.5, 0.8)	37.37	37.38	[63 56 57 52]
Position 6 (2.0, 2.0, 0.8)	38.16	38.16	[58 58 58 58]

positions near the corners of the room. A maximum gain in the capacity of approximately 6% is achieved at position 0 (0.5, 0.5, 0.8) for the variable EA system as compared to the fixed EA system as shown in Figure 4.4. The maximum gain at position 0 (0.5, 0.5, 0.8) is achieved because of its position. By having variable optimum EAs for all the PDs, the PDs are in a better position to receiver the incident photons. The channel

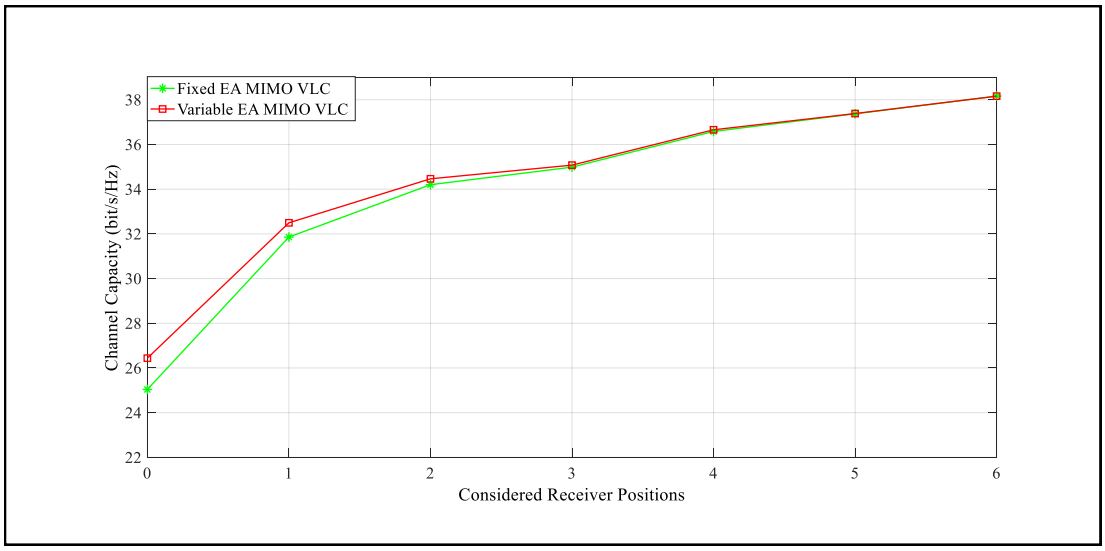

Figure 4.4. Maximum channel capacity for considered positions of fixed and variable EA MIMO-VLC systems

correlation is reduced as compared to fixed EA MIMO-VLC system. As we move towards the center of the room, the performance of fixed and variable EA systems gradually becomes identical. At position 6 (2.0, 2.0, 0.8), the optimum EA for PDs becomes equal for variable and fixed EA systems. As a result, the capacity of both the systems also becomes identical. However, the improvement in capacity comes at a cost of receiver's design complexity.

4.2.3. Maximum channel capacity comparison of 4x4 ADR and N-ADR based MIMO-VLC systems

The capacity performance of the indoor MIMO-VLC system depends on the rank of the channel matrix. A rank deficient channel matrix results in a poor capacity performance. ADRs are employed to generate a rank-full channel matrix and improve the performance of the MIMO-VLC system. For N-ADR, the horizontal orientation along with EA for PDs is assumed to be 0°. The rest of the parameters are assumed to be the same for both N-ADR and ADR based MIMO-VLC systems. The behavior of the N-ADR based MIMO-VLC system is the same as that of the ADR based MIMO-VLC system. The position 6 (2.0, 2.0, 0.8) results in the best performance resulting in a capacity of 21.41 bit/s/Hz whereas position 0 (0.5, 0.5, 0.8) can only attain a capacity of 13.77 bit/s/Hz. A comparison in terms of C_{max} values for the considered receiver positions is presented in Table 4.4.

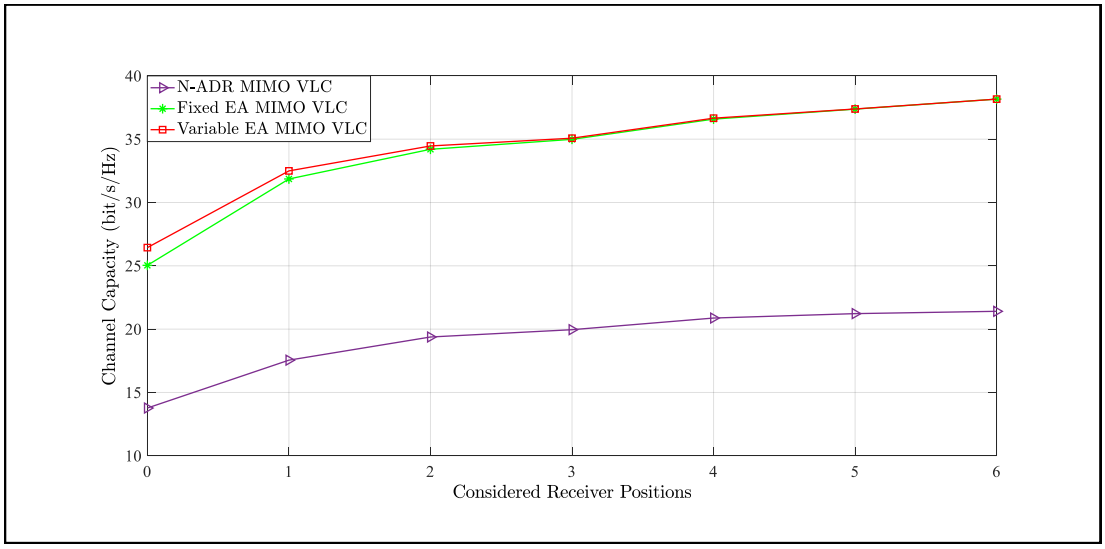

Figure 4.5. Maximum channel capacity comparison for 4x4 N-ADR and ADR based MIMO-VLC systems

Table 4.4. Maximum channel capacity for 4x4 N-ADR, fixed EA and variable EA MIMO-VLC systems

Considered Positions of the Receiver (x,y,z)	**C_{max} of the N-ADR system (bit/s/Hz)**	**C_{max} of the fixed EA system (bit/s/Hz)**	**C_{max} of the variable EA system (bit/s/Hz)**
Position 0 (0.5, 0.5, 0.8)	13.77	25.04	26.44
Position 1 (1.0, 1.0, 0.8)	17.55	31.86	32.50
Position 2 (1.5, 1.0, 0.8)	19.38	34.20	34.47
Position 3 (2.0, 1.0, 0.8)	19.96	34.99	35.08
Position 4 (1.5, 1.5, 0.8)	20.88	36.58	36.66
Position 5 (2.0, 1.5, 0.8)	21.22	37.37	37.38
Position 6 (2.0, 2.0, 0.8)	21.41	38.16	38.16

It can be very clearly observed that the ADR based MIMO-VLC systems result in a higher capacity as compared to the N-ADR based MIMO-VLC system. The difference in throughput between N-ADR and fixed and variable EA based MIMO-VLC systems at position 0 (0.5, 0.5, 0.8) is 11.27 bit/s/Hz and 12.67 bit/s/Hz, respectively. This difference shows an increasing trend in throughput values towards the center of the room as shown in Figure 4.5. At position 6 (2.0, 2.0, 0.8), a maximum difference of 16.75 bit/s/Hz is observed for fixed and variable EA MIMO-VLC systems.

4.2.4. Factors influencing the performance of 4x4 MIMO-VLC system

In this section, we will explore the impact on the performance of N-ADR and ADR based MIMO-VLC systems by different factors including the FOV angle, LED transmitter array length, and horizontal orientation of the receiver. We will change one of the factors at a time, by keeping the remaining parameters constant. This will provide us an insight into how the respective factor modifies the performance of the considered MIMO-VLC system.

4.2.4.1. FOV angle

The FOV angle is defined as the angle of receivable signal rays from LED to the receiver. FOV angle plays a very vital role in the performance of a MIMO-VLC system. Therefore, the selection of a suitable FOV angle is very vital for the performance of indoor MIMO-VLC system. In our simulations so far, we have used a FOV angle of 90°. However, now we will observe the performance of N-ADR and ADR based MIMO-VLC systems for a FOV angle of 60°. It has been observed that changing the FOV angle changes the capacity performance of the MIMO-VLC systems. For both fixed and variable EA MIMO-VLC systems, the respective optimum EA values also change resulting in a new optimized MIMO-VLC system. As can be seen from Figure 4.7, N-ADR based MIMO-VLC system shows no change in capacity performance. However, ADR based MIMO-VLC system i.e., fixed and variable EA systems have shown improvement in the capacity performance when the FOV angle is changed from 90° to 60°. The respective capacity values along with new optimum EA values for considered positions of the receiver are given in Table 4.5. This increase in capacity results from the fact that a smaller FOV angle allows data transmission at higher rates and reduces ISI interference. On the other hand, a smaller FOV angle also results in

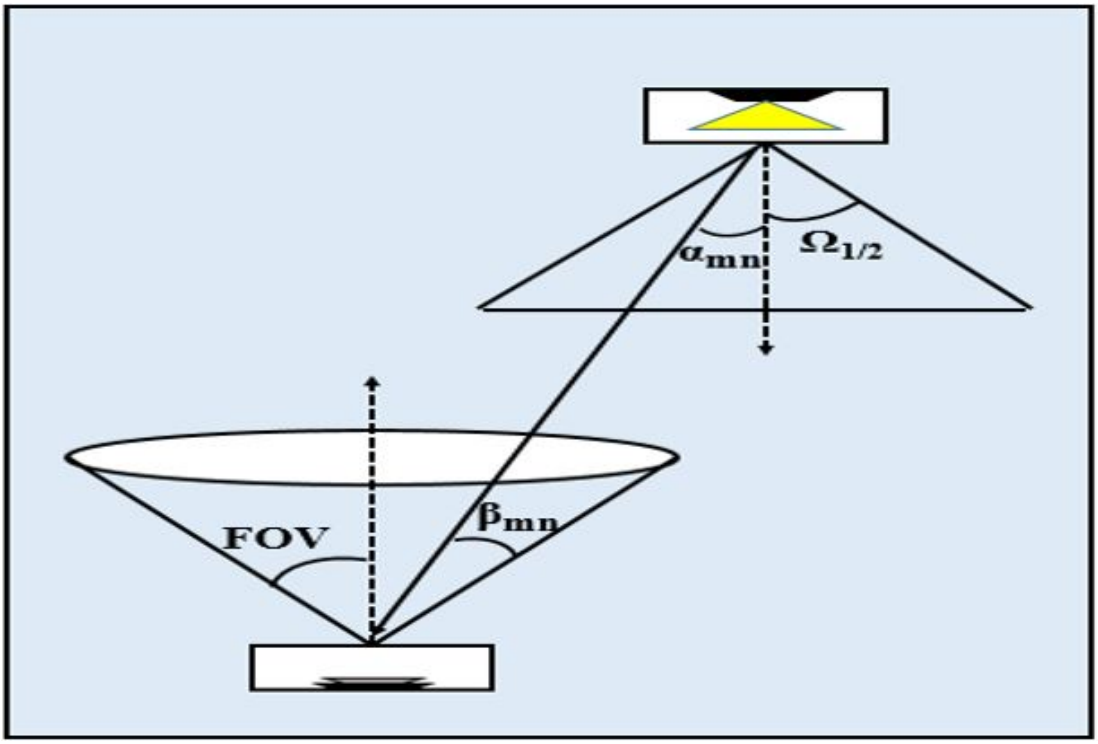

Figure 4.6. FOV angle for a VLC system

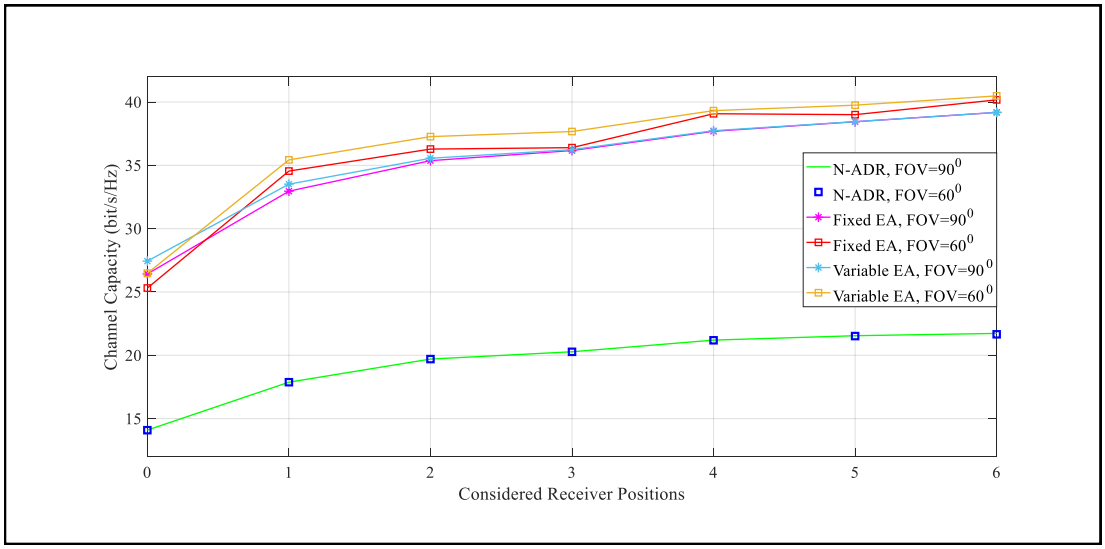

Figure 4.7. Maximum channel capacity comparison for FOV angles of 60° and 90°

Table 4.5. Capacity performance for fixed EA and variable EA MIMO-VLC systems when FOV= 60°

Considered positions of the receiver (x,y,z)	**C_{max} of the fixed EA system (bit/s/Hz)**	**Optimum EA (in Deg) of the fixed EA system $\theta_m^i = \theta_A$**	**C_{max} of the variable EA system (bit/s/Hz)**	**Optimum EAs (in Deg) of the variable EA system $[\theta_{m1}\ \theta_{m2}\ \theta_{m3}\ \theta_{m4}]$**
Position 0 (0.5, 0.5, 0.8)	25.31	[21 21 21 21]	26.48	[56 22 8 22]
Position 1 (1.0, 1.0, 0.8)	34.55	[31 31 31 31]	35.43	[56 36 18 36]
Position 2 (1.5, 1.0, 0.8)	36.28	[47 47 47 47]	37.27	[52 47 27 29]
Position 3 (2.0, 1.0, 0.8)	36.40	[40 40 40 40]	37.70	[64 48 24 38]
Position 4 (1.5, 1.5, 0.8)	39.07	[42 42 42 42]	39.32	[48 42 32 42]
Position 5 (2.0, 1.5, 0.8)	39.00	[45 45 45 45]	39.75	[58 43 37 45]
Position 6 (2.0, 2.0, 0.8)	40.17	[52 52 52 52]	40.48	[37 52 37 52]

uneven optical power distribution across the room, which is undesirable for an indoor MIMO-VLC system.

The capacity values for the FOV angle of 60° follows the same trend as observed for the FOV angle of 90°. The performance of the variable EA MIMO-VLC system is better as compared to the fixed EA system. The position 6 (2.0, 2.0, 0.8) presents the most suitable receiver position resulting in a capacity of 40.17 bit/s/Hz and 40.48 bit/s/Hz for fixed and variable EA MIMO-VLC systems, respectively. Similarly, as the position 0 (0.5, 0.5, 0.8) is very close to the corner of the room, the performance of position 0 (0.5, 0.5, 0.8) is worst among all the considered receiver positions, resulting in a capacity of 25.31 bit/s/Hz and 26.48 bit/s/Hz for fixed and variable EA MIMO-VLC systems, respectively.

4.2.4.2. LED transmitter array length

In order to explore the effect on the capacity performance of MIMO-VLC systems, we have considered position 1 (1.0, 1.0, 0.8) and position 6 (2.0, 2.0, 0.8) as our reference positions along with their respective optimum EA values. The position 0 (0.5, 0.5, 0.8) is located very close to the corner of the room, which always results in poor performance. Therefore, to have a fair comparison, we have selected position 1 (1.0, 1.0, 0.8) as a reference as compared to position 0 (0.5, 0.5, 0.8). Starting from the center of the room, we start varying the d_{tx} in a step size of 10 cm as shown in Figures 4.1 and 4.2. We

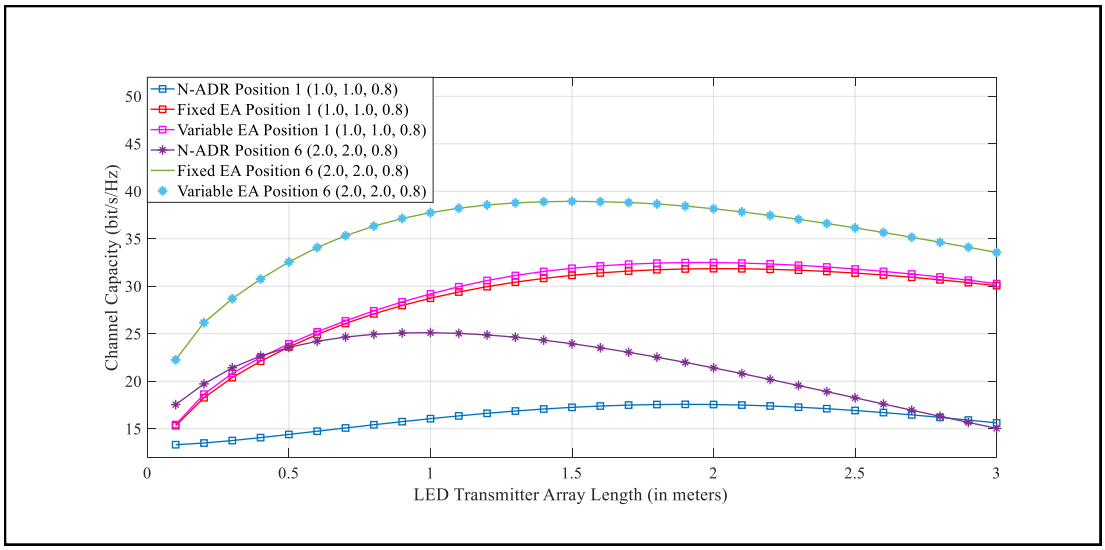

Figure 4.8. Capacity variation of a 4x4 MIMO-VLC system with d_{tx} when FOV= 90°

record the respective capacity performance of N-ADR and ADR based MIMO-VLC systems. As it can be seen from the Figure 4.8 that the throughput for N-ADR and ADR based MIMO-VLC system initially increases by increasing the d_{tx} until a maximum point i.e., $d_{tx\text{-}opt}$ is reached. This increase in throughput is the result of reduced channel correlation. However, a further increase in d_{tx} beyond $d_{tx\text{-}opt}$ results in reducing the received signal power. As a result of reduced signal power, the benefit of reduced channel correlation is lost and the capacity performance drops after $d_{tx\text{-}opt}$ is reached. The resulting capacity and $d_{tx\text{-}opt}$ values for N-ADR and ADR based MIMO-VLC systems is given in Table 4.6. As it can be seen from Table 4.6 that for the receiver positions near the corners of the room, a larger d_{tx} results in a better performance. However, for the receiver positions towards the center of the room, smaller d_{tx} values result in better capacity performance.

Table 4.6. Capacity variation of a 4x4 MIMO-VLC system with d_{tx} when FOV= 90°

Considered positions of the receiver (x,y,z)	**C_{max} of the N-ADR system (bit/s/Hz)**	**$d_{tx\text{-}opt}$ values (m)**	**C_{max} of the fixed EA system (bit/s/Hz)**	**$d_{tx\text{-}opt}$ values system (m)**	**$C_{max}$of the variable EA system (bit/s/Hz)**	**$d_{tx\text{-}opt}$ values (m)**
Position 0 (0.5, 0.5, 0.8)	14.60	3.0	25.80	2.7	27.01	2.6
Position 1 (1.0, 1.0, 0.8)	17.57	1.9	31.86	2.0	32.5	2.0
Position 2 (1.5, 1.0, 0.8)	19.87	1.5	34.3	1.8	34.62	1.8
Position 3 (2.0, 1.0, 0.8)	20.8	1.4	35.2	1.7	35.25	1.8
Position 4 (1.5, 1.5, 0.8)	22.75	1.2	37.03	1.6	37.23	1.6
Position 5 (2.0, 1.5, 0.8)	23.89	1.1	38.03	1.6	38.00	1.6
Position 6 (2.0, 2.0, 0.8)	25.12	1.0	38.94	1.5	38.94	1.5

4.2.4.3. Horizontal orientation of the receiver

The horizontal orientation of the receiver can be varied to decrease channel correlation. In our simulations, we have assumed the position of N-ADR along the surface of the table i.e., at a height of 0.8 m from the surface of the ground. Similarly, the horizontal orientation angle of N-ADR is also assumed to be 0° as shown in Figure 3.7. However, for ADR based MIMO-VLC system, the horizontal orientation of the receiver can be varied to explore the impact on the capacity performance of the system. In order to demonstrate the impact of horizontal orientation on the performance of ADR based MIMO-VLC systems, we have considered position 1 (1.0, 1.0, 0.8), position 4 (1.5, 1.5, 0.8), and position 6 (2.0, 2.0, 0.8) as reference positions along with their respective optimum EA values given in Tables 4.2 and 4.3.

As the LEDs are arranged symmetrically, the horizontal rotation is symmetric for every 45°. Therefore, the horizontal orientation is varied from 0° to 180°. As the horizontal rotation is symmetric for every 45°, the capacity initially rises with the horizontal orientation angle until C_{max} is reached at a horizontal angle of 45°. After 45°, the capacity decreases to a minimum capacity (C_{min}) which occurs at a horizontal angle of 90°. The cycle is repeated again from 90° to 180° as shown in Figure 4.9. The position 1 (1.0, 1.0, 0.8) of the variable EA based MIMO-VLC system does not follow the same trend in the second half i.e., from 90° to 180°. This behavior is caused by the respective

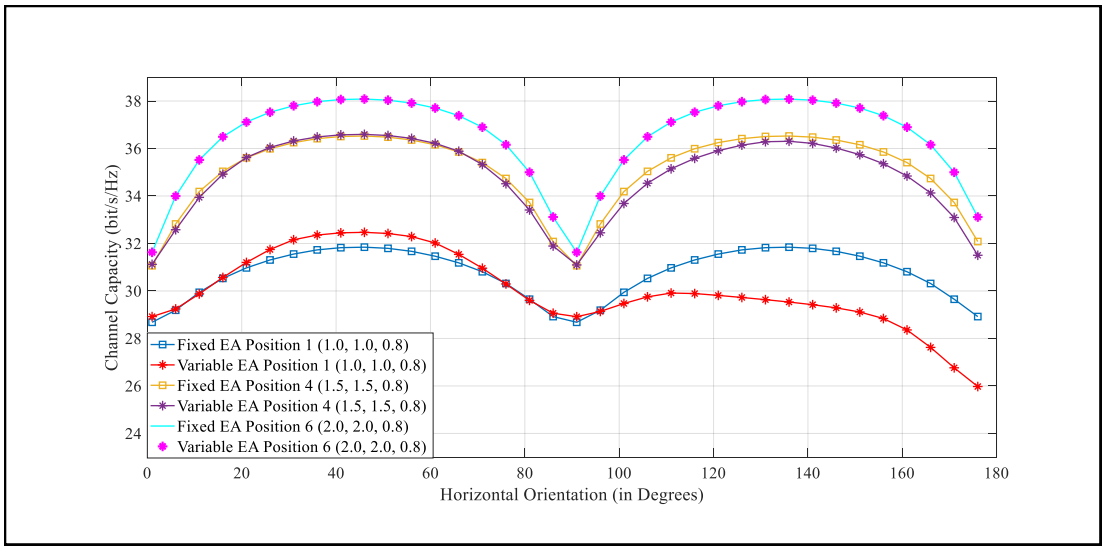

Figure 4.9. Capacity variation with respect to the horizontal orientation angle of the receiver

normal vectors resulting from different EAs of the MIMO-VLC system for position 1 (1.0, 1.0, 0.8).

4.2.5. Suitable receiver positions across the room

The room considered for simulation has 4 m x 4 m x 2.7 m dimensions. In our simulations, we have so far considered specific receiver positions across the room. However, in this section we provide the capacity distribution across the entire room for an FOV angle of 60°.

As can be seen from Figure 4.10 that the center of the room provides the best result in terms of capacity i.e., 40.48 bit/s/Hz. In the capacity variation around the center of the room, symmetry can be observed. The positions close to the corners of the room results in a comparatively poor capacity performance as compared to the positions close to the center of the room because of the LEDs placement i.e., d_{tx} is kept constant at 2 m. A meager capacity of around 26.48 bit/s/Hz is attained at the corners of the room. Thus, position 6 (2.0, 2.0, 0.8) presents an ideal position for the receiver.

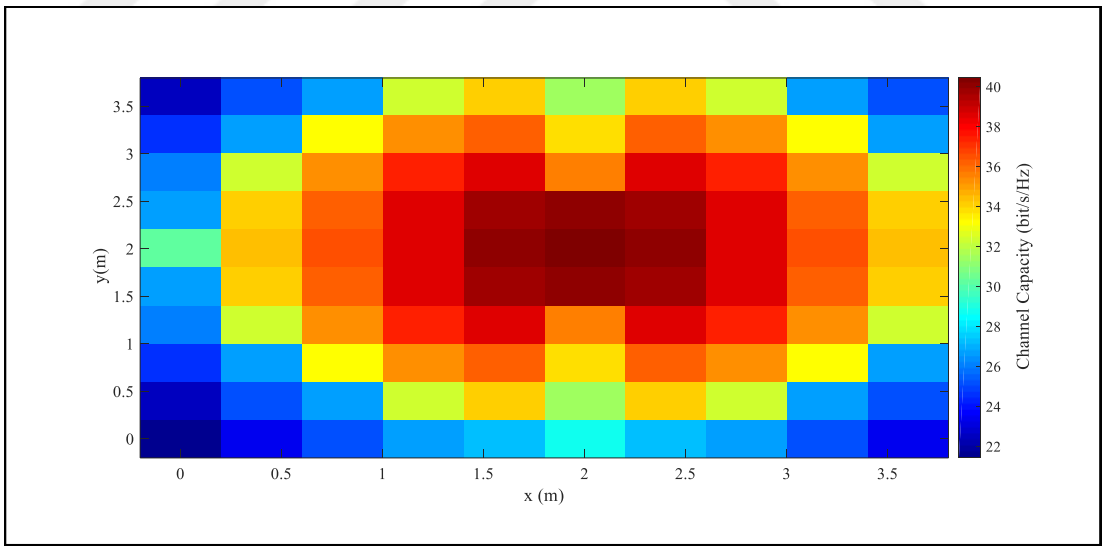

Figure 4.10. Capacity variation across entire room for the FOV angle of 60°

4.3. Capacity Performance of a 4x5 MIMO-VLC System

In this section, we will compare the capacity performance of a 4×5 fixed and variable EA indoor MIMO-VLC systems. The performance of ADRs is also compared with N-ADRs. Similarly, the variation in the capacity performance of the MIMO-VLC system

with respect to the FOV angle, LED transmitter array length and horizontal orientation angle of the receiver has also been explored in this section.

4.3.1. Capacity variation with respect to EA and fixed EA MIMO-VLC system

In order to explore the effect of EA on the capacity performance of a 4×5 MIMO-VLC system, we vary the EA in the range from 0° to 90°. As the position 6 (2.0, 2.0, 0.8) is located at the center of the room, the PDs are able to receive the incident photons from all the respective LEDs. As a result, the capacity performance of position 6 (2.0, 2.0, 0.8) is better as compared to other considered receiver positions achieving a C_{max} value of 39.18 bit/s/Hz as shown in Figure 4.11. The capacity performance deteriorates towards the corner of the room, where position 0 (0.5, 0.5, 0.8) results in a throughput value of only 26.42 bit/s/Hz. It can be seen from Figure 4.11 that at each respective receiver position, an optimum C_{max} value is achieved resulting in an optimum EA. This optimum EA is considered the same for all the PDs i.e., $\theta_m^i = \theta_A$. The optimum EAs along with C_{max} values and percentage gain when compared with 4×4 MIMO-VLC system are given in Table 4.7.

As it is evident from Table 4.7 that the maximum percentage gain in capacity is achieved at position 0 (0.5, 0.5, 0.8) when compared with 4×4 MIMO-VLC system. As we move away from the corner of the room, the percentage gain decreases until a minimum percentage gain of 2.66% is achieved at position 6 (2.0, 2.0, 0.8). Thus, placing an extra

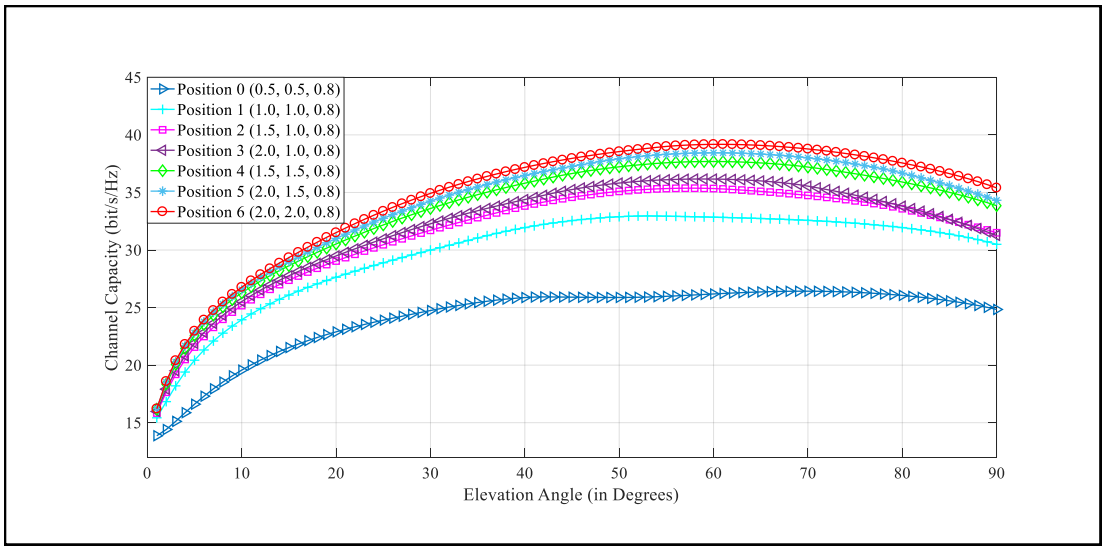

Figure 4.11. Capacity variation with EA for considered receiver positions

Table 4.7. Optimum fixed EAs that result in C_{max} & percentage gain for considered receiver positions for FOV angle of 90°

Considered Positions of the receiver (x,y,z)	**C_{max} of the fixed EA system (bit/s/Hz)**	**Optimum EAs (in Deg) of the fixed EA system $[\theta_{m1}\ \theta_{m2}\ \theta_{m3}\ \theta_{m4}]$**	**Capacity gain(%) w.r.t 4x4 fixed EA MIMO-VLC system**
Position 0 (0.5, 0.5, 0.8)	26.42	[70 70 70 70]	5.53
Position 1 (1.0, 1.0, 0.8)	32.96	[53 53 53 53]	3.46
Position 2 (1.5, 1.0, 0.8)	35.37	[58 58 58 58]	3.42
Position 3 (2.0, 1.0, 0.8)	36.17	[59 59 59 59]	3.38
Position 4 (1.5, 1.5, 0.8)	37.69	[60 60 60 60]	3.02
Position 5 (2.0, 1.5, 0.8)	38.44	[60 60 60 60]	2.86
Position 6 (2.0, 2.0, 0.8)	39.18	[61 61 61 61]	2.66

PD in the receiver can help us improve capacity performance at the corners of the room.

4.3.2. 4x5 Variable EA MIMO-VLC systems

The capacity performance of the variable EA system is better as compared to fixed EA MIMO-VLC system as shown in Figure 4.12. At position 0 (0.5, 0.5, 0.8), a maximum

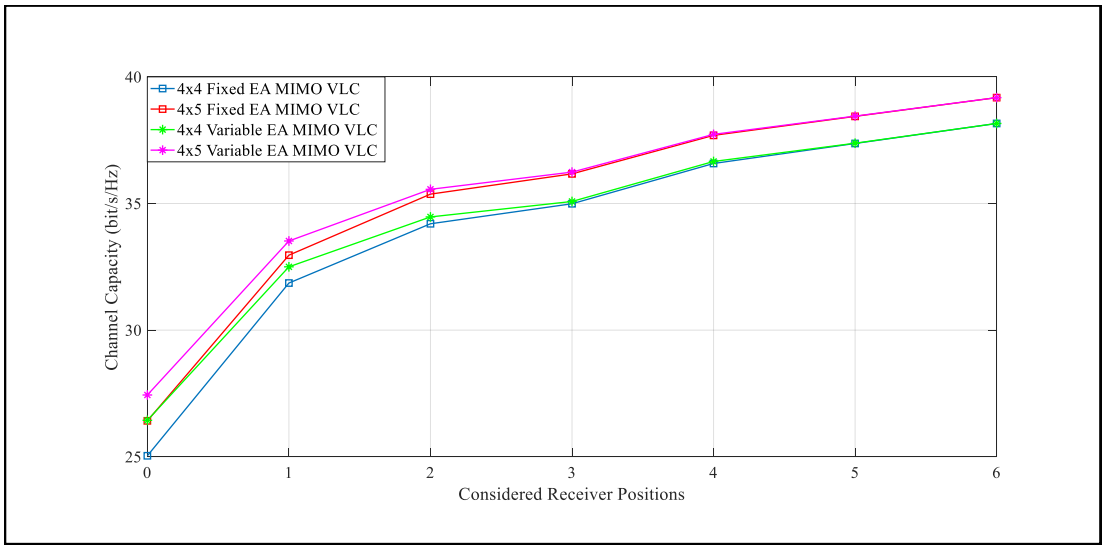

Figure 4.12. Maximum channel capacity comparison for considered positions of 4x4 and 4x5 MIMO-VLC systems

Table 4.8. Optimum variable EAs that result in C_{max} & capacity gain(%) for considered receiver positions for FOV angle of 90°

Considered Positions of the receiver (x,y,z)	**C_{max} of the variable EA system (bit/s/Hz)**	**Optimum EAs (in Deg) of the variable EA system $[\theta_{m1}\ \theta_{m2}\ \theta_{m3}\ \theta_{m4}]$**	**Capacity gain(%) w.r.t 4x4 variable EA MIMO-VLC system**
Position 0 (0.5, 0.5, 0.8)	27.44	[74 68 1 68]	3.78
Position 1 (1.0, 1.0, 0.8)	33.52	[68 65 41 64]	3.14
Position 2 (1.5, 1.0, 0.8)	35.56	[66 64 48 61]	3.19
Position 3 (2.0, 1.0, 0.8)	36.24	[64 65 55 55]	3.31
Position 4 (1.5, 1.5, 0.8)	37.73	[64 62 54 62]	2.94
Position 5 (2.0, 1.5, 0.8)	38.44	[62 62 59 59]	2.85
Position 6 (2.0, 2.0, 0.8)	39.18	[61 61 60 61]	2.66

capacity gain of 4% is achieved for the variable EA 4×5 MIMO-VLC system. The maximum gain at position 0 (0.5, 0.5, 0.8) results because of a lower channel correlation as compared to fixed EA MIMO-VLC system. As we move towards the center of the room, the respective fixed and variable EA becomes the same resulting in a similar capacity performance at the center of the room i.e., position 6 (2.0, 2.0, 0.8). The performance of 4×5 MIMO-VLC system is better as compared to 4×4 MIMO-VLC system as shown in Figure 4.12. As compared with the 4×4 variable EA MIMO-VLC system, a maximum gain in the capacity of 3.78% is achieved at position 0 (0.5, 0.5, 0.8) whereas a minimum gain in capacity of 2.66% is attained at position 6 (2.0, 2.0, 0.8). The capacity performance of the 4×5 variable EA MIMO-VLC system along with optimum EA values for individual PDs and capacity gain% as compared to 4×4 variable EA MIMO-VLC system is given in Table 4.8.

4.3.3. Maximum channel capacity comparison of 4x5 ADR and N-ADR based MIMO-VLC systems

For a 4×5 N-ADR based MIMO-VLC system, the simulation parameters are considered to be the same i.e., EA and horizontal orientation angle assumed to be 0°. The capacity

performance with respect to the position of the N-ADR based MIMO-VLC system is similar to the ADR based MIMO-VLC system and is given in Figure 4.13. The position 6 (2.0, 2.0, 0.8) being located at the center of the room, attains a maximum throughput of 21.73 bit/s/Hz. The position 0 (0.5, 0.5, 0.8) attains the lowest capacity of 14.09 bit/s/Hz.

When compared with 4×4 N-ADR based MIMO-VLC system, a maximum gain of 2.35% is achieved at the corner of the room i.e., position 0 (0.5, 0.5, 0.8). As we move towards the center of the room, the gain in capacity decreases with only a capacity gain of 1.50% at the center of the room i.e., position 6 (2.0, 2.0, 0.8). Thus, the capacity performance at the corners of the room can be improved by employing an extra PD at the center of the receiver. The respective throughput values for N-ADR and ADR based MIMO-VLC systems are represented in Table 4.9.

The capacity performance of the 4×5 ADR based MIMO-VLC system is much better as compared to the 4×5 N-ADR based MIMO-VLC system. A difference of 12.33 bit/s/Hz and 13.35 bit/s/Hz is recorded for fixed and variable EA MIMO-VLC systems, respectively. This difference in capacity increases towards the center of the room resulting in a difference of 17.45 bit/s/Hz and 17.45 bit/s/Hz at position 6 (2.0, 2.0, 0.8) for fixed and variable EA MIMO-VLC systems, respectively.

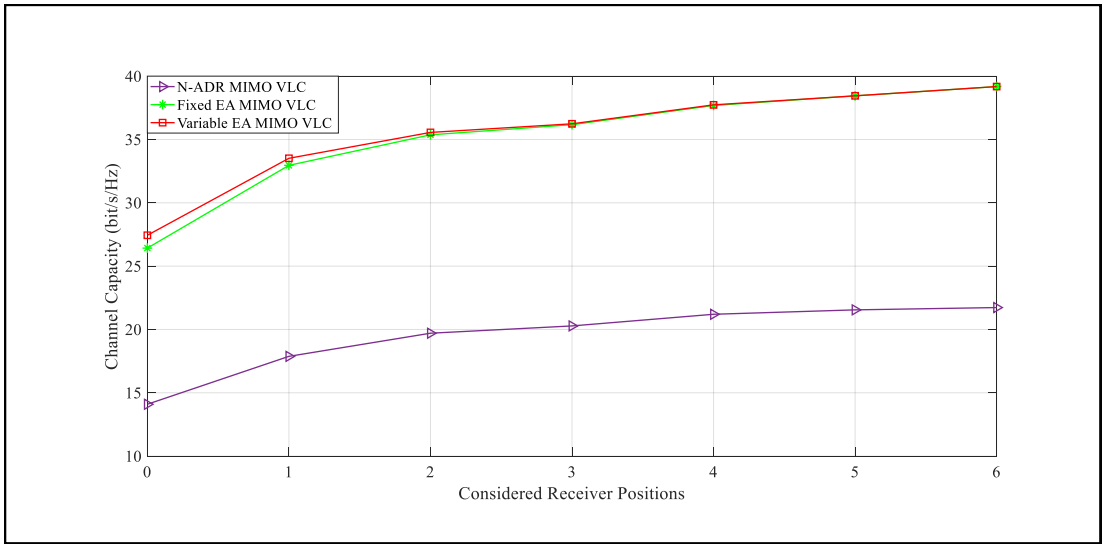

Figure 4.13. Maximum channel capacity comparison for 4x5 N-ADR and ADR based MIMO-VLC systems

Table 4.9. Maximum channel capacity for 4x5 N-ADR, fixed EA and variable EA MIMO-VLC systems

Considered Positions of the Receiver (x,y,z)	**C_{max} of the N-ADR system (bit/s/Hz)**	**C_{max} of the fixed EA system (bit/s/Hz)**	**C_{max} of the variable EA system (bit/s/Hz)**
Position 0 (0.5, 0.5, 0.8)	14.09	26.42	27.44
Position 1 (1.0, 1.0, 0.8)	17.88	32.96	33.52
Position 2 (1.5, 1.0, 0.8)	19.70	35.37	35.56
Position 3 (2.0, 1.0, 0.8)	20.28	36.17	36.24
Position 4 (1.5, 1.5, 0.8)	21.20	37.69	37.73
Position 5 (2.0, 1.5, 0.8)	21.55	38.44	38.45
Position 6 (2.0, 2.0, 0.8)	21.73	39.18	39.18

4.3.4. Factors influencing the performance of 4x5 MIMO-VLC system

The performance of a 4×5 MIMO-VLC system depends on many factors including the FOV angle, LED transmitter array length, and horizontal orientation of the receiver. To completely understand the impact on the performance of the MIMO-VLC system by a specific factor, we will change one factor at a time and keep the remaining factors unchanged. In this way, we will be able to explore the impact of the factor on the performance of the system.

4.3.4.1. FOV angle

The optimum capacity and EA values for 4×5 MIMO-VLC system recorded so far correspond to the FOV angle of 90°. However, the capacity performance of the N-ADR and ADR based MIMO-VLC systems changes as the FOV angle is changed from 90° to 60°. Similarly, the respective EA values of fixed and variable EA MIMO-VLC systems also change with the FOV angle. A very small decrease in capacity values has been observed for N-ADR based MIMO-VLC system. A maximum difference of 0.34% at position 6 (2.0, 2.0, 0.8) is observed for the new value of the FOV angle as shown in Figure 4.14.

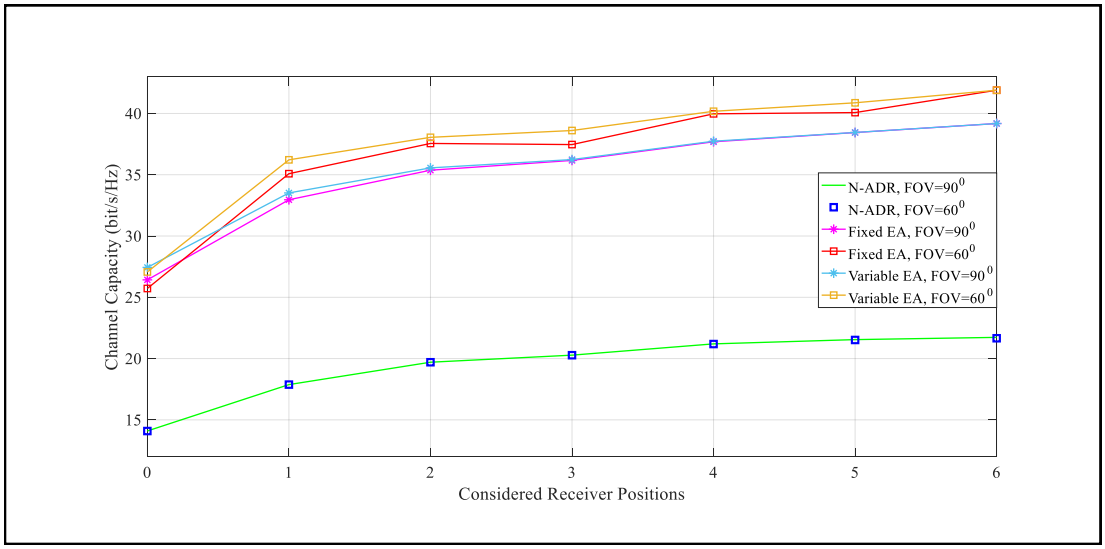

Figure 4.14. Maximum channel capacity comparison for FOV angles of 60° and 90°

Table 4.10. Maximum channel capacity for 4x5 fixed and variable EA MIMO-VLC systems when FOV= 60°

Considered positions of the receiver (x,y,z)	**C_{max} of the fixed EA system (bit/s/Hz)**	**Optimum EA (in Deg) of the fixed EA system $\theta_m^i = \theta_A$**	**C_{max} of the variable EA system (bit/s/Hz)**	**Optimum EAs (in Deg) of the variable EA system $[\theta_{m1}\ \theta_{m2}\ \theta_{m3}\ \theta_{m4}]$**
Position 0 (0.5, 0.5, 0.8)	25.72	[20 20 20 20]	27.07	[81 26 8 26]
Position 1 (1.0, 1.0, 0.8)	35.08	[35 35 35 35]	36.22	[60 40 18 40]
Position 2 (1.5, 1.0, 0.8)	37.52	[49 49 49 49]	38.05	[51 47 21 49]
Position 3 (2.0, 1.0, 0.8)	37.46	[43 43 43 43]	38.61	[64 47 38 24]
Position 4 (1.5, 1.5, 0.8)	39.97	[42 42 42 42]	40.18	[49 42 32 42]
Position 5 (2.0, 1.5, 0.8)	40.07	[58 58 58 58]	40.87	[66 66 45 45]
Position 6 (2.0, 2.0, 0.8)	41.90	[52 52 52 52]	41.90	[52 52 52 52]

The capacity values along with new optimum EAs for fixed and variable EA MIMO-VLC systems are given in Table 4.10. The capacity values for the FOV angle of 60° follow the same pattern. At position 0 (0.5, 0.5, 0.8), the performance of 60° employed FOV angle MIMO-VLC system is slightly poor as compared to 90° employed FOV angle MIMO-VLC system. However, for the rest of the considered positions, the performance of 60° employed FOV angle system is better than its counterpart as shown in Figure 4.14. The gain in channel capacity is achieved because a smaller FOV angle allows faster data transmission and low levels of ISI. The performance of the variable EA MIMO-VLC system is better as compared to the fixed EA MIMO-VLC system. The position 0 (0.5, 0.5, 0.8) presents the worst receiver position resulting in only 25.72 bit/s/Hz and 27.07 bit/s/Hz for fixed and variable EA MIMO-VLC systems, respectively. The position 6 (2.0, 2.0, 0.8) being located at the center of the room, exhibits the maximum throughput values of 41.90 bit/s/Hz for fixed and variable EA MIMO-VLC systems as shown in Figure 4.14.

4.3.4.2. LED transmitter array length

In this section, we have chosen two positions i.e., position 1 (1.0, 1.0, 0.8) and position 6 (2.0, 2.0, 0.8) as our reference positions to explore the impact on the capacity performance of N-ADR and ADR based MIMO-VLC systems. These positions are selected to have a fair comparison in terms of capacity. We start off from the center of

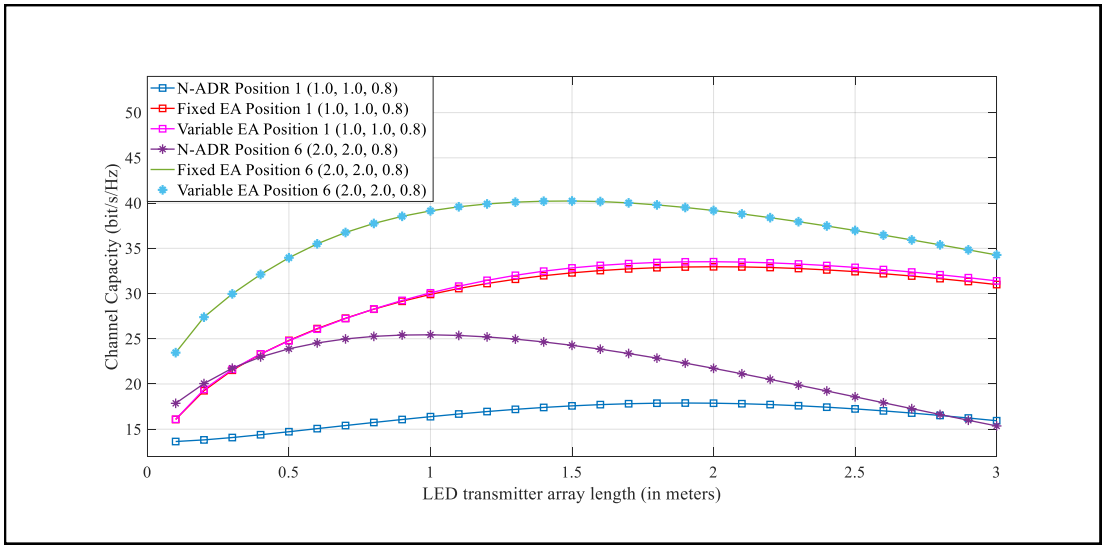

Figure 4.15. Capacity variation of a 4x5 MIMO-VLC system with d_{tx} when FOV= 90°

Table 4.11. Capacity variation of a 4x5 MIMO-VLC system with d_{tx} when FOV= 90°

Considered positions of the receiver (x,y,z)	**C_{max} of the N-ADR system (bit/s/Hz)**	**$d_{tx\text{-}opt}$ values (m)**	**C_{max} of the fixed EA system (bit/s/Hz)**	**$d_{tx\text{-}opt}$ values system (m)**	**$C_{max}$of the variable EA system (bit/s/Hz)**	**$d_{tx\text{-}opt}$ values (m)**
Position 0 (0.5, 0.5, 0.8)	14.92	3.0	27.01	2.6	28.00	2.7
Position 1 (1.0, 1.0, 0.8)	17.90	1.9	32.96	2.0	33.52	2.0
Position 2 (1.5, 1.0, 0.8)	20.20	1.5	35.53	1.8	35.71	1.8
Position 3 (2.0, 1.0, 0.8)	21.12	1.4	36.50	1.7	36.55	1.7
Position 4 (1.5, 1.5, 0.8)	23.07	1.2	38.31	1.6	38.34	1.6
Position 5 (2.0, 1.5, 0.8)	24.21	1.1	39.32	1.5	39.31	1.5
Position 6 (2.0, 2.0, 0.8)	25.44	1.0	40.23	1.5	40.23	1.5

the room and vary the d_{tx} in a step-size of 10 cm. We increase d_{tx} until 0.5 m is left from all sides of the room. The variation in capacity with the varying d_{tx} is plotted in Figure 4.15. The capacity of N-ADR and ADR based MIMO-VLC systems initially increases with d_{tx} until C_{max} is achieved at $d_{tx\text{-}opt}$. Till $d_{tx\text{-}opt}$, the improvement in capacity results from the fact that channel decorrelation is the prominent factor as compared to the reduction in signal strength. Beyond $d_{tx\text{-}opt}$, the reduction in signal strength becomes the prominent factor. As a result, the improvement resulted from the channel decorrelation is lost and the capacity starts dropping. As it can be seen from Table 4.11 that the positions near the corner of the room require comparatively larger d_{tx} values for improved performance as it minimizes the channel correlation. However, the positions towards the center of the room need smaller d_{tx} values for improved performance.

4.3.4.3. Horizontal orientation of the receiver

For the ADR based MIMO-VLC system, the horizontal orientation of the receiver can be varied to improve the capacity performance of the system. We have chosen three different positions i.e., position 1 (1.0, 1.0, 0.8), position 4 (1.5, 1.5, 0.8), and position 6 (2.0, 2.0, 0.8), as our reference positions to have a fair comparison. The position 0 (0.5, 0.5, 0.8) is not chosen as it always results in poor performance as it is located at the corner of the room. For the said positions, the remaining parameters along with optimum EA values are kept unchanged. The horizontal rotation for a 4×5 MIMO-VLC system is symmetric for every 45°, just like 4×4 MIMO-VLC system. The channel capacity also varies symmetrically as shown in Figure 4.16. The capacity rises with the varying horizontal orientation angle until C_{max} is achieved at 45°. After that, the capacity drops and attains C_{min} at 90°. The capacity again rises to C_{max} at 135° and drops back to C_{min} at 180°. The capacity values for positions 1 and 4 of variable EA MIMO-VLC systems are slightly higher than their respective counterparts in the first cycle i.e., from 0° to 90°. However, for the second cycle i.e., from 90° to 180°, the fixed EA capacity performance is better than the variable EA MIMO-VLC system. Thus, we can say that fixed EA MIMO-VLC systems follow perfect symmetry whereas variable EA MIMO-VLC system does not follow perfect symmetry because of having different EAs for the PDs.

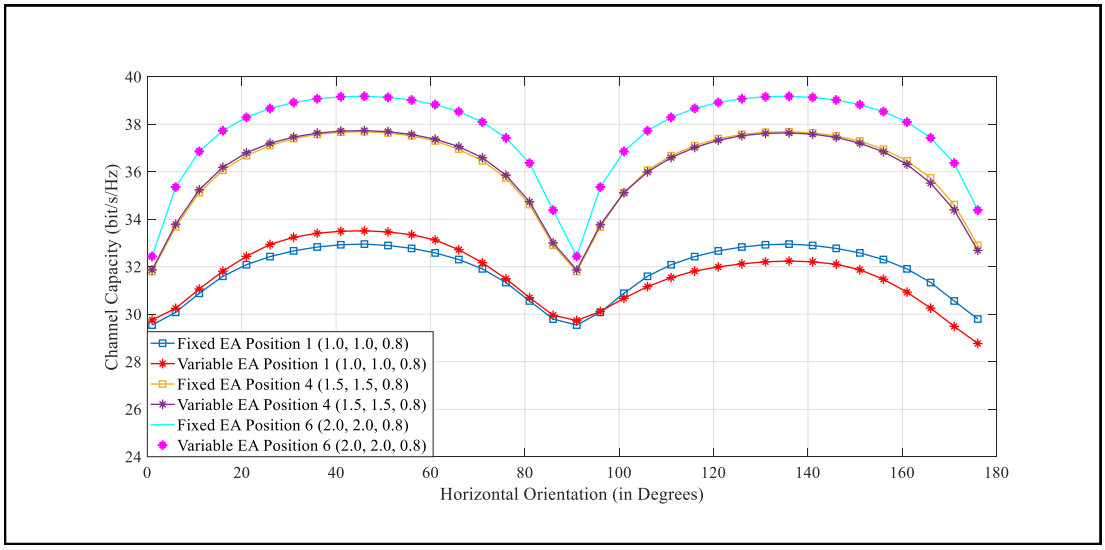

Figure 4.16. Capacity variation with respect to horizontal orientation angle of the receiver

4.3.5. Suitable receiver positions across the room

The suitable positions with respect to the capacity performance of the 4×5 MIMO-VLC system for a FOV angle of 60° are given in Figure 4.17. The positions near the corners of the room exhibit a poor capacity performance of 21.61 bit/s/Hz. The positions towards the center of the room present more suitable receiver positions, with the center of the room the most suitable receiver position with a capacity of 41.59 bit/s/Hz. A symmetry in the capacity performance of the 4×5 MIMO-VLC system can be observed around the center point i.e., x = y = 2m. However, due to the presence of the 5^{th} PD, the capacity performance of 4×5 MIMO-VLC system at corners of the room is better as compared to 4×4 MIMO-VLC system.

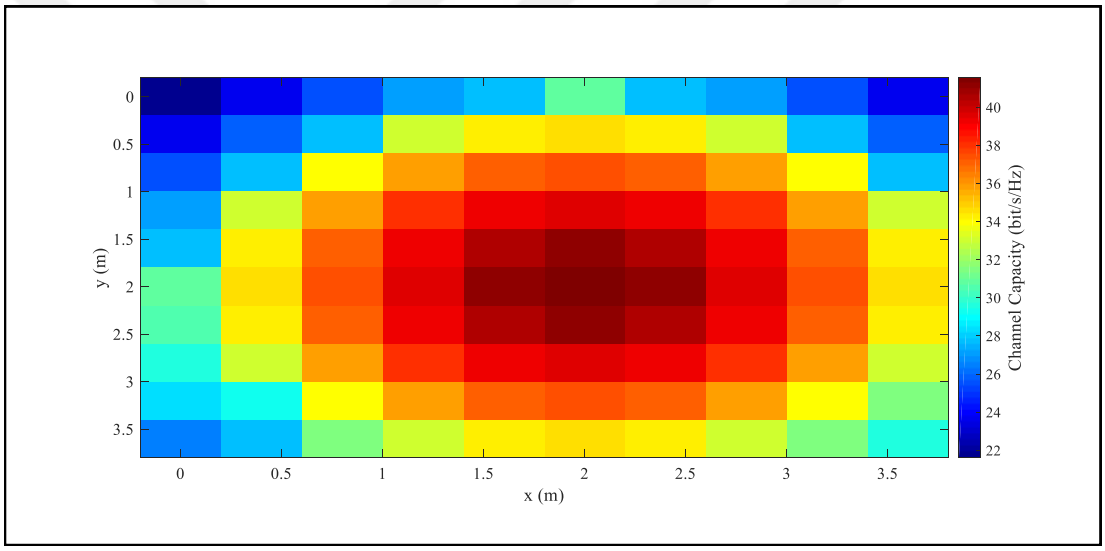

Figure 4.17. Capacity variation across entire room for the FOV angle of 60°

4.4. Capacity performance of a 5x5 MIMO-VLC system

The capacity performance of the 5×5 MIMO-VLC system is explored in this section. The difference in capacity performance for fixed and variable EA MIMO-VLC systems have also been highlighted in this section. Similarly, the impact on the performance of the 5×5 MIMO-VLC system by factors such as FOV angle, LED transmitter array length, and horizontal orientation angle of the receiver has also been explored and discussed in this section.

4.4.1. Capacity variation with respect to EA and fixed EA MIMO-VLC system

The EA for 5×5 MIMO-VLC system is also varied from 0° to 90°, just like its counterparts i.e., 4×4 and 4×5 MIMO-VLC systems. The FOV angle and transmitter array length are considered to be 90° and 2 m, respectively. The position 6 (2.0, 2.0, 0.8) being located at the center of the room, receives the information from all the LEDs. As a result, the capacity performance of position 6 (2.0, 2.0, 0.8) is better than the rest of the considered receiver positions. The position 6 (2.0, 2.0, 0.8) attains a C_{max} value of 45.44 bit/s/Hz. As we move away from the center of the room, the capacity performance degrades for the remaining positions. The position 0 (0.5, 0.5, 0.8) performs the worst of all the considered positions with a C_{max} value of 27.35 bit/s/Hz. For each respective position of the receiver, a C_{max} and EA value is attained as shown in Figure 4.18. This optimum EA value is assumed the same for all the PDs, which constitutes the fixed EA MIMO-VLC system. The respective C_{max} and optimum EA values are given in Table 4.12. When compared with a 4×4 fixed EA MIMO-VLC system, a maximum percentage gain in capacity is seen at position 6 (2.0, 2.0, 0.8) i.e., 19.07%. As we move towards the corner of the room, the percentage gain decreases for the respective

Table 4.12. Optimum fixed EAs that result in C_{max} & percentage gain for considered receiver positions for FOV angle of 90°

Considered Positions of the receiver (x,y,z)	**C_{max} of the fixed EA system (bit/s/Hz)**	**Optimum EAs (in Deg) of the fixed EA system $[\theta_{m1}\ \theta_{m2}\ \theta_{m3}\ \theta_{m4}]$**	**Capacity gain(%) w.r.t 4x4 fixed EA MIMO-VLC system**
Position 0 (0.5, 0.5, 0.8)	27.35	[70 70 70 70]	9.22
Position 1 (1.0, 1.0, 0.8)	35.49	[58 58 58 58]	11.40
Position 2 (1.5, 1.0, 0.8)	39.18	[61 61 61 61]	14.54
Position 3 (2.0, 1.0, 0.8)	40.56	[64 64 64 64]	15.93
Position 4 (1.5, 1.5, 0.8)	42.91	[66 66 66 66]	17.28
Position 5 (2.0, 1.5, 0.8)	44.18	[68 68 68 68]	18.22
Position 6 (2.0, 2.0, 0.8)	45.44	[70 70 70 70]	19.07

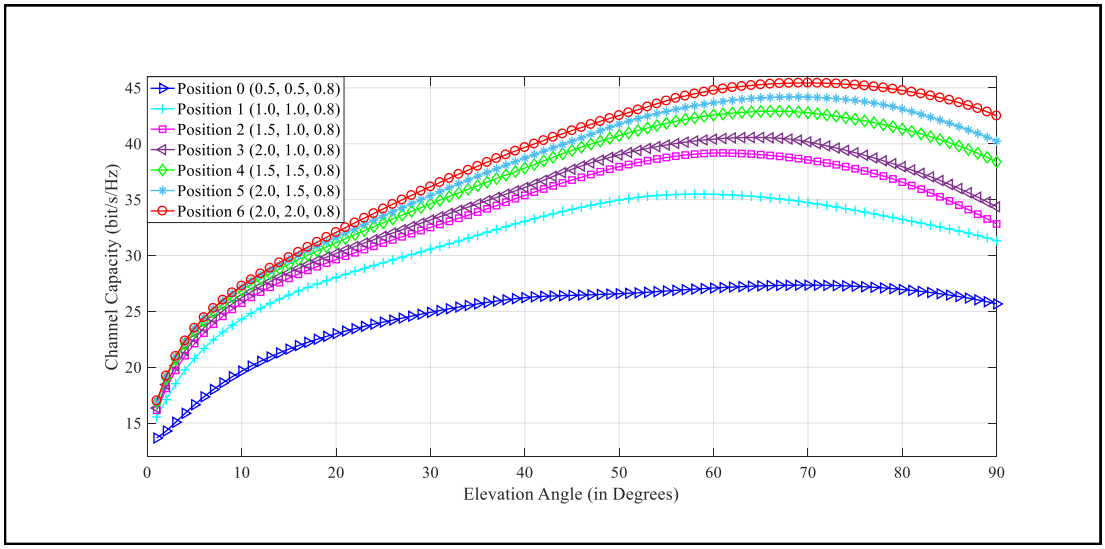

Figure 4.18. Capacity variation with EA for considered receiver positions

positions. At position 0 (0.5, 0.5, 0.8), a percentage gain of 9.22% is observed. As the M^{th} LED is placed at the center of the room i.e., (2.0, 2.0, 2.7), the maximum channel capacity improvement is observed for the position 6 (2.0, 2.0, 0.8).

4.4.2. 5x5 Variable EA MIMO-VLC system

The variable EAs for 5×5 MIMO-VLC system is found by varying the EA of individual PDs in the range from 0° to 90°. The performance of the variable EA MIMO-VLC system is better as compared to the fixed EA MIMO-VLC system as shown in Figure 4.19. The maximum gain in capacity is attained at position 0 (0.5, 0.5, 0.8). However,

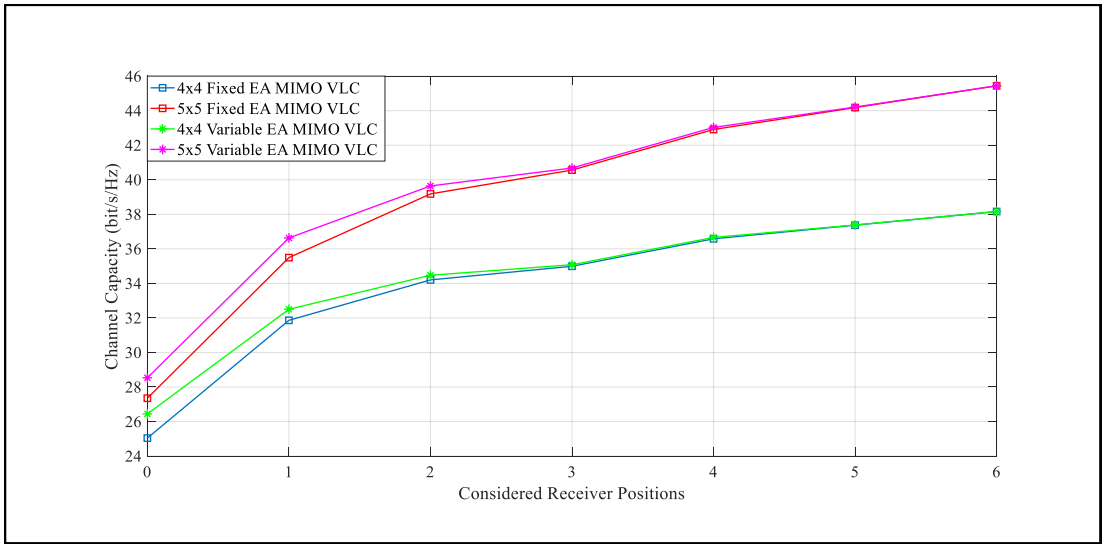

Figure 4.19. Maximum channel capacity comparison for considered positions of 4x4 and 5x5 MIMO-VLC systems

Table 4.13. Optimum variable EAs that result in C_{max} & capacity gain(%) for considered receiver positions for FOV angle of 90°

Considered Positions of the receiver (x,y,z)	**C_{max} of the variable EA system (bit/s/Hz)**	**Optimum EAs (in Deg) of the variable EA system $[\theta_{m1}\ \theta_{m2}\ \theta_{m3}\ \theta_{m4}]$**	**Capacity gain(%) w.r.t 4x4 variable EA MIMO-VLC system**
Position 0 (0.5, 0.5, 0.8)	28.53	[71 69 37 69]	7.91
Position 1 (1.0, 1.0, 0.8)	36.63	[73 70 49 69]	12.74
Position 2 (1.5, 1.0, 0.8)	39.64	[73 72 56 66]	15.03
Position 3 (2.0, 1.0, 0.8)	40.68	[73 73 61 61]	15.98
Position 4 (1.5, 1.5, 0.8)	43.03	[73 70 61 70]	17.38
Position 5 (2.0, 1.5, 0.8)	44.21	[72 72 66 66]	18.26
Position 6 (2.0, 2.0, 0.8)	45.44	[70 70 70 70]	19.07

as we move towards the center of the room, the gain in performance decreases. At position 6 (2.0, 2.0, 0.8), the capacity of the fixed and variable EA MIMO-VLC systems becomes equal as the EA values become the same. For each respective receiver position, the C_{max} value along with optimum variable EA is given in Table 4.13. The channel capacity of 5×5 MIMO-VLC system is better as compared to 4×4 MIMO-VLC system as shown in Figure 4.19. The percentage gain in capacity performance of 5×5 variable EA MIMO-VLC system when compared with 4×4 variable EA MIMO-VLC system is also provided in Table 4.13. The maximum capacity gain is achieved at the position 6 (2.0, 2.0, 0.8). Towards the corner of the room, the gain in capacity decreases resulting in only a meager capacity gain of 7.91%.

4.4.3. Maximum channel capacity comparison of 5x5 ADR and N-ADR based MIMO-VLC systems

The simulation parameters are kept constant in order to determine the performance of 5×5 N-ADR based MIMO-VLC system. The horizontal orientation angle and EA are assumed to be 0° as shown in Figure 3.7. The capacity performance of the 5×5 N-ADR based MIMO-VLC system follow the same trend as 5×5 ADR based MIMO-VLC

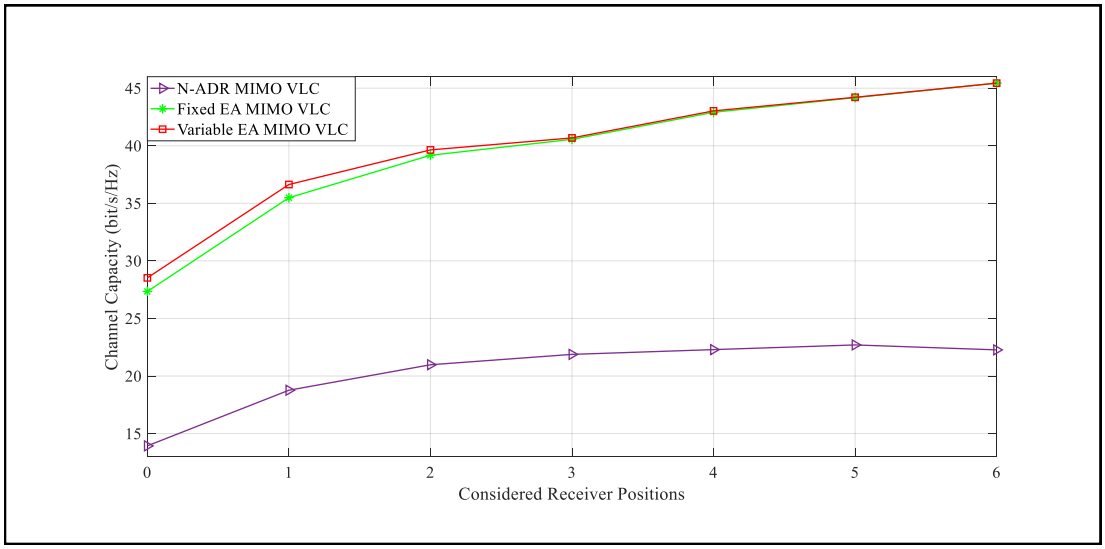

Figure 4.20. Maximum channel capacity comparison for 5x5 N-ADR and ADR based MIMO-VLC systems

system as shown in Figure 4.20. As the position 0 (0.5, 0.5, 0.8) is located very close to the corner of the room, it performs the worst among all the considered receiver positions. Only a throughput of 13.94 bit/s/Hz is recorded for position 0 (0.5, 0.5, 0.8). The position 5 (2.0, 1.5, 0.8) performs the best and attains a capacity of 22.71 bit/s/Hz. When compared with 4×4 N-ADR MIMO-VLC system, a minimum capacity gain of 1.24% is attained at position 0 (0.5, 0.5, 0.8). Towards the center of the room, the capacity gain increases, and maximum capacity gain of 9.64% is attained at position 3 (1.5, 1.0, 0.8). After position 3 (1.5, 1.0, 0.8), the capacity gain decreases slightly and a capacity gain of 4.11% is attained at position 6 (2.0, 2.0, 0.8). The variation in gain depends on the respective position of the receiver and channel correlation. The capacity values of N-ADR and ADR MIMO-VLC systems are given in Table 4.14. The performance of the 5×5 ADR based MIMO-VLC system is much better than 5×5 N-ADR based MIMO-VLC system as shown in Figure 4.20. A difference of 13.41 bit/s/Hz and 14.59 bit/s/Hz is observed for position 0 (0.5, 0.5, 0.8) of fixed and variable EA MIMO-VLC systems, respectively. As we move away from the corner of the room and towards the center of the room, the difference in capacity between ADR and N-ADR MIMO-VLC systems increases. At position 6 (2.0, 2.0, 0.8), the difference in the capacity of 23.17 bit/s/Hz is recorded for fixed and variable EA MIMO-VLC systems.

Table 4.14. Maximum channel capacity for 5x5 N-ADR, fixed EA and variable EA MIMO-VLC systems

Considered Positions of the Receiver (x,y,z)	**C_{max} of the N-ADR system (bit/s/Hz)**	**C_{max} of the fixed EA system (bit/s/Hz)**	**C_{max} of the variable EA system (bit/s/Hz)**
Position 0 (0.5, 0.5, 0.8)	13.94	27.35	28.53
Position 1 (1.0, 1.0, 0.8)	18.77	35.49	36.63
Position 2 (1.5, 1.0, 0.8)	20.98	39.18	39.64
Position 3 (2.0, 1.0, 0.8)	21.88	40.56	40.68
Position 4 (1.5, 1.5, 0.8)	22.30	42.91	43.03
Position 5 (2.0, 1.5, 0.8)	22.71	44.18	44.21
Position 6 (2.0, 2.0, 0.8)	22.29	45.44	45.44

4.4.4. Factors influencing the performance of 5x5 MIMO-VLC system

In this section, the impact of different factors on the performance of 5×5 MIMO-VLC system has been explored. One of the factors including the FOV angle, LED transmitter array length, and horizontal orientation angle is varied at a time and its impact on the performance of the MIMO-VLC system is explored accordingly.

4.4.4.1. FOV angle

The performance of the MIMO-VLC system is dependent on the FOV angle. The performance of the 5×5 MIMO-VLC system varies as the FOV angle is changed from 90° to 60°. As the capacity performances change with the FOV angle, so does the values of optimum EA values for fixed and variable EA MIMO-VLC systems. The performance of the N-ADR based MIMO-VLC system shows a slight change when the FOV angle is changed. However, the C_{max} value of the fixed and variable EA MIMO-VLC system improves as the FOV angle is changed from 90° to 60° as shown in Figure 4.21. The channel capacity performance improves as a narrow FOV angle results in a low ISI and a more direct beam from LEDs to PDs.

Table 4.15. Maximum channel capacity for fixed EA and variable EA MIMO-VLC systems when FOV= 60°

Considered positions of the receiver (x,y,z)	**C_{max} of the fixed EA system (bit/s/Hz)**	**Optimum EA (in Deg) of the fixed EA system $\theta_m^i = \theta_A$**	**C_{max} of the variable EA system (bit/s/Hz)**	**Optimum EAs (in Deg) of the variable EA system $[\theta_{m1}\ \theta_{m2}\ \theta_{m3}\ \theta_{m4}]$**
Position 0 (0.5, 0.5, 0.8)	29.29	[49 49 49 49]	32.50	[81 46 11 46]
Position 1 (1.0, 1.0, 0.8)	38.89	[52 52 52 52]	40.80	[72 52 24 52]
Position 2 (1.5, 1.0, 0.8)	41.00	[49 49 49 49]	43.52	[63 76 31 45]
Position 3 (2.0, 1.0, 0.8)	42.00	[48 48 48 48]	45.24	[79 79 38 38]
Position 4 (1.5, 1.5, 0.8)	45.80	[58 58 58 58]	47.49	[81 58 40 58]
Position 5 (2.0, 1.5, 0.8)	46.79	[70 70 70 70]	48.65	[70 70 49 49]
Position 6 (2.0, 2.0, 0.8)	49.82	[60 60 60 60]	49.82	[60 60 60 60]

The modified capacity values along with new optimum EA values for fixed and variable EA MIMO-VLC systems is given in TABLE 4.15. The performance of 60° employed ADR MIMO-VLC system is better than its counterpart i.e., 90° employed ADR MIMO-VLC system and follows the same trend. The performance of the variable EA MIMO-VLC system is better than the fixed EA MIMO-VLC system. At position 6 (2.0, 2.0, 0.8), the EA for fixed and variable EA MIMO-VLC systems becomes equal, resulting in a capacity of 41.82 bit/s/Hz. The position 6 (2.0, 2.0, 0.8) presents the most suitable location of the receiver in terms of capacity performance whereas position 0 (0.5, 0.5, 0.8) presents the worst position and attains a channel capacity of only 29.29 bit/s/Hz and 32.50 bit/s/Hz for fixed and variable EA MIMO-VLC systems, respectively.

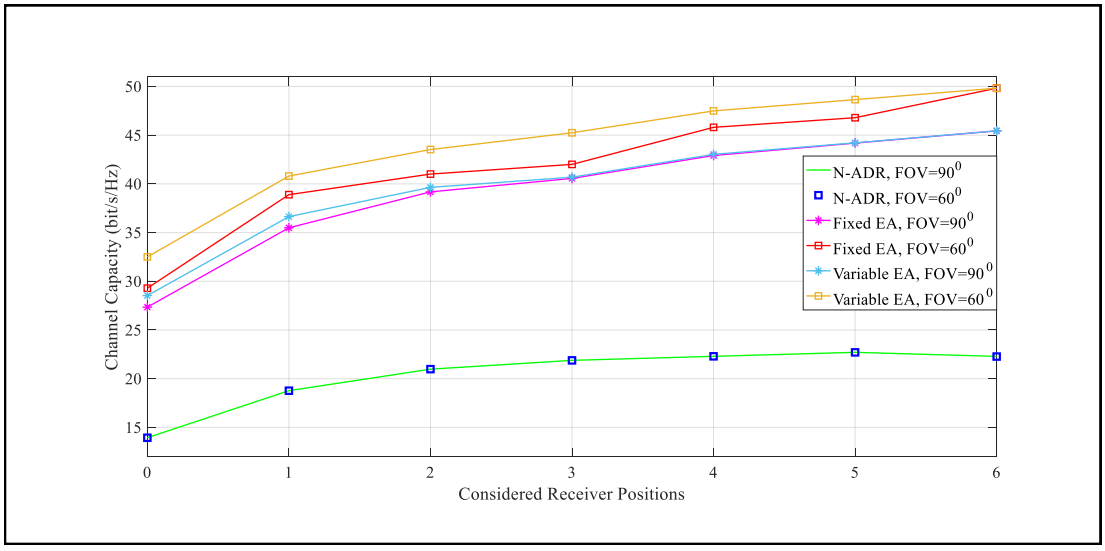

Figure 4.21. Maximum channel capacity for FOV angles of 60° and 90°

4.4.4.2. LED transmitter array length

We have selected position 1 (1.0, 1.0, 0.8) and position 6 (2.0, 2.0, 0.8) as our reference positions for performance comparison. We start varying the d_{tx} from the center of the room. The d_{tx} is varied in a step-size of 10 cm until we arrive close to the boundary of the room i.e., 0.5 m away from the boundary. The capacity variation with d_{tx} for the 5×5 MIMO-VLC system is given in Figure 4.22. The pattern of the capacity variation of 5×5 MIMO-VLC systems is the same as its counterparts. The capacity initially increases with the d_{tx} until $d_{tx\text{-}opt}$ is reached at which C_{max} is attained. After the $d_{tx\text{-}opt}$ any further increase in the d_{tx} results in a drop in the value of C_{max}. The respective

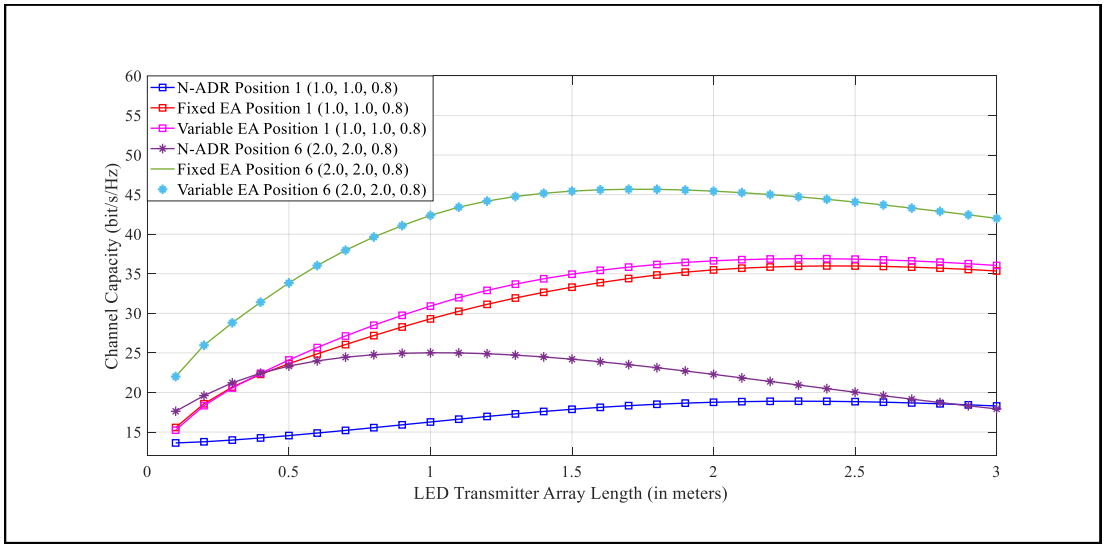

Figure 4.22. Capacity variation of a 5x5 MIMO-VLC system with d_{tx} when FOV= 90°

Table 4.16. Capacity variation of a 5x5 MIMO-VLC system with d_{tx} when FOV= 90°

Considered positions of the receiver (x,y,z)	**C_{max} of the N-ADR system (bit/s/Hz)**	**$d_{tx\text{-}opt}$ values (m)**	**C_{max} of the fixed EA system (bit/s/Hz)**	**$d_{tx\text{-}opt}$ values system (m)**	**$C_{max}$of the variable EA system (bit/s/Hz)**	**$d_{tx\text{-}opt}$ values (m)**
Position 0 (0.5, 0.5, 0.8)	15.60	3.0	29.21	3.0	30.48	3.0
Position 1 (1.0, 1.0, 0.8)	18.90	2.3	35.99	2.4	36.91	2.3
Position 2 (1.5, 1.0, 0.8)	21.01	1.9	39.23	2.1	39.67	2.1
Position 3 (2.0, 1.0, 0.8)	21.99	1.8	40.56	2.0	40.68	2.0
Position 4 (1.5, 1.5, 0.8)	23.15	1.4	42.94	1.9	43.07	1.9
Position 5 (2.0, 1.5, 0.8)	24.10	1.2	44.30	1.8	44.33	1.8
Position 6 (2.0, 2.0, 0.8)	25.02	1.0	45.68	1.7	45.68	1.7

C_{max} values along with $d_{tx\text{-}opt}$ for the considered receiver positions are given in Table 4.16. The values located towards the center of the room requires comparatively smaller d_{tx} values as compared to the receiver positions near the corners of the room. Thus, by adjusting the d_{tx} values, the performance of the MIMO-VLC system can be improved accordingly.

4.4.4.3. Horizontal orientation of the receiver

The performance of the ADR based MIMO-VLC system can be improved by selecting a suitable horizontal orientation angle with respect to the position of the receiver. We have considered the horizontal orientation and EA for N-ADR based MIMO-VLC system as 0° throughout this dissertation. We have selected position 1 (1.0, 1.0, 0.8), position 4 (1.5, 1.5, 0.8), and position 6 (2.0, 2.0, 0.8) for the purpose of performance comparison

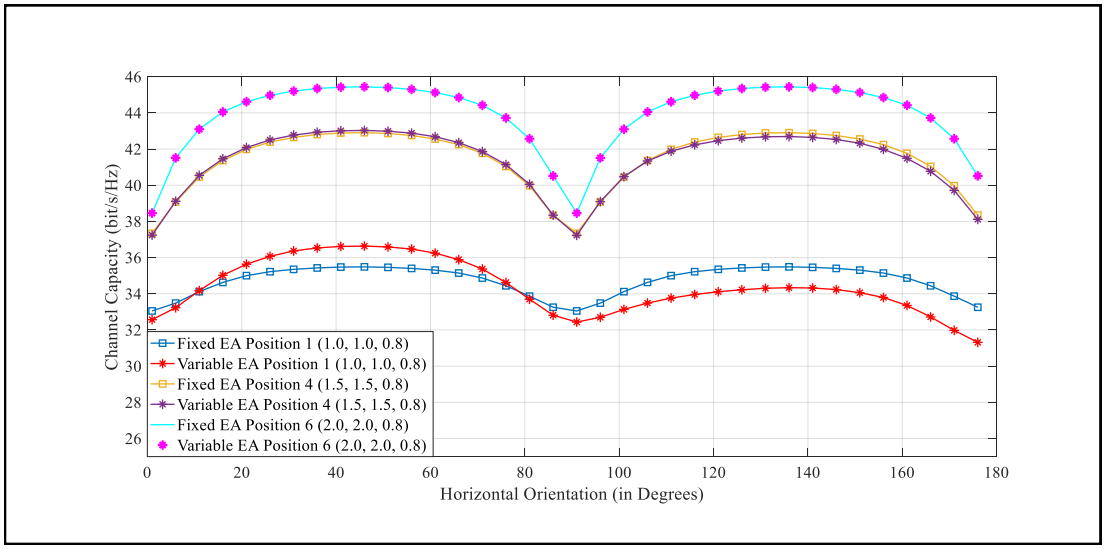

Figure 4.23. Capacity variation with respect to horizontal orientation angle of the receiver

for the ADR based MIMO-VLC system when the horizontal orientation angle is varied from 0° to 180°. Due to the symmetry of the MIMO-VLC system, the 5×5 MIMO-VLC system is symmetric for every 45°. The capacity of 5×5 MIMO-VLC system initially rises with the horizontal orientation angle to an angle of 45° at which C_{max} is attained. The capacity drops in the region 45° to 90° where C_{min} is reached at 90°. A similar trend is repeated in the second cycle for the ADR based MIMO-VLC system. A C_{max} is attained at an angle of 135° and a C_{min} is attained at an angle of 180° as shown in Figure 4.23. The fixed EA MIMO-VLC system follows a perfect symmetry whereas the variable EA MIMO-VLC system does not follow a perfect symmetry. The performance of variable EA is better as compared to the fixed EA MIMO-VLC system in the first cycle. However, in the second cycle. the performance of the variable EA MIMO-VLC system becomes worse than the fixed EA MIMO-VLC system as shown in Figure 4.23.

4.4.5. Suitable receiver positions across the room

The suitable positions in terms of channel capacity across the entire room for 5×5 MIMO-VLC system for a FOV angle of 60° is plotted in Figure 4.24. The center of the room presents an ideal position for the receiver, resulting in a C_{max} value of 49.69 bit/s/Hz. As we move away from the center of the room, the capacity performance slowly degrades. The corners of the room present the worst position for the receiver

resulting in a channel capacity of only 24.46 bit/s/Hz. However, across the entire room, the capacity performance of 5×5 MIMO-VLC system is much better as compared to 4×4 and 4×5 MIMO-VLC systems.

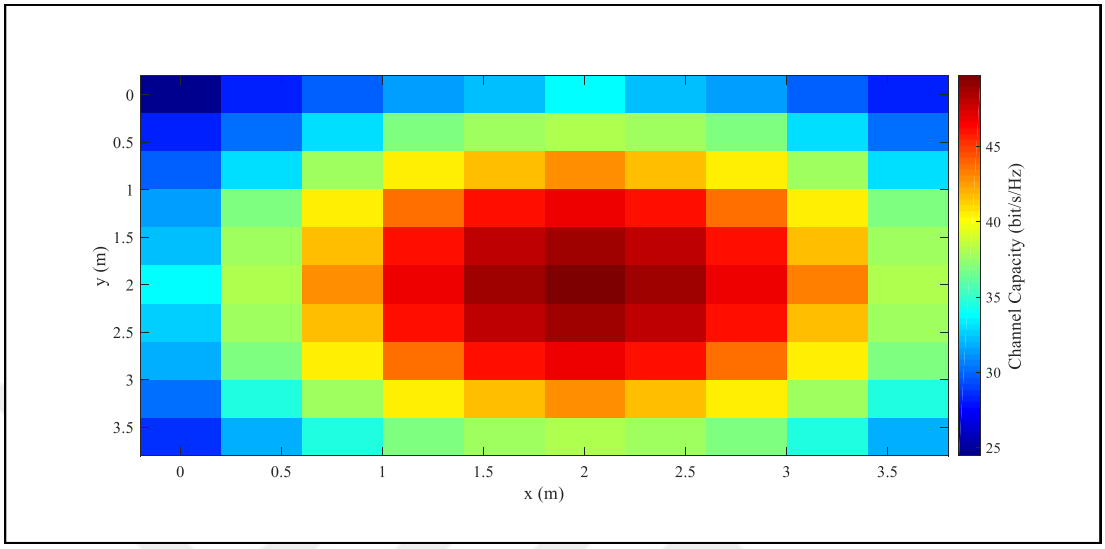

Figure 4.24. Capacity variation across entire room for the FOV angle of 60°

4.5. An overview of channel capacity for ADR and N-ADR 4x4, 4x5, and 5x5 MIMO VLC systems for FOV angle of 60° and 90°

In this section, we will provide an overview and comparison for channel capacity between N-ADR and ADR based different MIMO VLC systems. As it is very clear that by increasing the number of LEDs and PDs, the channel capacity of the MIMO-VLC system can be improved. The position 0 (0.5, 0.5, 0.8) always results in comparatively poor performance with respect to other receiver positions. Therefore, to have a fair comparison in terms of channel capacity, we have chosen position 1 (1.0, 1.0, 0.8), position 4 (1.5, 1.5, 0.8), and position 6 (2.0, 2.0, 0.8) for ADR and N-ADR based MIMO-VLC systems.

At first, we observe the channel capacity curve with EA for ADR-MIMO VLC systems. For N-ADRs, the horizontal orientation and EA is 0°. As we can see from the Figure 4.25, the channel capacity of the 5×5 MIMO-VLC system is better for all the considered receiver positions as compared to 4×4 and 4×5 MIMO-VLC systems. The channel capacity of position 4 (1.5, 1.5, 0.8) of the 5×5 MIMO-VLC system is better than position 6 (2.0, 2.0, 0.8) of the remaining considered MIMO-VLC systems. Similarly,

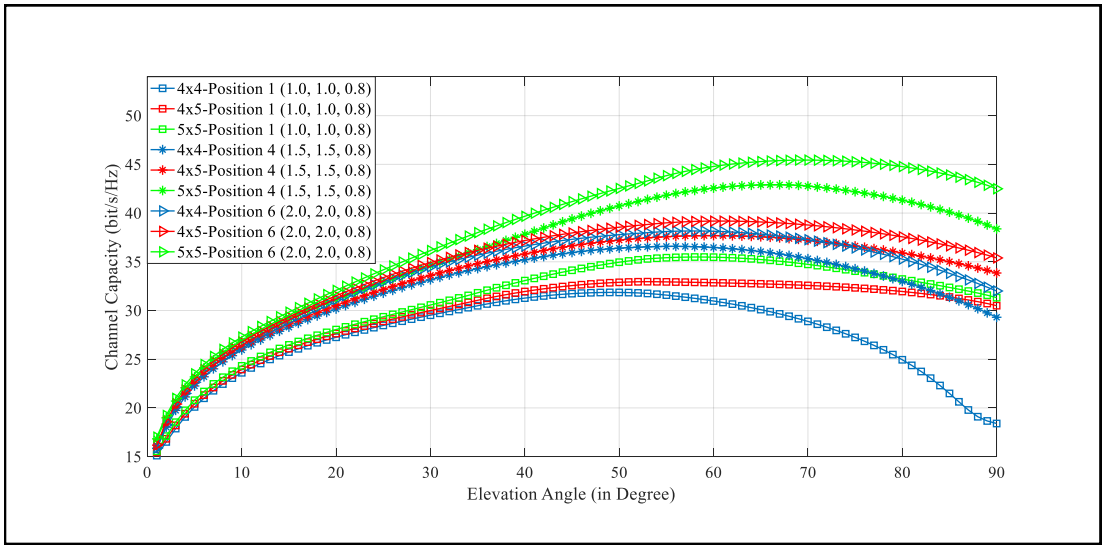

Figure 4.25. Channel capacity variation with respect to elevation angle of the receiver

the channel capacity of the 4×5 MIMO-VLC system is better as compared to the 4×4 MIMO-VLC system for all the considered positions of the receiver. Therefore, by the addition of a single PD and LED to a MIMO-VLC system, the channel capacity performance is improved significantly. The behavior of the channel capacity curves with EA is the same for all the MIMO-VLC systems. The channel capacity curve initially increases with EA until C_{max} is achieved at an optimum EA. After the optimum EA is achieved, the channel capacity starts dropping as shown in Figure 4.25.

A comparison in peak channel capacity of N-ADR and ADR based MIMO VLC systems for a FOV angle of 90° is shown in Figure 4.26. The ADR based MIMO-VLC system outperforms N-ADR based MIMO VLC system for all the considered receiver positions. Moreover, the channel capacity of a lower order i.e., 4×4 ADR MIMO-VLC system is better than a higher-order i.e., 5×5 N-ADR based MIMO VLC systems.

Similarly, for positions 1 and 4, the channel capacity of the variable EA MIMO-VLC system is always better than the fixed EA MIMO-VLC system. However, as the variable and fixed EAs become the same at the center of the room i.e., position 6 (2.0, 2.0, 0.8), the channel capacity values also become the same.

In a similar manner, the channel capacity for N-ADR and ADR based MIMO VLC systems are evaluated and given in Figure 4.27 for FOV angle of 60°. The ADR based MIMO-VLC systems outperforms the N-ADR MIMO-VLC system as shown in Figure

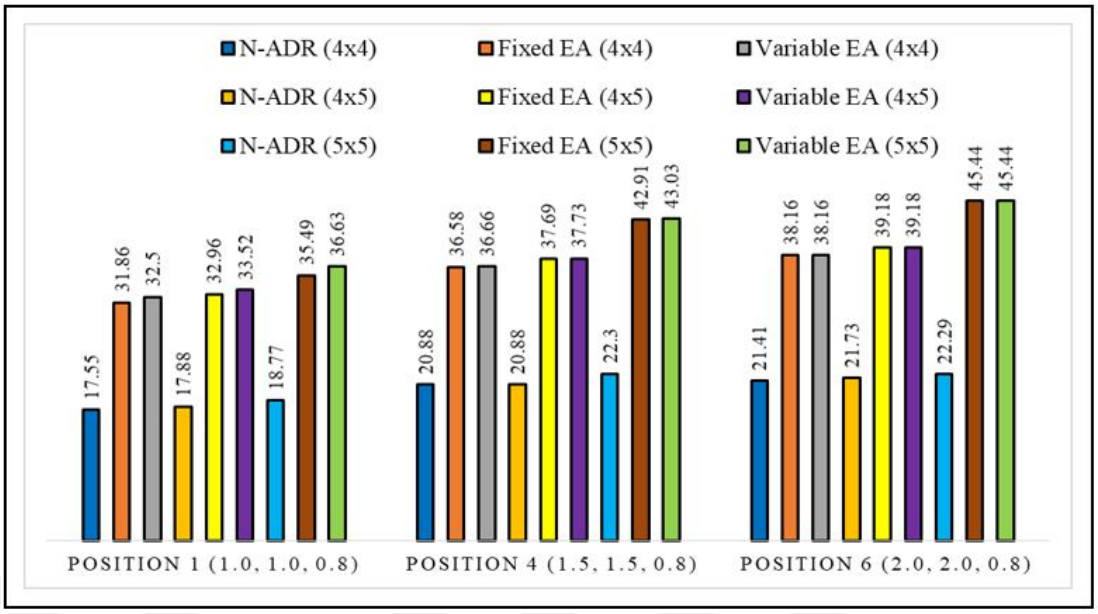

Figure 4.26. Peak channel capacity (bit/s/Hz) values of N-ADR, fixed and variable EA MIMO VLC system when FOV 90°

4.27. Similarly, the variable EA MIMO-VLC system results in a better performance than the fixed EA MIMO-VLC system. However, this channel capacity gain is achieved at the cost of the receiver design complexity.

The ADR based MIMO-VLC system results in higher peak values for FOV 60° as compared to FOV 90°. This gain in channel capacity results from the fact that a

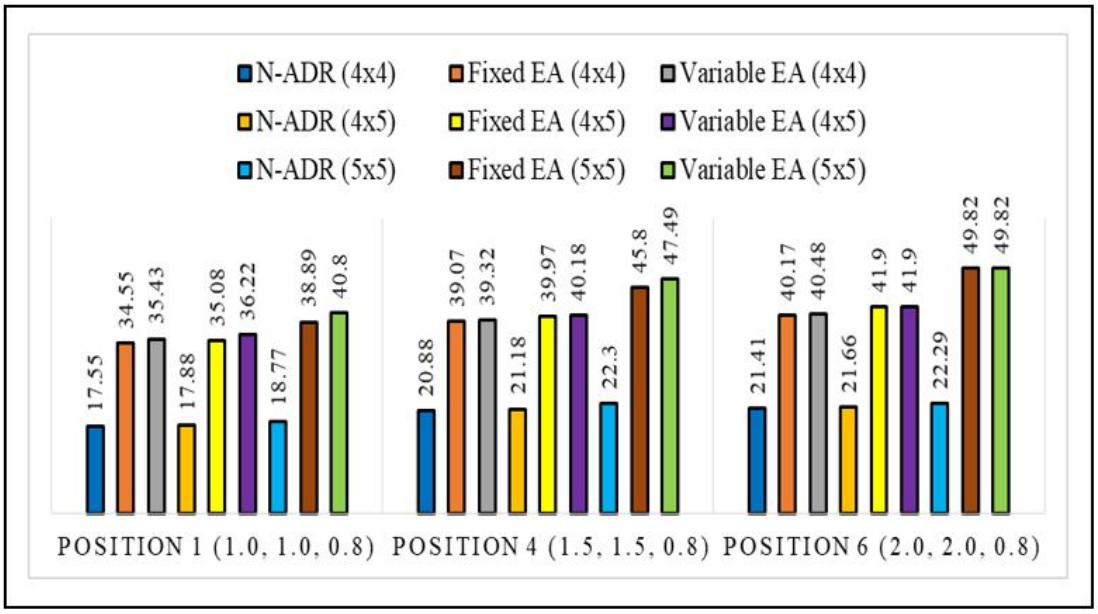

Figure 4.27. Peak channel capacity (bit/s/Hz) values of N-ADR, fixed and variable EA MIMO VLC system when FOV 60°

narrow FOV angle allows us to achieve a higher transmission rate and lower levels of ISI. However, a narrow FOV angle also results in uneven optical power distribution. Moreover, a narrow FOV angle may also result in limiting the viewing area of the PD, thus, creating blind spots. Therefore, it is important to select an optimal FOV angle to improve system performance.

The performance of the N-ADR based MIMO-VLC system remains the same for both FOV angles. The channel matrix entries for N-ADR MIMO VLC systems almost remains the same for both FOV angles, resulting in an almost similar performance. The channel capacity gain (%) for ADR based MIMO VLC system when FOV is varied from 90° to 60° is shown in the Figure 4.28.

The respective channel capacity gain (%) depends upon the position of the receiver and the respective channel capacity values. The 4×4 MIMO-VLC system shows a decreasing trend as we move from position 1 (1.0, 1.0, 0.8) to position 6 (2.0, 2.0, 0.8) for fixed and variable EA MIMO-VLC systems. Similarly, for the 5x5 variable EA MIMO-VLC system, a maximum gain (%) is observed at position 1 (1.0, 1.0, 0.8). For the rest of the considered position, maximum gain (%) is observed at position 6 (2.0, 2.0, 0.8).

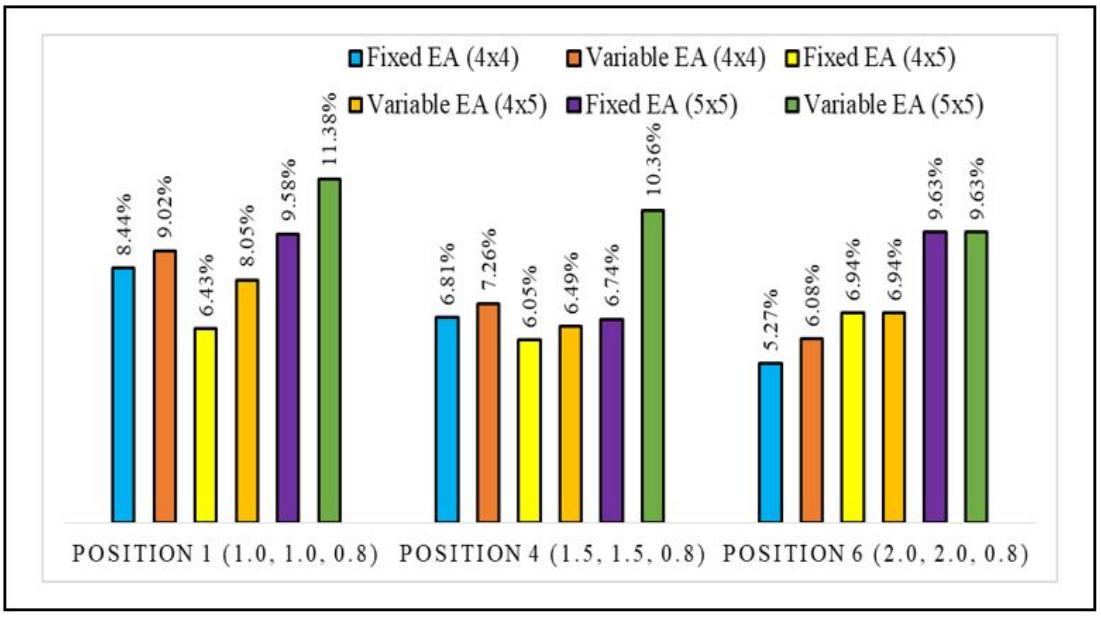

Figure 4.28. Channel capacity gain(%) when FOV angle is changed from 90° to 60°

4.6. BER Performance of MIMO-VLC Systems

In this section, we will evaluate and compare the BER performance of 4×4 and 5×5 MIMO-VLC systems. We have considered two transmission mechanisms i.e., RC and SMP. In order to conduct a fair comparison between the BER performance of the MIMO-VLC systems, we have considered the I and R_{spec} constant for both the transmission schemes. For the RC, the R_{spec} does not depend upon the number of LED transmitters i.e., $\log_2(K)$ whereas the R_{spec} of SMP depends on the number of LED transmitters i.e., M $\log_2(K)$ where M and K represent number of LED transmitters and signal constellation size, respectively.

4.6.1. 4x4 MIMO-VLC system

As explained in the Chapter 3, for a 4×4 MIMO-VLC system, we have considered R_{spec} of 4 bit/s/Hz and 8 bit/s/Hz. In order to keep the R_{spec} same, we have used 16-PAM and 256-PAM for RC employed MIMO-VLC systems whereas 2-PAM and 4-PAM are used for SMP employed MIMO-VLC systems.

We have selected three positions i.e., position 1 (1.0, 1.0, 0.8), position 4 (1.5, 1.5, 0.8), and position 6 (2.0, 2.0, 0.8) for BER performance comparison of fixed and variable EA MIMO-VLC systems. The BER performance of fixed and variable EA RC employed MIMO-VLC system is given in Figure 4.29. As it can be seen from Figure 4.29 that the

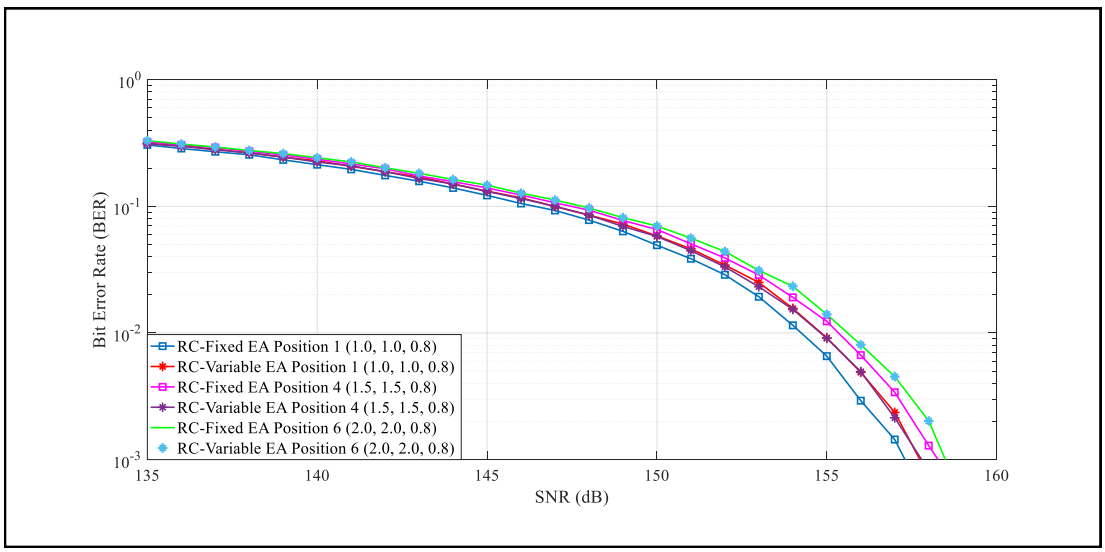

Figure 4.29. BER performance of RC employed MIMO-VLC system for R_{spec} = 4 bit/s/Hz

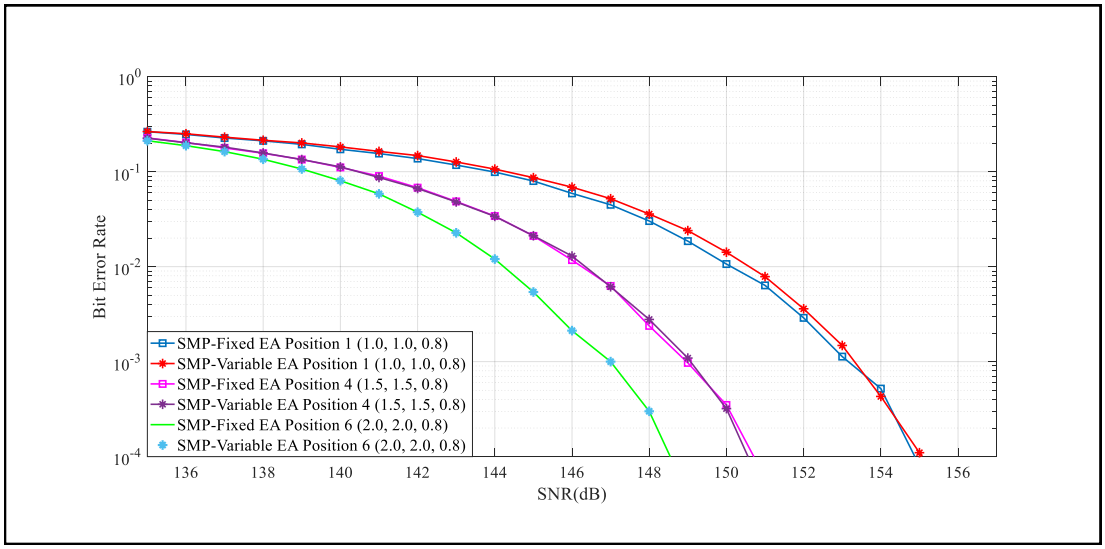

Figure 4.30. BER performance of SMP employed MIMO-VLC system for R_{spec} = 4 bit/s/Hz

BER performance of position 1 (1.0, 1.0, 0.8) is better as compared to position 4 (1.5, 1.5, 0.8) and position 6 (2.0, 2.0, 0.8). The performance of the fixed EA MIMO-VLC system is slightly better than the variable EA MIMO-VLC system. Similarly, the BER performance of the SMP employed MIMO-VLC system is given in 4.30. Position 6 (2.0, 2.0, 0.8) results in the best performance in an SMP employed MIMO-VLC system. For the SMP employed MIMO-VLC system, the performance of fixed and variable EA MIMO-VLC systems is almost the same.

A BER performance comparison between RC and SMP employed MIMO-VLC systems

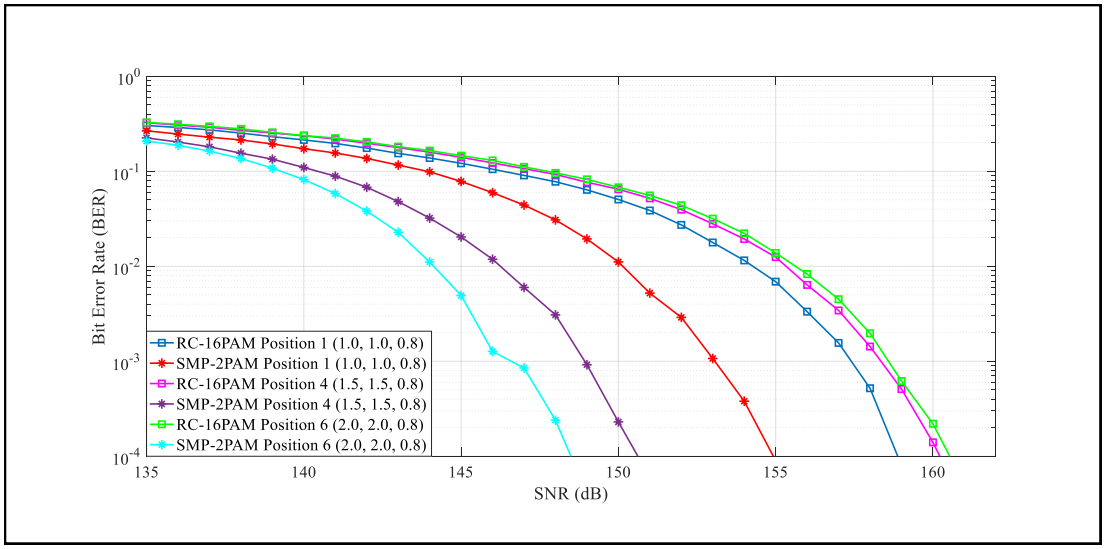

Figure 4.31. BER performance comparison of RC and SMP for R_{spec} = 4 bit/s/Hz

for R_{spec} of 4 bit/s/Hz is presented in Figure 4.31. The BER performance of the SMP employed MIMO-VLC system is much better as compared to RC employed MIMO-VLC system. For RC employed MIMO-VLC systems, we require a larger constellation size to attain the same R_{spec} as that of SMP employed MIMO-VLC systems. As a result of which RC employed MIMO-VLC systems performs worse than SMP employed MIMO-VLC systems.

In a similar manner, the BER performance of RC and SMP employed MIMO-VLC system is analyzed and compared for R_{spec} of 8 bit/s/Hz. The BER plot of RC employed MIMO-VLC is given in Figure 4.32. The BER performance of fixed and variable EA MIMO-VLC systems is almost identical. Moreover, the BER performance of position 1 (1.0, 1.0, 0.8) for RC employed MIMO-VLC system is better as compared to other considered positions. Similarly, the BER graph for SMP employed MIMO-VLC system is presented in Figure 4.33. In an SMP employed MIMO-VLC system, the BER performance of position 6 (2.0, 2.0, 0.8) is better than position 4 (1.5, 1.5, 0.8), which in turn, is better than position 1 (1.0, 1.0, 0.8). Just like its counterpart, the BER performance of fixed and variable EA MIMO-VLC systems is identical.

A comparison plot between RC and SMP employed MIMO-VLC systems for a R_{spec} of 8 bit/s/Hz is given in Figure 4.34. In order to meet the R_{spec} requirement, the RC employed MIMO-VLC systems require larger constellation sizes as compared to SMP

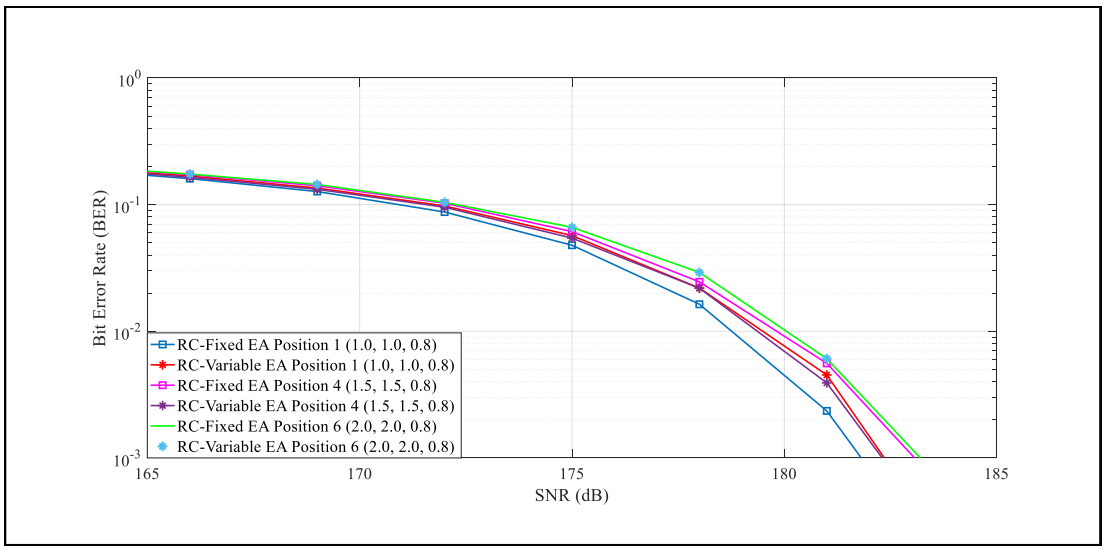

Figure 4.32. BER performance of RC employed MIMO-VLC system for R_{spec} = 8 bit/s/Hz

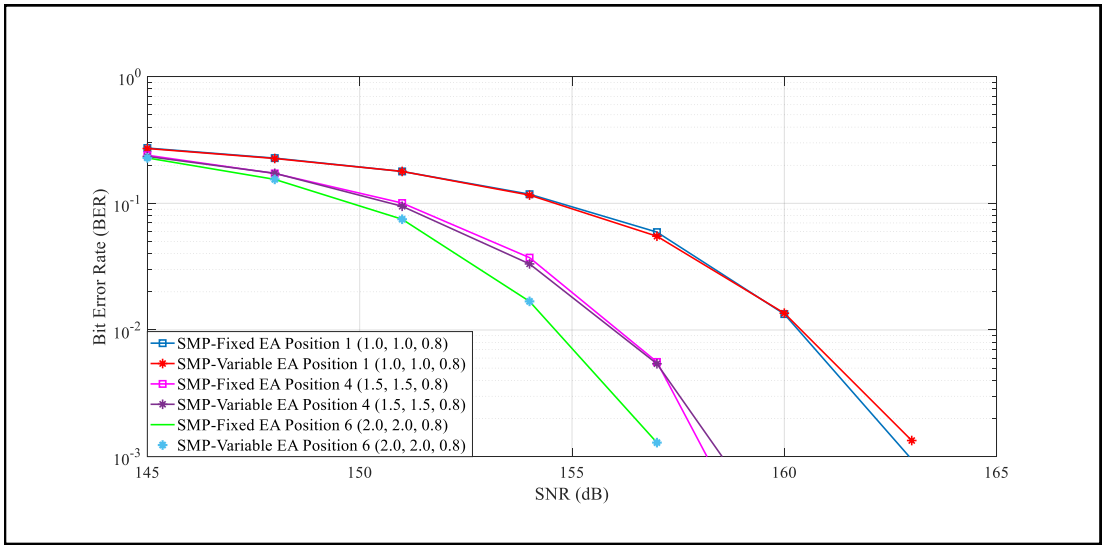

Figure 4.33. BER performance of SMP employed MIMO-VLC system for R_{spec} = 8 bit/s/Hz

employed MIMO-VLC systems. That's why we have used 16-PAM and 256-PAM for RC whereas 2-PAM and 4-PAM are used for SMP employed MIMO-VLC systems. Due to larger constellation sizes, the BER performance of RC is worse than SMP. A maximum difference of approximately 12.5 dB is observed for position 6 (2.0, 2.0, 0.8) of RC and SMP employed MIMO-VLC systems for the R_{spec} of 4 bit/s/Hz. Similarly, a maximum difference of 25 dB has been observed for position 6 (2.0, 2.0, 0.8) for the R_{spec} of 8 bit/s/Hz i.e., for RC to attain the same BER performance, an additional 25 dB is required.

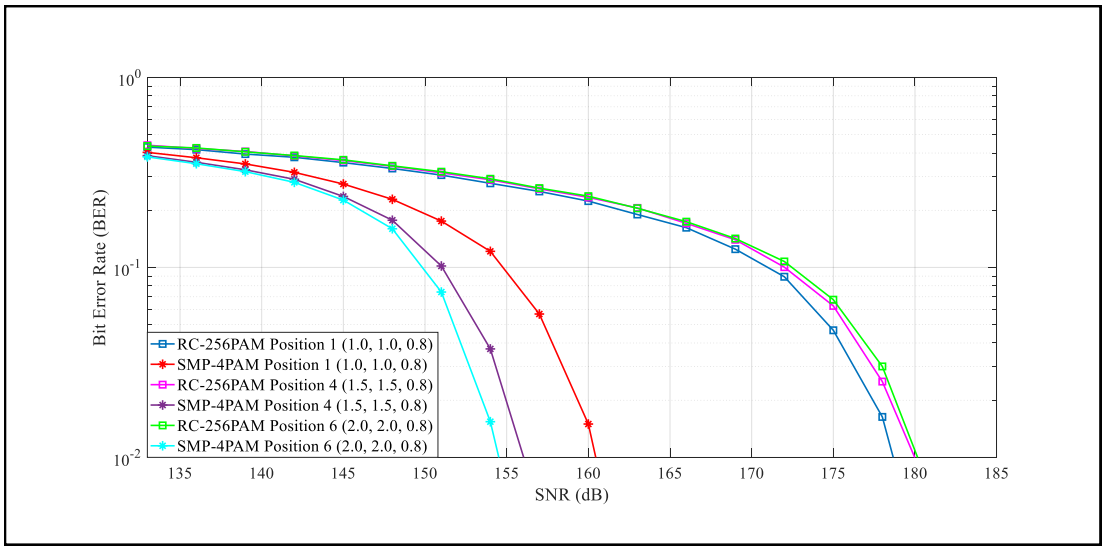

Figure 4.34. BER performance comparison of RC and SMP for R_{spec} = 8 bit/s/Hz

4.6.2. 5x5 MIMO-VLC system

For a 5×5 MIMO-VLC system, in order to have the same R_{spec} for performance comparison between RC and SMP employed MIMO-VLC systems, we have considered R_{spec} of 5 bit/s/Hz and 10 bit/s/Hz. We have used 32-PAM and 1024-PAM for RC employed MIMO-VLC systems whereas 2-PAM and 4-PAM are used for SMP employed MIMO-VLC systems.

To evaluate and compare the performance of 5×5 MIMO-VLC system, we have chosen position 1 (1.0, 1.0, 0.8), position 4 (1.5, 1.5, 0.8), and position 6 (2.0, 2.0, 0.8) as our reference positions. The BER performance of the RC employed MIMO-VLC system is shown in Figure 4.35. The BER performance of RC employed fixed and variable EA MIMO-VLC systems are very similar. position 6 (2.0, 2.0, 0.8) performs the best, followed by position 4 (1.5, 1.5, 0.8) and then position 1 (1.0, 1.0, 0.8). The maximum difference between BER performance of fixed and variable EA MIMO-VLC systems exists for position 1 (1.0, 1.0, 0.8) i.e., approximately 1 dB. For position 4 (1.5, 1.5, 0.8), the difference is extremely small whereas position 6 (2.0, 2.0, 0.8) results in the same performance. Similarly, the plot for the BER performance of SMP employed MIMO-VLC system is given in Figure 4.36. For a 5×5 SMP employed MIMO-VLC system, the BER performance of the variable EA is better for position 1 (1.0, 1.0, 0.8) as compared to the fixed EA MIMO-VLC system with a difference of 1 dB. For the rest

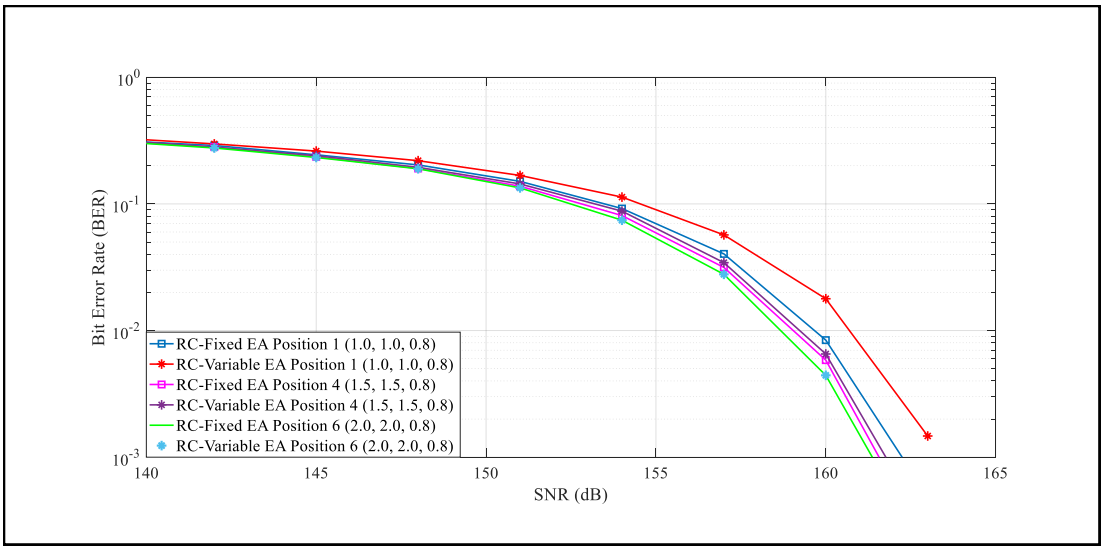

Figure 4.35. BER performance of RC employed MIMO-VLC system for R_{spec} of 5 bit/s/Hz

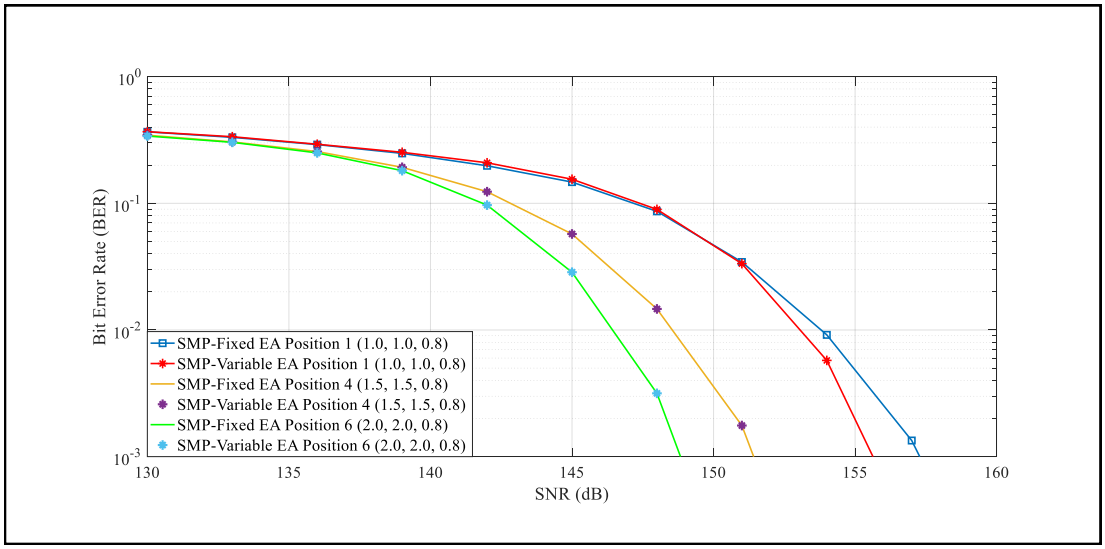

Figure 4.36. BER performance of SMP employed MIMO-VLC system for R_{spec} of 5 bit/s/Hz

of the considered positions i.e., position 4 (1.5, 1.5, 0.8) and position 6 (2.0, 2.0, 0.8), the BER performance of the fixed and variable EA MIMO-VLC systems is identical.

A comparison between the BER performance of RC and SMP employed MIMO-VLC systems for a R_{spec} of 5 bit/s/Hz is given in Figure 4.37. The performance of the SMP employed MIMO-VLC system is better as compared to RC employed MIMO-VLC system because of the fact that a smaller constellation size was required for SMP to attain the same R_{spec}.

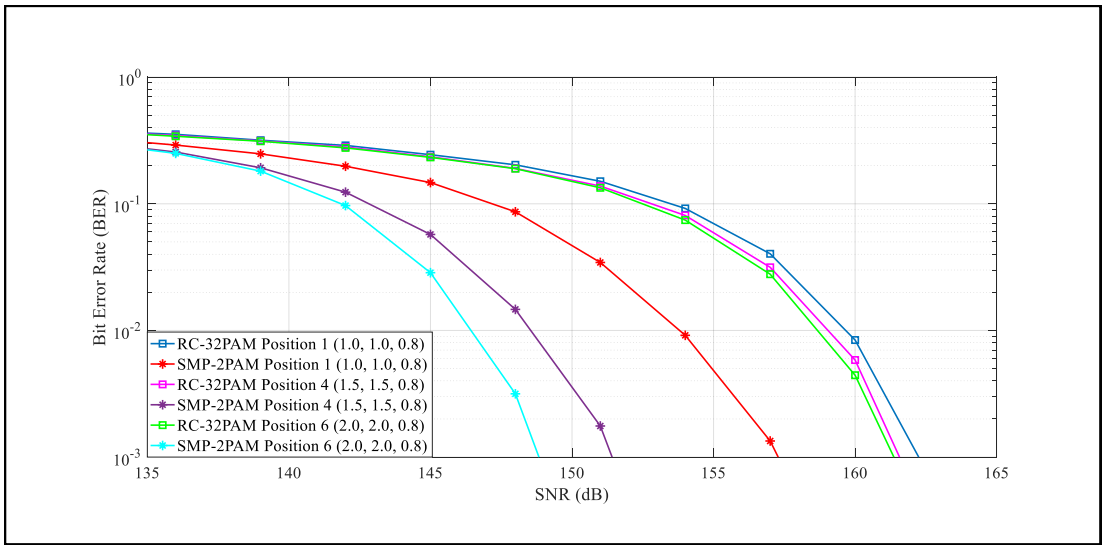

Figure 4.37. BER performance comparison of RC and SMP for R_{spec} = 5 bit/s/Hz

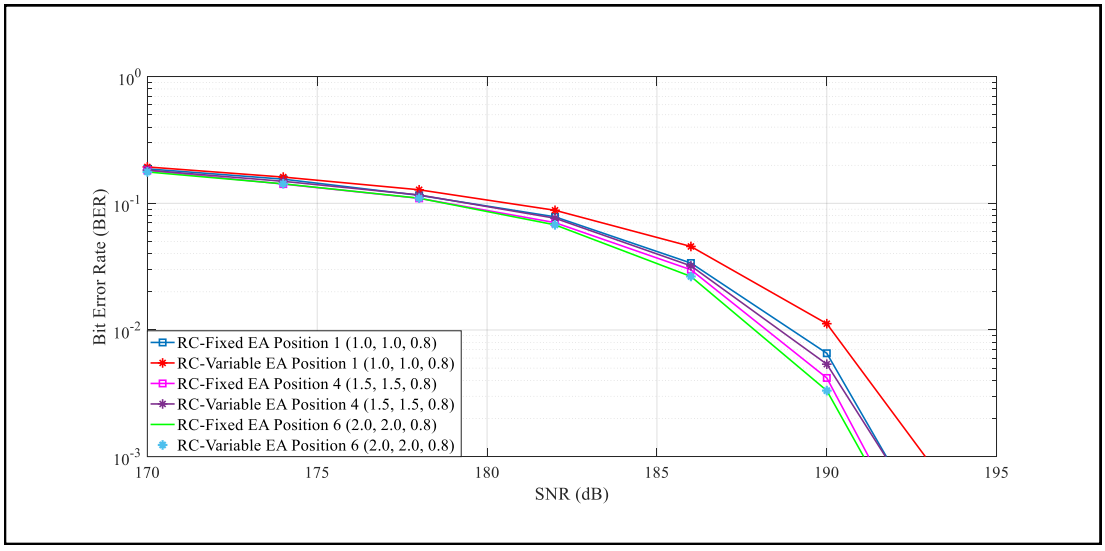

Figure 4.38. BER performance of RC employed MIMO-VLC system for R_{spec} of 10 bit/s/Hz

Similarly, the BER performance of the RC and SMP employed MIMO-VLC systems is explored for a R_{spec} of 10 bit/s/Hz. The BER performance of RC employed MIMO-VLC system is given in Figure 4.38. The BER performance of the fixed EA MIMO-VLC system is slightly better than the variable EA MIMO-VLC system for position 1 (1.0, 1.0, 0.8). The rest of the considered positions exhibits almost the same BER performance. Similarly, the BER plot for SMP is shown in Figure 4.39. A similar pattern is exhibited for the BER performance of SMP employed MIMO-VLC system. Position 6 (2.0, 2.0, 0.8) results in the best BER performance. The BER performance of fixed and variable EA MIMO-VLC systems for position 1 (1.0, 1.0, 0.8) and position 4

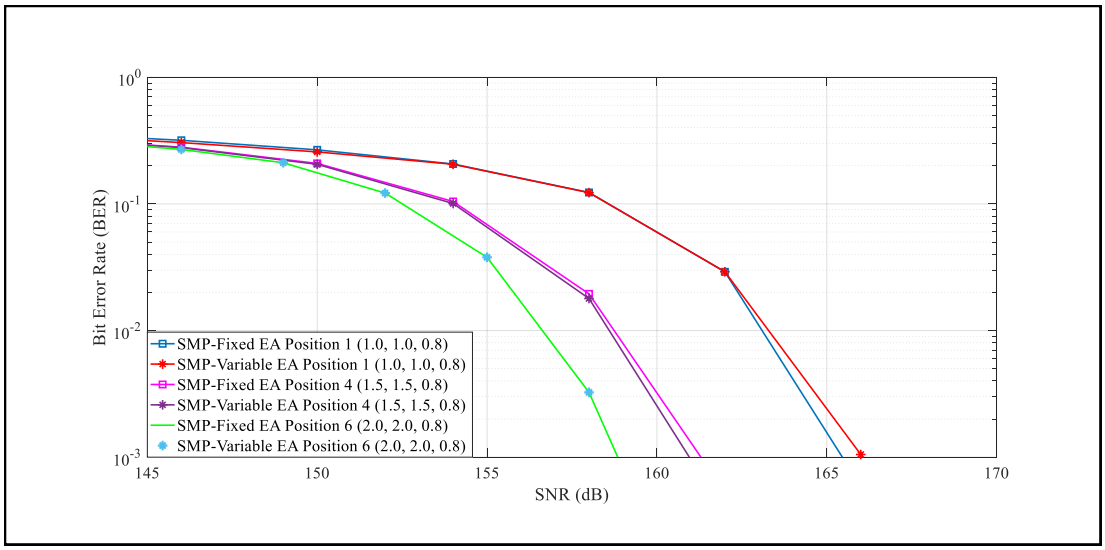

Figure 4.39. BER performance of SMP employed MIMO-VLC system

(1.5, 1.5, 0.8) is very close to one another as shown in Figure 4.39.

For R_{spec} of 10 bit/s/Hz, the BER performance of RC and SMP is compared and displayed in Figure 4.40. The SMP employed MIMO-VLC systems outperform the RC employed MIMO-VLC systems. A maximum difference in SNR required to attain the same BER performance is around 14 dB which is observed for position 6 (2.0, 2.0, 0.8) for a R_{spec} of 5 bit/s/Hz. Similarly, a maximum difference of around 33 dB is observed between position 6 (2.0, 2.0, 0.8) of RC and SMP employed MIMO-VLC systems for a R_{spec} of 10 bit/s/Hz. Due to larger constellation sizes adopted for RC i.e., 32-PAM and 1024-PAM as compared to 2-PAM and 4-PAM for SMP, the RC employed MIMO-VLC systems require an additional 14 dB and 33 dB to achieve the same BER performance for R_{spec} of 5 bit/s/Hz and 10 bit/s/Hz, respectively.

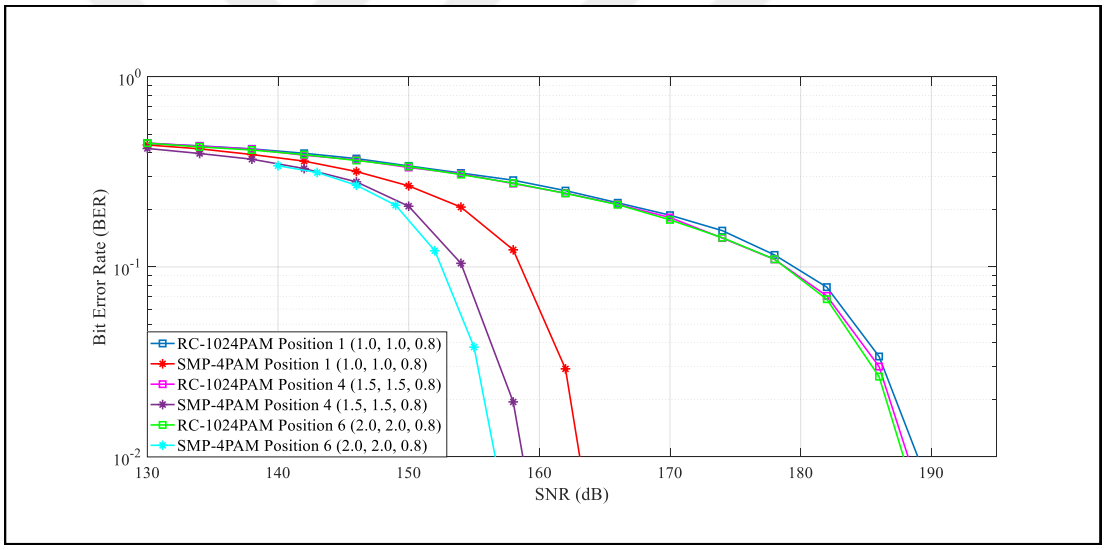

Figure 4.40. BER performance comparison of RC and SMP for R_{spec} = 10 bit/s/Hz

5. CONCLUSIONS AND FUTURE DIRECTIONS

The VLC has emerged as one of the most promising developments toward accommodating new users and provides seamless connectivity at very high data rates. The applications of VLC in the indoor environment has numerous advantages over traditional RF-based applications. However, channel correlation in an indoor MIMO-VLC system is one of the critical challenges of VLC, which degrades the overall performance of the MIMO system. Therefore, an appropriate mechanism is required to deploy and improve the performance of the indoor MIMO-VLC systems.

In this thesis, we focus on a special type of ADR called PR, to reduce the effects of channel correlation and improve the overall performance of the MIMO-VLC systems. In PR, the PDs are arranged in such a fashion that the normal vectors of the PDs point in different directions. The normal vectors depend upon the EA of PDs. Hence by carefully adjusting the EAs of PDs in an indoor MIMO-VLC system, channel correlation can be reduced. The performance of 4×4, 4×5, and 5×5 MIMO-VLC systems are compared for both fixed and variable EA for considered receiver positions. Similarly, the performance of the ADR based MIMO-VLC system is also compared with N-ADR based MIMO-VLC system.

Simulation results show that the variable EA based MIMO-VLC system outperforms the fixed EA based MIMO-VLC system for all the considered MIMO-VLC systems in terms of throughput. Moreover, the throughput performance of both, fixed and variable EA MIMO-VLC systems, is better for all the considered MIMO-VLC systems and receiver positions as compared to N-ADR based MIMO-VLC systems. Simulation has also shown that the capacity performance of the 4×5 MIMO-VLC system is better as compared to the 4×4 MIMO-VLC system. The maximum channel capacity gain of 5.53% and 3.78% is obtained for fixed and variable EA 4×5 MIMO-VLC system near the corners of the room. Thus, by adding an extra PD, the capacity performance near the corners of the room can be improved. Similarly, the channel capacity of the 5×5

MIMO-VLC system is better than both, the 4×4 and 4×5 MIMO-VLC systems. As the additional LED and PD is located at the center of the room, the maximum channel capacity gain of 19.07% is obtained with respect to 4×4 MIMO-VLC system at the center of the room. Thus, by the addition of an extra PD and LED, the channel capacity performance can be significantly improved.

It has also been observed that the FOV angle of 60° results in a better performance in terms of peak channel capacity values as compared to the FOV angle of 90°. As the FOV of the receiver is changed, the respective channel matrix entries are also changed resulting in a reduced channel correlation and ISI. As a result, the performance of 60° FOV employed MIMO-VLC system is better than its counterpart i.e., 90° FOV employed MIMO-VLC system. However, a narrow FOV angle results in uneven optical power distribution across the room, resulting in the creation of blind spots across the room. These blind spots result in degrading the performance of MIMO-VLC systems drastically and are undesirable in an indoor MIMO-VLC system.

Similarly, for each receiver position, an optimum LED transmitter array length exists, which results in C_{max}. It has been observed that the positions located closer to the center of the room requires a smaller LED transmitter array length as compared to the positions towards the corner of the room. The performance of all the considered MIMO-VLC systems is evaluated when the horizontal orientation angle of the receiver is varied from 0° to 180°. The capacity plots are evaluated for every receiver position and it has been observed that the fixed EA based MIMO-VLC system follows a perfect symmetry. However, the variable EA based MIMO-VLC systems do not follow the same symmetric cycle. In the first cycle i.e., 0° to 90°, the performance of the variable EA MIMO-VLC system is better. For the second cycle i.e., 90° to 180°, the variable EA MIMO-VLC system deviates from the symmetry and the performance of the variable EA MIMO-VLC system becomes slightly worse than the fixed EA MIMO-VLC system.

For the BER performance two different transmission schemes i.e., RC and SMP are considered. For performance comparison, the R_{spec} of both the transmission schemes is kept the same. As the R_{spec} of RC does not depend on the number of transmitters, a

larger constellation size has to be used to achieve the same R_{spec} as that of SMP. Due to a small constellation size, the performance of the SMP based MIMO-VLC system is much better than the RC based MIMO-VLC system. The BER performance of variable EA based MIMO-VLC systems is almost similar to the fixed EA MIMO-VLC systems. For the position away from the center of the room, the difference in the BER performance of fixed and variable EA is comparatively larger than the position near the center of the room. At the center of the room, as the fixed and variable EA values are the same, so does the BER performance. The BER performance depends on the LED transmitter array length. For very small values, the BER performance of RC becomes better than SMP. However, in our simulations for the BER performance analysis, we have kept the location of the LEDs fixed i.e., d_{tx} is kept 2 m. Therefore, an SMP employed MIMO-VLC system always outperforms an RC employed MIMO-VLC system.

This thesis essentially focuses on the performance of indoor MIMO-VLC systems. In this thesis, we have only considered LoS components. This system model can be extended to consider reflections from the walls of the room. By considering reflections, the channel capacity for the receiver positions close to the walls of the room can be improved.

In an indoor environment, RF sources are readily available. A VLC system can work in conjunction with an RF system resulting in a hybrid VLC/RF network. Such a network can result in significant improvement in throughput and coverage without any additional expenditure. In the future, this system can be extended to work in conjunction with RF. By adjusting the EAs of the PDs coverage can be provided to the parts of an indoor environment in which RF is not available.

REFERENCES

[1] Hanzo L., Haas H., Imre S., O'Brien D., Rupp M. and Gyongyosi L., Wireless myths, realities, and futures: from 3G/4G to optical and quantum wireless, *Proceedings of the IEEE*, 2012**, 100**(Special Centennial Issue), 1853–1888.

[2] Cisco VNI96, Cisco Visual Networking Index: Global Mobile Data Traffic Forecast, *Cisco White Paper*, 2019**, 1**(1), 1–10.

[3] Wang T.Q., He C. and Armstrong J., Performance analysis of aperture-based receivers for MIMO IM/DD visible light communications, *Journal of Lightwave Technology*, 2016**, 35**(9), 1513–1523.

[4] Nuwanpriya A., Ho S.W. and Chen C.S., Angle diversity receiver for indoor MIMO visible light communications, *2014 IEEE Globecom Workshops (GC Wkshps), IEEE*, 444–449, 2014.

[5] Nuwanpriya A., Ho S.W. and Chen C.S., Indoor MIMO visible light communications: Novel angle diversity receivers for mobile users, *IEEE Journal on Selected Areas in Communications*, 2015**, 33**(9), 1780–1792.

[6] Suh S., Bergesen J., Gibon TJ., Hertwich E. and Taptich M., Green Technology Choices: The Environmental and Resource Implications of Low-Carbon Technologies, *United Nations Environment Programme: Nairobi, Kenya*, 2017().

[7] Belkhir L. and Elmeligi A., Assessing ICT global emissions footprint: Trends to 2040 & recommendations, *Journal of Cleaner Production*, 2018**, 177**(), 448–463.

[8] Yining C., *Global LED Lighting Products Price Trend*, https://www.ledinside.com/news/2018/8/global_led_lighting_products_price_trend, (Access date: 22 March 2020).

[9] John D., Thibaut A. and Chiara D., *Tracking Buildings*, https://www.iea.org/reports/tracking-buildings/lighting/, (Access date: 22 March 2020).

[10] Dr. Peter L.W., *The Ozone Depletion Theory of Global Warming*, https://ozonedepletiontheory.info/ImagePages/electromagnetic-spectrum.html, (Access date: 22 March 2020).

[11] Khan A.U., Çelik Y. and Aldırmaz Çolak S., Capacity Variation of an Indoor MIMO VLC System for a Pyramid Receiver, *The 28th IEEE Conference on Signal Processing and Communications Applications*, In Press.

[12] Ma H., Lampe L. and Hranilovic S., Integration of indoor visible light and power line communication systems, *2013 IEEE 17th International Symposium on Power Line Communications and Its Applications, IEEE*, 291–296, 2013.

[13] Komine T. and Nakagawa M., Integrated system of white LED visible-light communication and power-line communication, *IEEE Transactions on Consumer Electronics*, 2003**, 49**(1), 71–79.

[14] Ndjiongue A.R., Ferreira H.C., Ouahada K. and Vinckz A.H., Low-complexity SOCPBFSK-OOK interface between PLC and VLC channels for low data rate transmission applications, *18th IEEE International Symposium on Power Line Communications and Its Applications, IEEE*, 226–231, 2014.

[15] Jovicic A., Li J. and Richardson T., Visible light communication: opportunities, challenges and the path to market, *IEEE Communications Magazine*, 2013**, 51**(12), 26–32.

[16] Pang G., Kwan T., Chan C. and Liu H., LED traffic light as a communications device, *Proceedings 199 IEEE/IEEJ/JSAI International Conference on Intelligent Transportation Systems (Cat. No. 99TH8383), IEEE*, 788–793, 1999.

[17] *Visible Light Communications Association*, http://vlca.net/standard, (Access date: 29 March 2020), 2018.

[18] Rehman S.U., Ullah S., Chong P.H.J., Yongchareon S. and Komosny D., Visible Light Communication: A System Perspective—Overview and Challenges, *Sensors*, 2019**, 19**(5), 1153.

[19] *IEEE Standard for Local and metropolitan area networks*, https://standards.ieee.org/standard/802_15_7-2018.html, (Access date: 30 March 2020).

[20] Saadi M. and Wuttisittikulkij L., Visible light communication–the journey so far, *Journal of Optical Communications*, 2019**, 40**(4), 447–453.

[21] World Health Organization, *Global status report on road safety 2015*, World Health Organization, 2015.

[22] Abualhoul M., Visible light and radio communication for cooperative autonomous driving: applied to vehicle convoy, PhD thesis, MINES ParisTech, 2016.

[23] Arnon S., Optimised optical wireless car-to-traffic-light communication, *Transactions on Emerging Telecommunications Technologies*, 2014**, 25**(6), 660–665.

[24] Luo P., Ghassemlooy Z., Le-Minh H., Bentley E., Burton A. and Tang X., Fundamental analysis of a car to car visible light communication system, *2014 9th International Symposium on Communication Systems, Networks & Digital Sign (CSNDSP), IEEE*, 1011–1016, 2014.

[25] Boubakri W., Abdallah W. and Boudriga N., A light-based communication architecture for smart city applications, *2015 17th International Conference on Transparent Optical Networks (ICTON), IEEE*, 1–6, 2015.

[26] Chowdhury H., Data download on the move in visible light communications: design and analysis. PhD thesis, University of Oulu, Finland, 2016.

[27] Zeng L., O'Brien D., Le-Minh H., Lee K., Jung D. and Oh Y., Improvement of date rate by using equalization in an indoor visible light communication system, *2008 4th IEEE International Conference on Circuits and Systems for Communications, IEEE*, 678–682, 2008.

[28] Le-Minh H., O'Brien D., Faulkner G., Zeng L., Lee K., Jung D. and Oh Y., 80 Mbit/s visible light communications using pre-equalized white LED, *2008 34th European Conference on Optical Communication, IEEE*, 1–2, 2008.

[29] Vučić J., Kottke C., Nerreter S., Langer K.D. and Walewski J.W., 513 Mbit/s visible light communications link based on DMT-modulation of a white LED, *Journal of lightwave technology*, 2010**, 28**(24), 3512–3518.

[30] Vučić J., Kottke C., Habel K. and Langer K.D., 803 Mbit/s visible light WDM link based on DMT modulation of a single RGB LED luminary, *2011 Optical Fiber Communication Conference and Exposition and the National Fiber Optic Engineers Conference, IEEE*, 1–3, 2011.

[31] Cossu G., Corsini R. and Ciaramella E., High-speed bi-directional optical wireless system in non-directed line-of-sight configuration, *Journal of Lightwave Technology*, 2014**, 32**(10), 2035–2040.

[32] Gomez A., Shi K., Quintana C., Sato M., Faulkner G., Thomsen B.C. and O'Brien D., Beyond 100-Gb/s indoor wide field-of-view optical wireless communications, *IEEE Photonics Technology Letters*, 2014**, 27**(4), 367–370.

[33] Zhan Z., Zhang M., Han D., Luo P., Tang X. and Lang L., 1.2 Gbps non-imaging MIMO-OFDM scheme based VLC over indoor lighting LED arrangments, July 2015, DOI: 10.1109/OECC.2015.7340270.

[34] Dissanayake S.D. and Armstrong J., Comparison of aco-ofdm, dco-ofdm and ado-ofdm in im/dd systems, *Journal of lightwave technology*, 2013**, 31**(7), 1063–1072.

[35] Başar E., Panayirci E., Uysal M. and Haas H., Generalized LED index modulation optical OFDM for MIMO visible light communications systems, *2016 IEEE International Conference on Communications (ICC), IEEE*, 1–5, 2016.

[36] Fath T. and Haas H., Performance comparison of MIMO techniques for optical wireless communications in indoor environments, *IEEE Transactions on Communications*, 2012**, 61**(2), 733–742.

[37] Ghassemlooy Z., Popoola W. and Rajbhandari S., *Optical wireless communications: system and channel modelling with Matlab*®, CRC press, 2019.

[38] Senior J.M. and Jamro M. Y., *Optical fiber communications: principles and practice*, Pearson Education, 2009.

[39] Ohno Y., Color rendering and luminous efficacy of white LED spectra, *Fourth International Conference on Solid State Lighting*, vol. 5530*, International Society for Optics and Photonics*, 88–98, 2004.

[40] Sheu J.K., Chang S.J., Kuo C.H., Su Y.K., Wu L.W., Lin Y.C., Lai W.C., Tsai J.M., Chi G.C. and Wu R.K., White-light emission from near UV InGaN-GaN LED chip precoated with blue/green/red phosphors, *IEEE Photonics Technology Letters*, 2003**, 15**(1), 18–20.

[41] Hernandez F.L., Poves E., Perez-Jimenez R. and Rabadan J., Low-cost diffuse wireless optical communication system based on white LED, *2006 IEEE International Symposium on Consumer Electronics, IEEE*, 1–4, 2007.

[42] He X., Cao G. and Zou N., Simulation of white light based on mixed RGB LEDs, 2011().

[43] Davis C.C., *Lasers and electro-optics: fundamentals and engineering*, Cambridge university press, 1996.

[44] Cui K., Chen G., Xu Z. and Roberts R.D., Line-of-sight visible light communication system design and demonstration, *2010 7th International Symposium on Communication Systems, Networks & Digital Signal Processing (CSNDSP 2010), IEEE*, 621–625, 2010.

[45] Street A.M., Stavrinou P.N., O'brien D.C. and Edwards D.J., Indoor optical wireless systems–a review, *Optical and Quantum Electronics*, 1997**, 29**(3), 349–378.

[46] Ciaramella E., Arimoto Y., Contestabile G., Presi M., D'Errico A., Guarino V. and Matsumoto M., 1.28 Terabit/s (32x40 Gbit/s) WDM transmission system for free space optical communications, *IEEE Journal on selected areas in communications*, 2009**, 27**(9), 1639–1645.

[47] Carruther J.B. and Kahn J.M., Angle diversity for nondirected wireless infrared communication, *IEEE Transactions on Communications*, 2000**, 48**(6), 960–969.

[48] Carruthers J.B. and Carroll S.M., Statistical impulse response models for indoor optical wireless channels, *International Journal of Communication Systems*, 2005**, 18**(3), 267–284.

[49] Kahn J.M. and Barry J.R., Wireless infrared communications, *Proceedings of the IEEE*, 1997**, 85**(2), 265–298.

[50] Kotzin M.D. and van den Heuvel A.P., A duplex infra-red system for in-building communications, *36th IEEE Vehicular Technology Conference*, vol. 36*, IEEE*, 179–185, 1986.

[51] Kahn J.M., Krause W.J. and Carruthers J.B., Experimental characterization of non-directed indoor infrared channels, *IEEE Transactions on Communications*, 1995**, 43**(2/3/4), 1613–1623.

[52] Burton A., Le-Minh H., Ghassemlooy Z., Bentley E. and Botella C., Experimental Demonstration of 50-Mb/s Visible Light Communications Using 4×4 MIMO, *IEEE Photonics Technology Letters*, 2014**, 26**(9), 945–948.

PUBLICATIONS AND WORKS

Khan A. U., Çelik Y., Aldırmaz Çolak S., Capacity Variation of an Indoor MIMO VLC System for a Pyramid Receiver, *28th IEEE Conference on Signal Processing and Communications Applications*, 2020, In Press.

Suleman M. and **Khan A. U.**, Efficient Jamming of Electromagnetic Spectrum of Frequency Modulation Technique, *2nd International Students Science Congress*, Abstract Book (2018), Page 94.

Shakir M., Rehman O.U., **Khan A. U.**, Abbasi M.A., Khan M.A., Optimal Performance of Wireless Body Area Networks in Varying Postural Orientations, *Technical Journal of the Faculty of Engineering University of Zulia*, 2015.

BIOGRAPHY

Aamir Ullah Khan received his Bachelor of Science in Electrical (Telecommunication) Engineering from COMSATS Institute of Information Technology (now known as COMSATS University) Islamabad, Pakistan. After graduation, he was associated with Telecom Services and Consultants Pvt. Ltd as Associate VoIP Engineer from March 2015 to August 2015. He was associated with the National University of Computer and Emerging Sciences (FAST-NU) as a Lab Engineer from August 2015 to June 2017. He is also a Huawei Certified Systems Instructor (HCSI) of HCNA (R&S). He completed his Master of Science in Electronics and Communications Engineering at Kocaeli University, Kocaeli, Turkey. He is working in the field of wireless communications and networking and his research interests include Visible Light Communication (VLC) systems, hybrid VLC/RF technologies, green technologies, and Wireless Communications Technologies for Beyond 5G/6G Networks.